Technical University of Lisbon

Faculty of Human Kinetics

Functional Assessment after Peripheral Nerve Injury

- Kinematic Model of the Hindlimb of the Rat

Thesis submitted in the fulfilment of the requirements for the Degree of Doctor in

Motricidade Humana, speciality of Fisioterapia

SANDRA CRISTINA FERNANDES AMADO

Advisor: Doutor António Prieto Veloso

Co-advisor: Doutora Ana Colette Pereira de Castro Osório Maurício

Jury

President:
Reitor da Universidade Técnica de Lisboa

Vogals:

Doutor António José de Almeida Ferreira, Professor Catedrático da Faculdade de Veterinária da Universidade Técnica de Lisboa;
Doutor António Prieto Veloso, Professor Catedrático da Faculdade de Motricidade Humana da Universidade Técnica de Lisboa;
Doutora Ana Colette Pereira de Castro Osório Maurício, Professora Associada com Agregação do Instituto de Ciências Biomédicas Abel Salazar da Universidade do Porto;
Doutora Maria Margarida Marques Rebelo Espanha, Professora Associada da Faculdade de Motricidade Humana da Universidade Técnica de Lisboa;
Doutor Artur Severo Proença Varejão, Professor Auxiliar com Agregação da Escola de Ciências Agrárias e Veterinárias da Universidade de Trás-os-Montes e Alto Douro;
Doutor Paulo Alexandre Silva Armada da Silva, Professor Auxiliar da Faculdade de Motricidade Humana da Universidade Técnica de Lisboa

2012

The following parts of this thesis have been published or submitted for publication:

(1) Amado S, Simões MJ, Armada da Silva PAS, Luís AL, Shirosaki Y, Lopes MA, et al. Use of hybrid chitosan membranes and N1E-115 cells for promoting nerve regeneration in an axonotmesis rat model. [Internet]. Biomaterials. 2008 Nov ;29(33):4409-19.

(2) Amado S, Rodrigues JM, Luís AL, Armada-da-Silva P a S, Vieira M, Gartner A, et al. Effects of collagen membranes enriched with in vitro-differentiated N1E-115 cells on rat sciatic nerve regeneration after end-to-end repair. [Internet]. Journal of neuroengineering and rehabilitation. 2010 Jan; 7:7.

(3) Amado S, Armada-da-Silva P, João F, Mauricio AC, Luis AL, Simões MJ, et al. The sensitivity of two-dimensional hindlimb joints kinematics analysis in assessing function in rats after sciatic nerve crush. Behavioural brain research. 2011 (submitted);

(4) S Amado, AL Luis, S Raimondo, M Fornaro, MG Giacobini-Robecchi, S Geuna, F João, AP Veloso, AC Maurício , PAS Armada-da-Silva. 2012 *Neuroscience* (submitted)

OTHER PUBLICATIONS

(4) A Gärtner, AC Maurício, T Pereira, PAS Armada-da-Silva, S Amado, AP Veloso, AL Luís, ASP Varejão, S Geuna (2011). Cellular systems and biomaterials for nerve regeneration in neurotmesis injuries. In Biomaterials / Book 3. Editor Prof. Rosario Pignatello. InTech (ISBN 979-953-307-295-0).

(5) João, F., Amado, S., Veloso, A., Armada-da-silva, P., & Maurício, Ana C. (2010). Anatomical reference frame versus planar analysis: implications for the kinematics of the rat hindlimb during locomotion. *Reviews in the neurosciences*, *21*(6), 469.

(6) Simões, M. J., Amado, S., Gärtner, A., Armada-Da-Silva, P. a S., Raimondo, S., Vieira, M., et al. (2010). Use of chitosan scaffolds for repairing rat sciatic nerve defects. *Italian journal of anatomy and embryology = Archivio italiano di anatomia ed embriologia*, *115*(3), 190-210.

ORAL PRESENTATIONS

(7) Armada-da-Silva P, Amado S, Borges M, Simões MJ, João F, Maurício AC, et al. Nerve Decompression Does Not Improve Sciatic Function in Chronic Constriction Injury in the Rat. In: 2nd International Fascia Research Congress. Amsterdam: 2009.

(8) Amado S, Veloso A, Armada-da-Silva P, João F, Simões MJ, Vieira M, et al. Biomechanical and Morphological Approach to Assess Recovery After Peripheral Nerve Injury in Animal Model. In: 2nd International Fascia Research Congress. Amsterdam: 2009.

(9) Amado S, Veloso AP, Armada-da-silva P, João F, Luís AL, Geuna S, et al. Análise biomecâanica da recuperação funcional na reparação de lesõoes do nervo periférico num modelo animal. In: 3º Congresso Nacional de Biomecânica da Sociedade Portuguesa de Biomecânica. Bragança: 2009.

(10) João F, Amado S, Veloso A, Armada-da-Silva P, Mauricio A. Segmental Kinematic Analysis using a tridimensional reconstruction of rat hindlimb: comparison between 2D and 3D joint angles. In: ISB 2010.

Contents

CONTENTS VII

ACKNOWLEDGEMENTS IX

SUMMARY XI

RESUMO XII

CHAPTER 1 – INTRODUCTION AND MAIN OBJECTIVES 1

CHAPTER 2 – METHODOLOGICAL CONSIDERATIONS 19

CHAPTER 3 - USE OF HYBRID CHITOSAN MEMBRANES AND N1E-115 CELLS FOR PROMOTING NERVE REGENERATION IN AN AXONOTMESIS RAT MODEL 39

CHAPTER 4 - EFFECTS OF COLLAGEN MEMBRANES ENRICHED WITH IN VITRO-DIFFERENTIATED N1E-115 CELLS ON RAT SCIATIC NERVE REGENERATION AFTER END-TO-END REPAIR 77

CHAPTER 5 - THE SENSITIVITY OF TWO-DIMENSIONAL HINDLIMB JOINTS KINEMATICS ANALYSIS IN ASSESSING FUNCTION IN RATS AFTER SCIATIC NERVE CRUSH 105

CHAPTER 6 - THE EFFECT OF ACTIVE AND PASSIVE EXERCISE IN NERVE REGENERATION AND FUNCTIONAL RECOVERY AFTER SCIATIC NERVE CRUSH IN THE RAT 135

CHAPTER 7 - GENERAL DISCUSSION AND CONCLUSIONS 165

Acknowledgements

Institutional support and partnership was crucial for the successful development of scientific work. The experimental work was possible to be performed at the Instituto Nacional Ricardo Jorge and Faculdade de Medicina Veterinaria de Lisboa. I would like to gratefully acknowledge the valuable support by Doutor José Manuel Correia Costa, from Laboratório de Parasitologia, Instituto Nacional de Saúde Dr. Ricardo Jorge (INSRJ), Porto, Portugal and by Doutora Belmira Carrapiço, from Faculdade de Medicina Veterinária de Lisboa.

I would like to thanks to the Universidade Técnica de Lisboa (UTL) rector, the president of scientific committee and the president of Faculdade de Motricidade Humana, also of Instituto Ciências Biomédicas Abel Salazar – Universidade do Porto, ICETA-CECA, and Escola Superior de Saúde de Leiria - Instituto Politécnico de Leiria.

I wish to express my sincere appreciation and gratitude to all of those who have made this thesis possible. In particular I would like to thank:

Professor António Prieto Veloso, my supervisor, and the head of Neuromechanics Research Group, for your never-ending patience and generous giving of your time and skills. I am very grateful for you guiding me through this work.

Professor Ana Colette de Castro Osório Maurício, my co-supervisor, for your enthusiastic support, your door always being open, for you being a great human. I have learnt a lot from you. Special thanks also to Henrique…

Professor Paulo Armada-da-Silva, my co-author, for your generous giving of feedback and input during the work with the research projects.

Professor Ana Lúcia Luís, my co-author, for her microsurgery skills and for all fruitful discussions and advices regarding science and life in general. Thank you also to her family, Fernando and Rita.

Professor Jorge Rodrigues, my co-author, for his microsurgery skills and for being a great example of Human Professional.

Professor Stefano Geuna and his team, my co-authors, for his stereological techniques that stimulated my interest about nerve morphology.

Professor José Domingues and Ascenção Lopes, my co-authors, for the great opportunity to work at experimental level with biomaterials, regenerative medicine and tissue engineering.

Maria João Simões, Márcia Vieira, my co-authors, for the patience during the hours spent at the lab performing the videos.

Filipa João, my co-author, for the enthusiastic interest about rats *in silica*…!

My former research colleagues at the Neuromechanics group: Professors **Filomena Carnide, Filomena Vieira and Carlos Andrade. Maria Machado (Didi), Vera Moniz-Pereira, Filipa João, Liliana, Silvia Cabral, Ricardo Matias, Wangdoo Kim** thank you for all the great time we have spent together in the lab and of course during all of our parties.

Professor Carlos Ferreira, thank you for the "Master thesis" format.

Professor Hugo Gamboa and **Neuza Nunes** for encouraging the study of pattern recognition.

To all my patients that understood the need felt to initiate a different way to answer their questions…. Thank you.

For students and my colleagues at Escola Superior de Saúde de Leiria, a special thanks to: Ana Roque, José Vital, Luís Eva Ferreira, Sílvia Jorge, Dulce Gomes e Sónia Pós de Mina, Susana Custódio, Sílvia Gonzaga, Filipa Soares.

My **friends** and **family** for the time not spent with them… **My parents** and **sister** for always being there and supporting me in every aspects of life. For your never-ending encouragement to fully explore my curiosity. My gratitude and my admiration see no limitations.

To **Francisco**, for the unconditional love, and **Claudio** that supported the day-by-day basis.

My research has been supported by **Fundação para a Ciência e Tecnologia (FCT)** from Ministério da Ciência e Ensino Superior (MCES), Portugal, through the financed grant SFRH/BD/30971/2006 and research project PTDC/CTM/64220/2006. Part of the work was also supported by PRIN and FIRB grants from the Italian MIUR (Ministero dell'Istruzione, dell'Università e della Ricerca), by the Regione Piemonte (Programma di Ricerca Sanitaria Finalizzata)

Summary

Gait analysis is increasingly used on research methodology to assess dynamics aspects of functional recovery after peripheral nerve injury in the rat model, which ultimately is the goal of treatment and rehabilitation. In this thesis we studied nerve regeneration using techniques of molecular and cellular biology. Functional recovery was evaluated using the sciatic functional index (SFI), the static sciatic index (SSI), the extensor postural thrust (EPT), the withdrawal reflex latency (WRL) and hindlimb kinematics. Nerve fiber regeneration was assessed by quantitative stereological analysis and electron microscopy. From our results, hybrid chitosan membranes after sciatic nerve crush, either alone or enriched with N1E-115 neural cells, may represent an effective approach for the improvement of the clinical outcome in patients receiving peripheral nerve surgery. Collagen membrane, with or without neural cell enrichment, did not lead to any significant improvement in most of functional and stereological predictors of nerve regeneration that we have assessed, with the exception of EPT. Extending the kinematic analysis during walking to the hip joint improved sensitivity of this functional test. For motor rehabilitation, either active or passive exercises positively affect sciatic nerve regeneration after a crush injury, possibly mediated by a direct mechanical effect onto the regenerating nerve.

Keywords: functional assessment, rat, joint kinematics, neurorehabilitation, peripheral nerve, biomaterials.

Resumo

A crescente utilização da análise da marcha após lesão do nervo periférico no modelo do rato relaciona-se com a necessidade de avaliar aspectos dinâmicos da recuperação funcional. Na presente tese estudámos a regeneração do nervo com utilização de técnicas moleculares e celulares. A recuperação funcional foi avaliada com uso de Índice de funcionalidade do ciático, índice estático do ciático, reflexo extensor postural, latência do reflexo flexor e cinemática do membro posterior. A regeneração da fibra nervosa foi avaliada com técnicas estereológicas e microscopia electrónica. Dos nossos resultados concluímos que as membranas híbridas de quitosano após lesão de esmagamento do nervo ciático, com ou sem enriquecimento de células neurais N1E-115, podem representar uma abordagem efetiva para a melhoria dos resultados clínicos dos pacientes sujeitos a cirurgia do nervo periférico. As membranas de colageneo, com ou sem enriquecimento de células neurais, não repercutiram nenhuma melhoria significativa nos parâmetros preditores funcionais e estereologicos de regeneração do nervo. Verificámos que a inclusão da articulação da coxo-femoral na analise cinemática de marcha aumentou a sensibilidade deste teste funcional. Para a reabilitação motora, quer o exercício ativo quer passivo influenciou a regeneração do nervo após esmagamento, possivelmente devido a um efeito mecânico na regeneração do nervo periférico.

Palavras-chave: avaliação funcional, rato, cinemática, neuroreabilitação, nervo periférico, biomateriais

Chapter 1 – Introduction and Main Objectives

1 Introduction and main objectives

This thesis was focused on the study of functional recovery after biological therapeutic strategies for repair of peripheral nerve axonotmesis and neurotmesis injuries with experimental model of the rat. The available background regarding peripheral nerve repair suggests that: 1) Biomaterials are important for peripheral nerve repair after injury with promising functional results; 2) Functional recovery is the golden standard to ascertained efficacy of interventions and results transposition from *in vivo* experiments; 3) the description of functional movement of the ankle i.e. ankle kinematics during stance phase is an accurate method for functional assessment. So, the aims of this thesis were: 1) to evaluate functional recovery after a moderate i.e axonotemesis and severe i.e neurotemesis sciatic nerve injury and verify if various types of biomaterials, would affect functional recovery and the morphology of nerve fibers, with emphases on evaluation of kinematic analysis of the rat ankle; 2) to improve kinematic model for assessment of functional recovery after sciatic nerve crush injury; 3) to verify if therapeutic exercise would induce changes on kinematics of gait and nerve morphology.

After peripheral nerve injury, its inner capability of repair is a remarkable reality. Previously, our research group reported *in vitro* results that highlighted the relevance of Ca^{2+} (1; 2) and results leads to a significant research to know which biological element might contribute to synergistically optimize effects of microsurgical techniques and improve morphological and functional recovery (3-5). Neurotrophic factors have been the target of intensive research - their role in nerve regeneration and the way they influence neural development, survival, outgrowth, and branching (6). Among neurotrophic factors, neurotrophins have been heavily investigated in nerve regeneration studies. They include the nerve growth factor (NGF), brain-derived neurotrophic factor (BDNF), neurotrophin-3 (NT-3), and neurotrophin-4/5 (NT-4/5) (7). Neurotrophic factors promote a variety of neural responses, including survival and outgrowth of the motor and sensory nerve fibers, and spinal cord regeneration (8). However, *in vivo* responses to neurotrophic factors can vary due to the method of their delivering. Therefore, the development and use of controlled delivery devices are required for the study of complex systems.

A multidisciplinary team, including Veterinaries, Engineers, Medical doctors like neurologists and surgeons, through Experimental Surgery has a crucial role in the development of biomaterials associated to these cellular systems, and in testing the surgical techniques that involve their application, always considering animal welfare

and the most appropriate animal model. Rodents, particularly the rat and the mouse, have become the most frequently utilized animal models for the study of peripheral nerve regeneration because of the widespread availability of these animals as well as the distribution of their nerve trunks which is similar to humans (9). Although other nerve trunks, especially in the rat forelimb, are getting more and more used for experimental research (10; 11), the rat sciatic nerve is still the far more employed experimental model as it provides a nerve trunk with adequate length and space at the mid-thigh for surgical manipulation and/or introduction of grafts or guides (9). Although sciatic nerve injuries themselves are rare in humans, this experimental model provides a very realistic testing bench for lesions involving plurifascicular mixed nerves with axons of different size and type competing to reach and reinnervate distal targets (9). Common types of experimentally induced injuries include focal crush or freeze injury that causes axonal interruption but preserves the connective sheaths (axonotmesis), complete transection disrupting the whole nerve trunk (neurotmesis) and resection of a nerve segment inducing a gap of certain length. Several biomaterials developed by our research group (including PLGA with a novel proportion 90:10 of the two polymers, poly(L-lactide):poly(glycolide), hybrid chitosan and collagen) or available already in the market like Neurolac® (made of poly-ε-caprolactone) have been tested associated to cellular systems to promote nerve regeneration after axonotmesis and neurotmesis injuries in the sciatic nerve experimental model. The cellular systems that have been studied in this context include an immortalized neural cell line N1E-115.

One primary cause of poor recovery after long-term denervation is a profound reduction in the number of axons that successfully regenerate through the deteriorating intramuscular nerve sheaths. Muscle force capacity is further compromised by the incomplete recovery of muscle fibres from denervation atrophy. Progressive muscle atrophy and changes in muscle fibres composition are consequences of peripheral nervous system injury that interrupts communication between skeletal muscle and neurons. After peripheral nerve injury, alterations of gait pattern are the most relevant observation (5; 12). Functional recovery stills the main limitation to achieve results translation, and the understanding of such limitation is greatly dependent also on research methods and on therapeutic strategies. Choosing the correct functional assay in the rat model for peripheral nerve injury (13) and spinal cord injury (14) is a question of intensive research interest as an experimental model. After peripheral nerve injury there are neural and mechanical disturbances and the amount of sensory endings that exist is one of the major limitations to study the functional meaning of recovery and thus, the biomechanical model has been increasingly used. For most recently published studies, functional tests consider analysis of voluntary movement and reflex

activity. Gait function represents the integration of motor and sensory function and several gait parameters were considered with significant relationship for functional evaluation of experimental rat model, only during the last decade it has been studied with biomechanics research methods. Previously, we have highlighted the importance of both functional and morphological methods in this model (5) already reported by Varejão et al. (15), which make possible to have different levels of complexity to study the peripheral nerve repair process. In experimental laboratory animal model it is a great advance to measure observable functional gains, until now impossible to obtain since they were considered subjective behavioral measurements.

Locomotion, from a mechanical point of view, is characterized by a repetitious sequence of limb motion to move the body forward while maintaining the stance balance. There are three basic approaches to analyze gait (16): 1) subdividing the cycle according to the variations in reciprocal floor contact by the two feet; 2) using the time and distance qualities of the stride; 3) identifying the functional significance of the events within the gait cycle and designate these intervals as the functional phases of gait. According to the variations in reciprocal floor contact by the two feet, as the body moves forward, one limb serves as mobile source of support while the other limb advances itself to a new support site. Stance phase designates the entire period during which the foot is on the ground and begins with initial contact (IC). Swing phase is the phase of the normal gait cycle during which the foot is off the ground. The swing phase follows the stance phase and is divided into the initial swing, the midswing, and the terminal swing stages.

Analysis of the free walking pattern of the rat is the method mostly used for assessment of motor function through motion analysis. Although locomotor activity in an open field is a stable behavioural test and may be used as an index of the behavioural-physiological coping style of an individual rat (Basso, Beatie and Bresnahan (BBB) Locomotor Rating Scale) (17), the information obtained is qualitative, range from 0 to 21 and distinguish between locomotor features such as flaccid paralysis, isolated hind-limb joint movements, weight-supported plantar stepping, coordination, and details of locomotion (eg, toe clearance, paw position) (18). Specifically for peripheral nerve injury, it was developed a method to measure a combination of motor and sensory recovery: Sciatic Functional Index (SFI) (19). They calculated an index of the functional condition of rat sciatic nerve (SFI) that consists on expressing as a percentage the difference between the measurements of injured hind paw parameters and the intact contralateral hind paw parameters obtained from footprints. The main objective of these methods was to extrapolate the nerve function

recovery considering its action on innervated muscles. After sciatic nerve injury, footprints reveal differences between the normal and experimental print length with the last one being the largest. Although SFI is a quantitative method, it is dependent on the pressure exerted by the foot on the floor, and it is restricted to a point in time, which limits the information obtained. Automutilation, inversion or eversion deformations often limit the functional assessment with the use of SFI (20), despite this limitation it is a widely used parameter because of its reliability (21). Bervar (2000) described an alternative video analysis of static footprint video analysis (SSI) to assess functional loss following injury to the rat sciatic nerve, during animal standing or periodic rest on a flat transparent surface used motion analysis with the utilization of video analysis. SSI static sciatic index was developed based on the premise that the recovery of muscle tone after nerve injury is a constituent part of integral nerve and muscle functional recovery and forces acting on the body i.e. body weight and postural muscle tone during standing influenced footprint parameters (22). The main difference between SFI and SSI was that the distance between the tip of the third toe and the posterior margin of the sole discoloured area (PLF), defined as the print length parameter, was not considered. The authors considered this parameter the most difficult part of the video analysis and it was subject to observer's misinterpretation and unwilling measuring errors with excessive variability and poor correlation between static video method and dynamic ink track method. They found better reproducibility, high accuracy, more precise quantification of the degree of functional loss and there are few non-measurable footprints with SSI.

Walking pattern is the result of several signs that contributes to the performance of movement (23). Understanding adaptive changes in motor activity associated with functional recovery following muscle denervation can be achieved with biomechanical research methods. In biomechanics, movement is studied in order to understand the underlying mechanisms involved in the movement or in the acquisition and regulation of skill. Biomechanics involves mechanical measurements used in conjunction with biological interpretations (24). Mechanicaly, motion production also depends on the geometry of bones and muscles, which reflects the moment pattern of motion.

The development of scientific methods of monitoring locomotion is based on computational and mathematical principles. Biomechanics is based on Newton´s equation of motion. There are some assumptions about Biomechanics to simplify the complex musculoskeletal system and eliminate the necessity of quantifying the changes in mass distribution caused by tissue deformation and movement of bodily fluids: body segments behave as rigid bodies during movements, and in addition, segmental mass distribution is similar among members of a particular population (23).

Over the last years, the number of parameters used for ankle joint motion analysis has been increasing, most likely reflecting advances in computer-based video and motion analysis. In a first use of ankle joint kinematics in peripheral nerve research, Santos et al. (25) proposed a 2D geometrical model of the joint using two intersecting lines joining the knee and ankle and the fifth metatarsal head to the ankle. They demonstrated an increase in joint angle during the swing phase after a crush injury of the peroneal nerve. After this early study, Lin et al. (26) examined the angular changes of the ankle joint during the rat walk after sciatic nerve transection and autografting using a single parameter: the joint angle at mid-stance. Changes in this angle were reported as being sensitive to assess functional impairment after sciatic nerve injury after several months of the sciatic transection, when compared to non-injured controls. More recently, Varejão et al. (27) contributed significantly to improve ankle joint kinematic analysis in the rat sciatic nerve model by proposing a more thorough analysis of ankle motion during the stance phase that takes into account well-defined time events. These authors measured the angle of the ankle joint at initial (toe) contact (IC), opposite toe-off (around 20% of the duration of stance phase), heel raise (around 40% of the duration of stance phase), and at toe-off (TO) (27; 28). Using these measurements, the authors could demonstrate the presence of functional deficit beyond 8 weeks after sciatic nerve crush, in clear contrast to SFI measures. By this time of recovery after sciatic crush, SFI measures usually show complete recovery (5; 15).

More recently, the use of digital 2D video analysis of ankle motion in rat peripheral nerve models also includes the swing phase of walking (29). Also using 2D video analysis and dedicated software for motion analysis, our group reported recently measures of both angle and angular velocity of the ankle joint during the stance phase (5). Angular velocity data were calculated in an attempt to raise the precision of ankle motion analysis and to increase its power in detecting subtle differences in functional recovery when testing alternative treatments after sciatic crush (27; 28). We reasoned that functional deficits during walking in rat nerve models may be masked by the high redundancy and adaptability of the motor apparatus in response to sensorimotor alterations (5; 15). From a biomechanical perspective, joint rotational velocity has a more direct relationship with the forces actuating onto the hindlimb segments and therefore velocity measures may be better indicators of dysfunction caused by nerve injury. Moreover, ankle position data is sometimes difficult to interpret, for example in those cases where ankle joint angle remains unaffected in the weeks immediately after

sciatic nerve crush (27; 28). This shows that measures of ankle joint angle taken at snapshots during walking may lack sensitivity to assess functional impairment.
Increasing the number of measures may not improve the precision of functional evaluation. In fact, including more kinematic variables in walking analysis may otherwise raise uncertainty in interpreting data. For example, Varejão et al. (15) report that ankle angles at TO were similar before and after 4 weeks of sciatic crush, whereas ankle angles were clearly affected post-injury at other time points during the stance phase. Similar inconsistency in kinematic measurements of ankle joint motion in rats after sciatic crush injury has been also reported by us (30). This latter study was designed in order to prolong the observation up to 12 weeks. A full functional recovery was predicted by SFI/SSI, Extensor Postural Trust (EPT) and Withdrawal Reflex Latency (WRL) but not by all ankle kinematics parameters. Moreover, only two morphological parameters (myelin thickness/axon diameter ratio and fiber/axon diameter ratio) returned to normal values. Although these results may reflect phenomena related to nerve regeneration and end-organ reinnervation, such as motor axons misdirection (34), they also suggest that kinematic parameters display distinct ability to demonstrate functional alterations after peripheral nerve injury.

Damage to any portion of the reflex arc, including the sciatic nerve can result in loss or slowing of the reflex response. Reflex activity refers to the neural activity in which a particular stimulus, by exciting an afferent nerve, produces a stereotyped, immediate response of muscle. Considering motor control, it is related with sensory feedback control. Marshal Hall was the first neurologist who has introduced the term reflex into biology in the 19th century. He thought of the muscle as reflecting a stimulus as a wall reflects a ball thrown against it. Reflex was defined as the automatic response of a muscle or several muscles to a stimulus that excites an afferent nerve. The anatomical pathway used in a reflex is called the reflex arc and it consists of an afferent nerve, one or more interneurons within the central nervous system and an efferent nerve. Reflexes are considered unlearned, rapid, predictable motor responses to a stimulus, and occur over a highly specific neural pathway called reflex arc. Thalhammer and collaborators, (36), originally proposed the Extensor Postural Trust (EPT) as a part of the evaluation of motor function in the rat after sciatic nerve injury. It is classified as a postural reflex reaction. For this test, the entire body of the rat, excepting the hindlimbs, was wrapped and supporting the animal by the thorax and lowering the affected hindlimb towards the platform of a digital balance, elicits the EPT. As the animal is lowered to the platform, it extends the hindlimb, anticipating the contact made by the distal metatarsus and digits. The force applied to the platform balance was recorded. Sensory function is usually

assessed with the nociceptive withdrawal reflex (WRL), also called the flexion reflex. The flexor, or withdrawal, reflex is initiated by a painful stimulus and causes automatic withdrawal of the endangered body part from the stimulus. It was adapted from the hotplate test as described by Masters and collaborators in 1993 (35) and involves a protective response to withdraw the site from the stimulus when cutaneous receptors (Group III and IV afferents) sense a noxious stimulus. It is a polysynaptic reflex that is induced by noxious stimulation of the limb and its latency, amplitude, and duration depends on stimulus intensity (28). Although WRL reflex was originally termed flexion-withdrawal reflex (37), it has since been shown to involve other muscles besides flexors (38). The WRL can be variable because it depends on which afferents are activated by the stimulus and is transmitted over polysynaptic pathways, which means that the input signal can be modified along its path.

Quantification of the number of myelinated fibers in peripheral nerve is one of the main indicators of success of peripheral nerve repair. Number, density and diameter of the nervous fibers are the main variables considered. However, sampling scheme is crucial to avoid systematic errors of estimation (39) due to, for instance, anisotropy of the nervous fibres along the nerve and consequent tendency of grouping fibers related with their diameter (40). The golden standard is the designed-based sampling also recognized as systematic random sampling scheme. Previously, we have reported that 12 weeks after injury, regenerated nerves have higher mean density and total number of myelinated axons as lower mean fiber diameter and myelin thickness. Fiber density and number in crushed nerves is still significantly higher than normal nerves while size is still significantly lower (5). It has been hypothesized that one explanation could be the occurrence of a sprouting of more than one growth cone from each severed axon leading to the presence of an abundance of small regenerating axons that cross the lesion site and grow to innervate the end organs (46). The primary function of peripheral nerves is communication. Thus, electrical and/or chemical messages are passed from neuron to neuron or from neuron to target organ. Curiously, early work on impulse conduction along peripheral fibers by Erlanger and Gasser (for which they shared the Nobel Prize in 1942) demonstrated remarkable relationships between the conduction velocity of the axons and the type of information that was conveyed. In what concerns nerve morphology, peripheral nerves demonstrate a wide variety of axonal types, from myelinated axons of 20 microns in diameter, to very fine nonmyelinated axons as small as 0.2 microns in diameter. Significant correlation and internal consistency between electrophysiological and morphological parameters (i.e. conduction velocity and fiber diameter) make available information and guidelines for

parameter selection based upon the specific question being investigated (36). The largest motor fibers (13-20 um, conducting at velocities of 80 -120 m/s) innervate the extrafusal fibers of the skeletal muscles, and smaller motor fibers (5-8 um, conducting at 4-24 m/s) innervate intrafusal muscle fibers. The largest sensory fibers (13-20 μm) innervate muscle spindles and Golgi tendon organs (both conveying unconscious proprioceptive information), the next largest (6-12 μm) convey information from mechanoreceptors in the skin, and the smallest myelinated fibers 1 – 5 μm) convey information from free nerve endings in the skin, as well as pain, and cold receptors. Non myelinated peripheral C fibers (0.2 – 1.5 μm) carry information about pain and warmth.

In our fist study (chapter 3) functional recovery was assessed after different therapeutic strategies to improve sciatic nerve repair after axonotemesis injury. The experimental model based on the induction of a crush injury (axonotmesis) in the rat sciatic nerve provides a very realistic testing bench for lesions involving plurifascicular mixed nerves with axons of different size and type competing to reach and re-innervate distal targets (35). This type of injury is thus appropriate to investigate the cellular and molecular mechanisms of peripheral nerve regeneration, to assess the role of different factors in the regeneration process (36) and to perform preliminary *in vivo* testing of biomaterials that will be useful in tube-guide fabrication for more serious injuries of the peripheral nerve, such as neurotmesis. Reflex activity, gait function, motion analysis during gait and nerve morphology were assessed with EPT and WRL, SFI, ankle kinematics and nerve histomorphometry respectively. Motion pattern of ankle joint was studied performing 2-D biomechanical analysis (sagital plan) during stance phase of gait. It was carried out applying a two-segment model of the ankle joint. It was characterized with four time events: Initial Contact, Opposite Toe-Off, Hell Rise, and Toe-Off as described above. We brought together two of the more promising recent trends in nerve regeneration research: 1) local enwrapping of the lesion site of axonotmesis by means of hybrid chitosan membranes; 2) application of a cell delivery system to improve local secretion of neurotrophic factors. First, type I, II and III chitosan membranes were screened by an *in vitro* assay, in terms of physical, mechanical and cytocompatibility properties. Then, membranes were evaluated *in vivo* to assess their biocompatibility and their effects on nerve fiber regeneration and nerve recovery in a standardized rat sciatic nerve crush injury model (37). Among the various substances proposed for the fashioning of nerve conduits, chitosan attracted particular attention because of its biocompatibility, biodegradability, low toxicity, low cost, enhancement of wound-healing and antibacterial effects (38). In addition, the potential application of

chitosan in nerve regeneration has been demonstrated both *in vitro* and *in vivo* (39). Chitosan is a partially deacetylated polymer of acetyl glucosamine obtained after the alkaline deacetylation of chitin (40).

In our second study (chapter 4) different therapeutic strategies were developed to improve sciatic nerve repair after a different, more severe lesion i.e. neurotmesis with and without gap. The aim of this study was to verify if rat sciatic nerve regeneration after end-to-end reconstruction can be improved by seeding *in vitro* differentiated N1E-115 neural cells on a type III equine collagen membrane and enwrap the membrane around the lesion site. Reflex activity, gait function, motion analysis during gait and nerve morphology were assessed with EPT and WRL, SSI, ankle kinematics and nerve morphometry respectively. 2-D biomechanical analysis (sagital plan) was carried out applying a two-segment model of the ankle joint. As in the previous study, we only considered the stance phase.

In chapter 5, it is described a third group of experiments, that established different levels of functional dysfunction by evaluating sciatic-crushed rats: 1) in the denervation phase (one week after injury), 2) in the reinnervated phase: 12 weeks after injury, and 3) sham-operated controls. We considered the entire gait cycle i.e. stance and swing phases, which were characterized with four time events: Initial Contact, Midstance, Toe-Off and Midswing. Peak values of joint angle and angular velocity were studied in both phases: stance and swing. Additionally, all hindlimb joints were studied: ankle, knee and hip, allowing the study of 2-D motion analysis (sagital plan) and interjoint coordination. Gait was also characterized in terms of spatiotemporal parameters (gait velocity, step length, swing and stance phase duration), which allowed having insights about its mechanical characteristics. An important statistical question was raised with this study: Increasing the number of ankle motion measures is also not statistically desirable, particularly if these carries redundancy and lowers sensitivity. Studies in animal models of peripheral nerve injury are usually constrained by low number of subjects according to international welfare laws. When kinematic measures are applied to determine changes at behavioural level, less than 10 animals per group are commonly used (41-45). Therefore the decision of which kinematic variables should be used to assess functional recovery in peripheral nerve research should be based on an evaluation of their sensitivity to detect functional changes of different levels of severity. A proper selection of kinematic variables would give researchers a tool to monitor functional recovery after nerve injury and to detect long term functional changes caused by incomplete recovery or adaptive changes in motor patterns. We performed a

discriminant analysis of the kinematic parameters to verify if 2D joint motion analysis is highly sensitive and specific to identify functional deficits caused by acute sciatic crush in the rat. The sensitivity and specificity of a given set or battery of tests may be evaluated using discriminant analysis. This statistical technique builds a predictive model to detect membership based on a set of independent variables. This technique may be applied to evaluate the sensitivity and specificity of a set of testing variables since it measures the ability of these tests in classifying elements in a specific group. While assessing sensitivity, discriminant analysis also determines the relative importance of the independent variables in classifying observations and to discard variables with little importance in-group segregation. These applications of discriminant analysis will help to select which of the potentially large number of variables related to segmental motions during walking will be most important in assessing functional recovery after a peripheral nerve injury in the rat. Therefore, this study evaluates the sensitivity and specificity of ankle joint motion kinematic measures in detecting motion abnormalities as a result of sciatic nerve crush by employing discriminant analysis. Different levels of functional dysfunction in this study were established by evaluating sciatic-crushed rats: 1) in the denervation phase (one week after injury), 2) in the reinnervated phase: 12 weeks after injury, and 3) sham-operated controls.

Our fourth study (chapter 6) aimed to verify if active and passive exercise would elicit changes in functional recovery after sciatic nerve crush detected by hindlimb kinematics and nerve morphology. Progressive muscle atrophy and changes in muscle fibres composition are consequences of peripheral nervous system injury that interrupts communication between skeletal muscle and neurons. Many strategies have been used to maintain the muscle activity during the time of reinnervation (46). Exercise is an important activity in the management of neuromuscular disease. It might improve return of sensorymotor function. Exercise performed after peripheral nerve injury acts on muscle properties (histochemical muscle fiber alteration, contractile properties, enzyme activities, and muscle weight) and nerve properties (axonal regrowth and myelinization of axons). Most investigations have frequently used the motorized treadmill in *in vivo* studies since it offers a controlled and convenient strategy for testing and training. Twelve weeks after crush injury without exercise protocol, functional recovery is not full and nerve morphology remains significant different in control and injured animals as well as ankle joint motion during walk (47). Although many studies have studied the effects of exercise in functional recovery, biomechanical evaluation was not considered. Previous studies (48) suggested that functional reinnervation of hindlimb muscles begins 2 or 3 weeks post sciatic nerve crush in rats

and that overwork of muscle before this period can be harmful (41-45), but the reason for the negative effect of exercise is still unknown. Therefore, in our study we performed four groups of animals: two groups of animals started an exercise training protocol 2 weeks after injury (week 2). Groups (1) sciatic-crushed rats that performed treadmill walking; (2) sciatic-crushed rats that performed passive muscle stretch (3) sham-operated controls and (4) sciatic-crushed controls. The exercise groups ended the program at week-12 post injury. Each rat received 2 weeks of training before surgery. All rats were subjected to walk/run with no incline at a treadmill speed of 10 m/min continuously, 30 min/day, for 5 days/week during 10 consecutive weeks. Training was performed on a specially constructed treadmill for rodents developed in our laboratory with a 10-lane motor-driven conveyer belt with adjustable speed and inclination. Biomechanical analysis of rat walk was performed every 2 weeks on a purpose-developed walkway integrating two miniature force plates and a motion capture system with four high-speed Oqus cameras (Qualysis Systems).

REFERENCES

1. Rodrigues JM, Luís AL, Lobato JV, Pinto MV, Faustino A, Hussain NS, et al. Intracellular Ca2+ concentration in the N1E-115 neuronal cell line and its use for peripheric nerve regeneration. [Internet]. Acta médica portuguesa. 2005 ;18(5):323-8.
2. Rodrigues JM, Luís AL, Lobato JV, Pinto MV, Lopes MA, Freitas M, et al. Determination of the intracellular Ca2+ concentration in the N1E-115 neuronal cell line in perspective of its use for peripheric nerve regeneration. [Internet]. Biomedical materials and engineering. 2005 Jan ;15(6):455-65.
3. Luis A, Amado S, Geuna S, Rodrigues J, Simoes M, Santos JD, et al. Long-term functional and morphological assessment of a standardized rat sciatic nerve crush injury with a non-serrated clamp [Internet]. Journal of neuroscience methods. 2007 ;16392–104.
4. Luis AL, Rodrigues JM, Amado S, Veloso AP, Armada-Da-silva PAS, Raimondo S, et al. PLGA 90/10 and caprolactone biodegradable nerve guides for the reconstruction of the rat sciatic nerve [Internet]. Microsurgery. 2007 ;27(2):125–137.
5. Luís AL, Amado S, Geuna S, Rodrigues JM, Simões MJ, Santos JD, et al. Long-term functional and morphological assessment of a standardized rat sciatic nerve crush injury with a non-serrated clamp. [Internet]. Journal of neuroscience methods. 2007 Jun ;163(1):92-104.
6. Schmidt CE, Leach JB. Neural tissue engineering: strategies for repair and regeneration. [Internet]. Annual review of biomedical engineering. 2003 Jan ;5293-347.
7. Lundborg G, Dahlin L, Danielsen N, Zhao Q. Trophism, tropism, and specificity in nerve regeneration. [Internet]. Journal of reconstructive microsurgery. 1994 Sep ;10(5):345-54.
8. Frykman GK, McMillan PJ, Yegge S. A review of experimental methods measuring peripheral nerve regeneration in animals. [Internet]. The Orthopedic clinics of North America. 1988 Jan ;19(1):209-19.
9. Mackinnon SE, Hudson AR, Hunter DA. Histologic assessment of nerve regeneration in the rat. [Internet]. Plastic and reconstructive surgery. 1985 Mar ;75(3):384-8.
10. Sinis N, Schaller H-E, Becker ST, Lanaras T, Schulte-Eversum C, Müller H-W, et al. Cross-chest median nerve transfer: a new model for the evaluation of

nerve regeneration across a 40 mm gap in the rat. [Internet]. Journal of neuroscience methods. 2006 Sep 30;156(1-2):166-72.

11. Papalia I, Tos P, Scevola A, Raimondo S, Geuna S. The ulnar test: a method for the quantitative functional assessment of posttraumatic ulnar nerve recovery in the rat. [Internet]. Journal of neuroscience methods. 2006 Jun 30;154(1-2):198-203.
12. Varejão ASP, Cabrita AM, Geuna S, Patrício J a, Azevedo HR, Ferreira AJ, et al. Functional assessment of sciatic nerve recovery: biodegradable poly (DLLA-epsilon-CL) nerve guide filled with fresh skeletal muscle. [Internet]. Microsurgery. 2003 Jan ;23(4):346-53.
13. Nichols CM, Myckatyn TM, Rickman SR, Fox IK, Hadlock T, Mackinnon SE. Choosing the correct functional assay: a comprehensive assessment of functional tests in the rat. [Internet]. Behavioural brain research. 2005 Sep ;163(2):143-58.
14. Sedý J, Urdzíková L, Jendelová P, Syková E. Methods for behavioral testing of spinal cord injured rats. [Internet]. Neuroscience and biobehavioral reviews. 2008 Jan ;32(3):550-80.
15. Varejão ASP, Cabrita AM, Meek MF, Bulas-Cruz J, Melo-Pinto P, Raimondo S, et al. Functional and morphological assessment of a standardized rat sciatic nerve crush injury with a non-serrated clamp. [Internet]. Journal of neurotrauma. 2004 Nov ;21(11):1652-70.
16. Perry J. Gait analysis: Normal and Pathological Function. SLACK Incorporated; 1992.
17. Basso DM, Beattie MS, Bresnahan JC. A sensitive and reliable locomotor rating scale for open field testing in rats. [Internet]. Journal of neurotrauma. 1995 Feb ;12(1):1-21.
18. Basso DM. Experimental Spinal Cord Injury : Implications of Basic Science Research for Human Spinal Cord Injury. 2000 ;80(8):808 - 817.
19. Medinaceli L de, Freed WJ, Wyatt RJ. An index of the functional condition of rat sciatic nerve based on measurements made from walking tracks. [Internet]. Experimental neurology. 1982 Sep ;77(3):634-43.
20. Yu P, Matloub HS, Sanger JR, Narini P. Gait analysis in rats with peripheral nerve injury. [Internet]. Muscle & nerve. 2001 Feb ;24(2):231-9.
21. Meek MF, Den Dunnen WF, Schakenraad JM, Robinson PH. Long-term evaluation of functional nerve recovery after reconstruction with a thin-walled biodegradable poly (DL-lactide-epsilon-caprolactone) nerve guide, using walking

track analysis and electrostimulation tests. [Internet]. Microsurgery. 1999 Jan ;19(5):247-53.

22. Bervar M. Video analysis of standing--an alternative footprint analysis to assess functional loss following injury to the rat sciatic nerve. [Internet]. Journal of neuroscience methods. 2000 Oct ;102(2):109-16.
23. Robertson GM, Hamill J, Caldwell G, Kamen G, Whittlesey S. Research Methods in Biomechanics [Internet]. Human Kinetics Publishers; 2004.
24. Higgins S. Movement as an emergent form: Its structural limits [Internet]. Human Movement Science. 1985 Jun ;4(2):119-148.
25. Santos PM, Williams SL, Thomas SS. Neuromuscular evaluation using rat gait analysis. [Internet]. Journal of neuroscience methods. 1995 ;61(1-2):79-84.
26. Lin FM, Pan YC, Hom C, Sabbahi M, Shenaq S. Ankle stance angle: a functional index for the evaluation of sciatic nerve recovery after complete transection. [Internet]. Journal of reconstructive microsurgery. 1996 Apr ;12(3):173-7.
27. Varejão ASP, Cabrita AM, Meek MF, Bulas-Cruz J, Gabriel RC, Filipe VM, et al. Motion of the foot and ankle during the stance phase in rats. [Internet]. Muscle & nerve. 2002 Nov ;26(5):630-5.
28. Varejão ASP, Cabrita AM, Meek MF, Bulas-Cruz J, Filipe VM, Gabriel RC, et al. Ankle kinematics to evaluate functional recovery in crushed rat sciatic nerve [Internet]. Muscle & nerve. 2003 ;27(6):706–714.
29. Ruiter GC de, Spinner RJ, Alaid AO, Koch AJ, Wang H, Malessy MJ a, et al. Two-dimensional digital video ankle motion analysis for assessment of function in the rat sciatic nerve model. [Internet]. Journal of the peripheral nervous system : JPNS. 2007 Sep ;12(3):216-22.
30. Luís AL, Rodrigues JM, Geuna S, Amado S, Simões MJ, Fregnan F, et al. Neural cell transplantation effects on sciatic nerve regeneration after a standardized crush injury in the rat. [Internet]. Microsurgery. 2008 Jan ;28(6):458-70.
31. Luís AL, Rodrigues JM, Geuna S, Amado S, Shirosaki Y, Lee JM, et al. Use of PLGA 90:10 scaffolds enriched with in vitro-differentiated neural cells for repairing rat sciatic nerve defects. [Internet]. Tissue engineering. Part A. 2008 Jun ;14(6):979-93.
32. Canu M-H, Garnier C. A 3D analysis of fore- and hindlimb motion during overground and ladder walking: comparison of control and unloaded rats. [Internet]. Experimental neurology. 2009 Jul ;218(1):98-108.

33. Canu M-H, Garnier C, Lepoutre F-X, Falempin M. A 3D analysis of hindlimb motion during treadmill locomotion in rats after a 14-day episode of simulated microgravity. [Internet]. Behavioural brain research. 2005 Feb ;157(2):309-21.
34. Ruiter GCW de, Malessy MJ a, Alaid AO, Spinner RJ, Engelstad JK, Sorenson EJ, et al. Misdirection of regenerating motor axons after nerve injury and repair in the rat sciatic nerve model. [Internet]. Experimental neurology. 2008 Jun ;211(2):339-50.
35. Masters DB, Berde CB, Dutta SK, Griggs CT, Hu D, Kupsky W, et al. Prolonged regional nerve blockade by controlled release of local anesthetic from a biodegradable polymer matrix. [Internet]. Anesthesiology. 1993 Aug ;79(2):340-6.
36. Thalhammer JG, Vladimirova M, Bershadsky B, Strichartz GR. Neurologic Evaluation of the Rat during Sciatic Nerve Block with Lidocaine [Internet]. Anesthesiology. 1995 Apr ;82(4):1013-1025.
37. Sherrington CS. Flexion-reflex of the limb, crossed extension-reflex, and reflex stepping and standing. [Internet]. The Journal of physiology. 1910 Apr ;40(1-2):28-121.
38. Schouenborg J, Holmberg H, Weng HR. Functional organization of the nociceptive withdrawal reflexes. II. Changes of excitability and receptive fields after spinalization in the rat. [Internet]. Experimental brain research. Experimentelle Hirnforschung. Expérimentation cérébrale. 1992 Jan ;90(3):469-78.
39. Geuna S, Gigo-Benato D, Rodrigues A de C. On sampling and sampling errors in histomorphometry of peripheral nerve fibers. [Internet]. Microsurgery. 2004 Jan ;24(1):72-6.
40. Torch S, Usson Y, Saxod R. Automated morphometric study of human peripheral nerves by image analysis. [Internet]. Pathology, research and practice. 1989 Nov ;185(5):567-71.
41. Yuan Y, Zhang P, Yang Y, Wang X, Gu X. The interaction of Schwann cells with chitosan membranes and fibers in vitro. [Internet]. Biomaterials. 2004 Aug ;25(18):4273-8.
42. Wang W, Itoh S, Matsuda A, Ichinose S, Shinomiya K, Hata Y, et al. Influences of mechanical properties and permeability on chitosan nano/microfiber mesh tubes as a scaffold for nerve regeneration. [Internet]. Journal of biomedical materials research. Part A. 2008 Feb ;84(2):557-66.

43. Chandy T, Sharma CP. Chitosan--as a biomaterial. [Internet]. Biomaterials, artificial cells, and artificial organs. 1990 Jan ;18(1):1-24.
44. Shirosaki Y, Tsuru K, Hayakawa S, Osaka A, Lopes MA, Santos JD, et al. In vitro cytocompatibility of MG63 cells on chitosan-organosiloxane hybrid membranes. [Internet]. Biomaterials. 2005 Feb ;26(5):485-93.
45. Yamaguchi I, Itoh S, Suzuki M, Osaka A, Tanaka J. The chitosan prepared from crab tendons: II. The chitosan/apatite composites and their application to nerve regeneration. [Internet]. Biomaterials. 2003 Aug ;24(19):3285-92.
46. Mackinnon SE, Dellon AL, O'Brien JP. Changes in nerve fiber numbers distal to a nerve repair in the rat sciatic nerve model. [Internet]. Muscle & nerve. 1991 Nov ;14(11):1116-22.
47. Dellon AL, Mackinnon SE. Selection of the appropriate parameter to measure neural regeneration. [Internet]. Annals of plastic surgery. 1989 Sep ;23(3):197-202.
48. Marqueste T, Alliez J-R, Alluin O, Jammes Y, Decherchi P. Neuromuscular rehabilitation by treadmill running or electrical stimulation after peripheral nerve injury and repair. [Internet]. Journal of applied physiology (Bethesda, Md. : 1985). 2004 May ;96(5):1988-95.
49. Senel S, McClure SJ. Potential applications of chitosan in veterinary medicine. [Internet]. Advanced drug delivery reviews. 2004 Jun ;56(10):1467-80.

Chapter 2 – Methodological considerations

1 Animals

During this chapter we will describe the methods used for the following chapters.
Experiments were performed in rats (Wistar or Sprague-Dawley) weighing 250-300g (Charles River Laboratories, Barcelona, Spain). Animals were housed for 2 weeks before entering the experiment and experimental groups were defined with six or eight animals each depending on the study. Two animals were housed per cage (Makrolon type 4, Tecniplast, VA, Italy), in a temperature and humidity controlled room with 12-12h light / dark cycles, and were allowed normal cage activities under standard laboratory conditions. The animals were fed with standard chow and water *ad libitum*. Adequate measures were taken to minimize pain and discomfort taking into account human endpoints for animal suffering and distress. Moreover, after surgical intervention cage environment was enriched for all animals with the goal of minimize stress.
All procedures were performed with the approval of the Veterinary Authorities of Portugal in accordance with the European Communities Council Directive of November 1986 (86/609/EEC).

Injury	Group	n	Intervention	Follow-up (weeks)
Axonotmesis	1	6	Chitosan Type II	12
	2	6	Chitosan Type II + neural cells	12
	3	6	Chitosan Type III	12
	4	6	Chitosan Type III + neural cells	12
	5	6	Control Axonotmesis	12
Neurotmesis	6	6	Control End-to-End	20
	7	6	End-to-End + collagen memb.	20
	8	6	End-to-End + collagen memb	20
Axonotmesis	9	8	Control "Sham"	12
	10	8	Control Axonotmesis	12
	11	8	Active Exercise	12
	12	8	Passive Exercice	12

Handling

The handling was performed to familiarize animals with the experimenter, with the environment in which the studies would be performed, and with the manipulations involved in the neurologic evaluation. This familiarization minimizes the stress-response during the experimental period. The experimental animals were observed for exploratory activity, and the latency of grooming was everyday monitored.

2 Microsurgical procedures

Our experimental work, concerning the *in vivo* testing of neurotmesis and axonotmesis injury and regeneration, was based on the use of Sasco Sprague-Dawley rat sciatic nerve. Usually, the surgeries are performed under an M-650 operating microscope (Leica Microsystems, Wetzlar, Germany). Under deep anaesthesia (ketamine 9 mg/100 g; xylazine 1.25 mg/100 g, atropine 0.025 mg/100 body weight, intramuscular), the right sciatic nerve is exposed through a skin incision extending from the greater trochanter to the distal mid-half followed by a muscle splitting incision. After nerve mobilisation, a transection injury is performed (neurotmesis) using straight microsurgical scissors. The nerve must be injured at a level as low as possible, in general, immediately above the terminal nerve ramification. For neurotmesis without gap, the nerve is reconstructed with an end-to-end suture, with two epineural sutures using de 7/0 monofilament nylon. For axonotmesis we used a standardized clamping procedure that was described in details in previous works (1-4). After nerve mobilisation, a non-serrated clamp (Institute of Industrial Electronic and Material Sciences, University of Technology, Vienna, Austria) exerting a constant force of 54 N, was used for a period of 30 seconds to create a 3-mm-long crush injury, 10 mm above the bifurcation into tibial and common peroneal nerves (4; 5). The starting diameter of the sciatic nerve was about 1 mm, flattening during the crush to 2 mm, giving a final pressure of $p = 9$ MPa. The nerves were kept moist with 37ºC sterile saline solution throughout the surgical intervention. Finally the skin and subcutaneous tissues are closed with a simple-interrupted suture of a non-absorbable filament (Synthofil®, Ethicon). An antibiotic (enrofloxacin, Alsir® 2.5 %, 5 mg / kg b.w., subcutaneously) is always administered to prevent any infections. To prevent autotomy a deterrent substance must be applied to rats' right foot (6; 7). All procedures must be performed with the approval of the Veterinary Authorities of Portugal in accordance with the European Communities Council Directive of November 1986 (86/609/EEC).

3 Methods for Functional Assessment of Reinnervation

Biomechanical model - Kinematic analysis

The first step to perform a biomechanical analysis of body motion is the definition of a mechanical rigid body model that is an idealized form of simplification the structural differences of bones and represents a system. The definition of the numbers of body segments is dependent on the movement that we want to analyze. To study ankle joint movement during locomotion, we defined two rigid bodies: foot and shank.
Considering the computational setting used, to be possible to detect an object/body moving, it must recognize the body that moves within a recognized and well-defined area. Therefore, we have to define the 1) segments of the body we want to evaluate; 2) the reference system;
Motion analysis software provides time-dependent quantitative data, which can be obtained from stick figures or from volumetric models representing the animal body.

- Digital video images record

Animals walked on a Perspex track with length, width and height of respectively 120, 12, and 15 cm (Figure 1). In order to ensure locomotion in a straight direction, the width of the apparatus was adjusted to the size of the rats during the experiments, and a darkened cage was connected at the end of the corridor to attract the animals. The rats' gait was video recorded at a rate of 100 Hz images per second (JVC GR-DVL9800, New Jersey, USA). The camera was positioned at the track half-length where gait velocity was steady, and 1 m distant from the track obtaining a visualization field of 14 cm wide. Reference system was defined with four points to perform the area: 0.03m x0.015m.
Only walking trials with stance phases lasting between 150 and 400 ms were considered for analysis, since this corresponds to the normal walking velocity of the rat (20–60 cm/s) (8; 9).

- Digital video images analysis - Two-dimensional joint kinematic analysis

The video images were stored in a computer hard disk for latter analysis using an appropriate software APAS® (Ariel Performance Analysis System, Ariel Dynamics, San Diego, USA). Image data were trimmed using APAS-Trimmer: five frames before Initial contact of the fingers on the floor and five after Toe Off. Data were digitized manually

(APAS-Digitize and -Transform) to perform image representation and filtered with low pass digital filter at 6 Hz (APAS filter) to determine coordinates for skin landmarks; and to obtain kinematic parameters of angular displacement and velocity of joint using DLT (Direct linear transformation) by Abdel-Aziz and Karara (1971). 2-D biomechanical analysis (sagital plan) was carried out applying a two-segment model of the ankle joint, adopted from the model firstly developed by Varejão and co-workers (9). Skin landmarks were tattooed at 3 points: the proximal edge of the tibia, the lateral malleolus and, the fifth metatarsal head (Figure 2). The definition of the segments foot and shank was performed manually with digitalization of these points after selecting the total frames that fulfilled the stance phase (Figure 3). The rats' ankle angle was determined using the scalar product between a vector representing the foot and a vector representing the lower leg. Four complete walking cycles were analysed per rat. With this model, positive and negative values of position of the ankle joint indicate dorsiflexion and plantarflexion, respectively. For each stance phase the following time points were identified (Figure 4): initial contact (IC), opposite toe-off (OT), heel-rise (HR) and toe-off (TO) (10; 11), and were time normalized for 100% of the stance phase. The normalized temporal parameters were averaged over all recorded trials. Angular ankle's velocity was also determined (negative values correspond to dorsiflexion).

Figure 1- Track where animals walked, (Perspex 120cm length, 12cm width, and 15cm height)

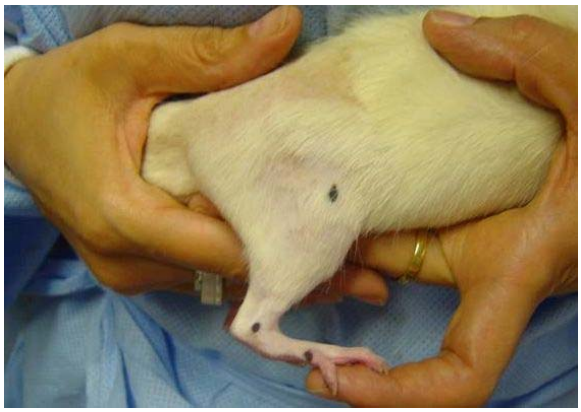

Figure 2 - Skin landmarks were tattooed at 3 points: the proximal edge of the tibia, the lateral malleolus and, the fifth metatarsal head

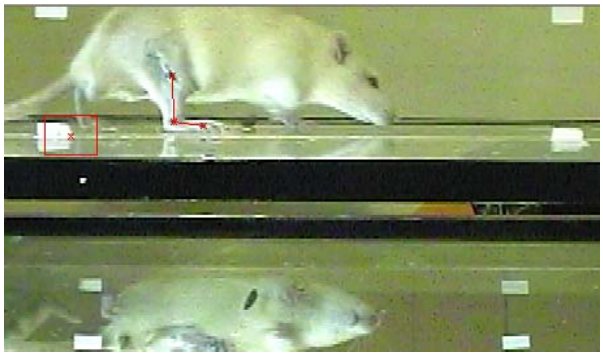

Figure 3 - Video image of the stance phase of rats locomotion

Figure 4 - Time points during stance phase: initial contact (IC), opposite toe-off (OT), heel-rise (HR) and toe-off (TO)

- Motion capture - Optoelectronic system

With technical advances in computer science and the continuous development of mathematical models, biomechanical modeling has improved. Optoelectronic system of infrared cameras (Oqus-300, Qualisys, Sweden) operating at a frame rate of 200Hz tracks the motion of small reflective markers placed on the hindlimb using two infra-red video cameras and has been used to quantify locomotor motion. To obtain three-dimensional co-ordinate data for a marker, two cameras must record the marker

position in space. Image-processing software identified the marker locations in each two-dimensional infra-red camera image to compute its three-dimensional location relative to a calibration plate that was positioned in the data collection corridor. Two additional cameras can be used to ensure that data from at least two cameras is always recorded. Prior to recording movements, the cameras must be calibrated by way of an object with an array of markers whose positions in space are certified to a known accuracy. Motion capture (MOCAP) allows the assessment of the instantaneous positions of markers located on the surface of the skin and, thus, a kinematics analysis of movement. Passive marker based systems use markers coated with a retroreflective material to reflect light back that is generated near the cameras lens. The camera's threshold can be adjusted so only the bright reflective markers will be sampled. We used an optoelectronic system of six infrared cameras (Oqus-300, Qualisys, Sweden) operating at a frame rate of 200Hz was used to record the motion of right hindlimb during the gait cycle. A new corridor was conceptualized and constructed with force platform system with four load cells (two for vertical force component and two for anterior-posterior force component) (Figure 5). Animals walked on a Perspex track with length, width and height of respectively 120, 12 and 15cm. Two darkened cages were connected at the extremities of the corridor to facilitate walking.

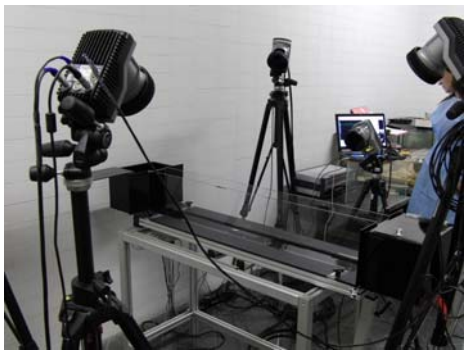

Figure 5 - Set-up of cameras and corridor for motion capture using optoelectronic system

After shaving, seven reflective markers with 2mm diameter were attached to the right hindlimb at bony prominences (Figure 6): 1) tip of fourth finger, 2) head of fifth metatarsal, 3) lateral malleolus, 4) lateral knee joint, 5) trochanter major, 6) anterior superior iliac spine, and 7) ischial tuberosity. The same operator placed all markers and the rat was maintained static in a similar position to the walking position with the aim of minimizing the error introduced by the mobility of skin in relation to the bony references. All rats previously performed two or three conditioning trials to be familiarized with the corridor. Initial trials are often rejected because rats stop or rise on

their hindlimbs to explore the track. Sometimes another rat was placed inside the cage to encourage the trial rat to walk along the track toward it. Cameras were positioned to minimize light reflection artifacts and to allow recording 4-5 consecutive walking cycles, defined as the time between two consecutive initial ground contacts (IC) of the right fourth finger. The motion capture space was calibrated regularly using a fixed set of markers and a wand of known length (20 cm) moved across the recorded field. Calibration was accepted when the standard deviation of wand's length measure was below 0.4 mm.

Figure 6 - Reflective markers with 2mm diameter were attached to the right hindlimb at bony prominences: (1) tip of fourth finger, (2) head of fifth metatarsal, (3) lateral malleolus, (4) lateral knee joint, (5) trochanter major, (6) anterior superior iliac spine, and (7) ischial tuberosity and three non-colinear markers.

- Motion analysis - Two-dimensional joint kinematic analysis

In chapters 5 and 6, the kinematic analysis was performed with Visual3D software.

An absolute reference system (ARS), direction of lab co-ordinate, was defined: a right-handed orthogonal triad <X, Y, Z> fixed in the track ground. Each of the axes is defined as: +X axis pointing rightward, +Y axis pointing anteriorly and +Z axis pointing upward. Additionally, a segmental reference system (SRS) is defined. This system uses Cartesian coordinates fixed to the rigid body and also has clear anatomical meanings such as proximal-distal, lateral-medial and anterior-posterior.

A gait cycle was defined as the time interval between two consecutive IC of the right fifth metatarsal. The definition of a static position as a reference frame to define the position of the segments was conventionally at TO event (Figure 7). Time events (IC and TO) were detected manually during a first trial by analysing coordinate data from head of fifth metatarsal marker. IC was defined when the data values became constant, and TO when data values increased, with visual inspection of the movement. The axis considered for analysis was that of the direction of locomotion. After the definition of the event on the first cycle, it was applied a target pattern recognition for others trials of the same group.

Six walking cycles were analyzed for each animal. Temporal parameters were normalized to the total duration of the gait cycle. A spline interpolation (performing a least-squares fit of a 3rd order polynomial to 10 points) and a 2nd order Butterworth lowpass filter (cut-off frequency of 6Hz, determined by analysis of the difference residuals between filtered and non-filtered data (12) were applied to the original marker coordinates data. Joint angle and joint angular velocity were calculated by dot product and first derivative of joint angle, respectively, between adjacent segments: shank and foot for ankle joint; shank and thigh for the knee joint; thigh and pelvis for the hip joint.

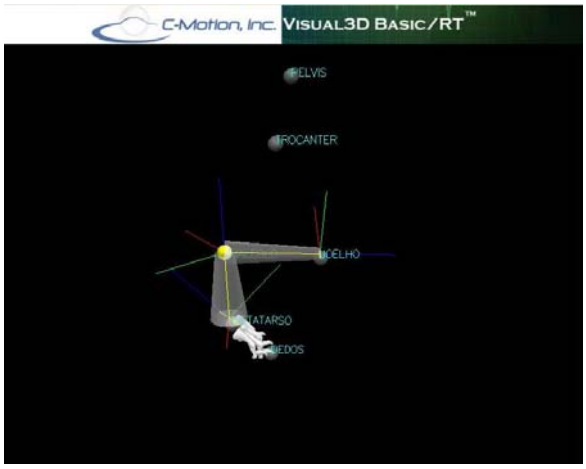

Figure 7 - Reference frame to define the position of the segments, conventionally at TO event.

Sciatic Functional Index (SFI) and Static Sciatic Index (SSI)

For SFI, animals were tested in a confined walkway measuring 42-cm-long and 8.2-cm-wide, with a dark shelter at the end. A white paper was placed on the floor of the rat walking corridor. The hindpaws of the rats were pressed down onto a finger paint-soaked sponge, and they were then allowed to walk down the corridor leaving its hind footprints on the paper (Figure 8). Often, several walks were required to obtain clear print marks of both feet. Prior to any surgical procedure, all rats were trained to walk in the corridor, and a baseline walking track was recorded. Subsequently, walking tracks were recorded every week until the week-8 postoperatively and then on weeks 10 and 12 or on weeks 16 and 20 for axonotmesis and neurotemesis injury, respectively.

Figure 8 - Paint-soaked sponge and corridor where rats leave its hind footprints on the paper (13).

Several measurements were taken from the footprints (Figure 9): (I) distance from the heel to the third toe, the print length (PL); (II) distance from the first to the fifth toe, the toe spread (TS); and (III) distance from the second to the fourth toe, the intermediary toe spread (ITS). For both dynamic (SFI) and static assessment (SSI), all measurements were taken from the experimental (E) and normal (N) sides. Prints for measurements were chosen at the time of walking based on clarity and completeness at a point when the rat was walking briskly. The mean distances of three measurements were used to calculate the following factors (dynamic and static):

Toe spread factor (TSF) = (ETS – NTS)/NTS

Intermediate toe spread factor (ITSF) = (EITS – NITS)/NITS

Print length factor (PLF) = (EPL – NPL)/NPL

Where the capital letters E and N indicate injured (experimental) and non-injured side (normal), respectively.

SFI was calculated as described by (14) according to the Equation 1:

SFI = -38.3 (EPL – NPL)/NPL + 109.5(ETS-NTS)/NTS + 13.3(EIT-NIT)/NIT – 8.8 = (-38.3 x PLF) + (109.5 x TSF) + (13.3 x ITSF) – 8.8

Equation 1 - SFI

Static footprints were obtained at least during four occasional rest periods. For the sciatic static index (SSI) only the parameters TS and ITS, were measured (15) (Equation 2).

SSI = [(108.44 x TSF) + (31.85 x ITSF)] - 5.49

Equation 2 – SSI

Normal(N) Experimental(E)

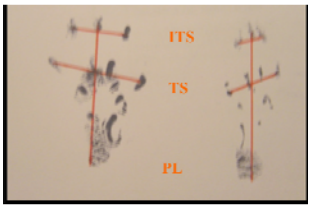

Figure 9 - Measurements from the footprints: (PL) distance from the heel to the third toe, the print length; (TS) distance from the first to the fifth toe, the toe spread; and (ITS) distance from the second to the fourth toe, the intermediary toe spread (13)**.**

For both SFI and SSI, an index score of 0 is considered normal and an index of -100 indicates total impairment. When no footprints were measurable, the index score of -100 was given (11). Reproducible walking tracks could be measured from all rats. In each walking track three footprints were analysed by a single observer, and the average of the measurements was used in SFI calculations.

Extensor Postural Thrust (EPT) - Motor reflex function

The Extensor Postural Trust was originally proposed by Thalhammer and collaborators, (17) as a part of the neurological recovery evaluation in the rat after sciatic nerve injury. For EPT test, the entire body of the rat, except the hindlimbs, was wrapped in a surgical towel and supported by the thorax (Figure 10). The affected hindlimb was then lowered towards the platform of a digital balance (model PLS 510-3, Kern & Sohn GmbH, Kern, Germany) to elicit the EPT. As the animal was lowered over the platform, it extended the hindlimb, anticipating the contact made by the distal metatarsus and digits. The force in grams applied to the digital platform balance was recorded (digital scale range 0-500 g). The reduction in this force, representing reduced extensor muscle tone, was considered a deficit of motor function. The same procedure was applied to the contra-lateral, unaffected limb. The affected and normal limbs were tested 3 times, with an interval of 2 minutes between consecutive tests, and the three values were averaged to obtain a final result. The normal (unaffected limb) EPT (NEPT) and experimental EPT (EEPT) values were incorporated into an equation Equation **(11)** to derive the percentage of functional deficit, as described in the literature by (16):

% Motor deficit = [(NEPT – EEPT)/NEPT] x 100

Equation (11) **- EPT**

Figure 10 - Extensor Postural Thrust (13)

Withdrawal Reflex Latency - Nociception

The rat was wrapped in a surgical towel above its waist and then positioned to stand with the affected hindpaw on a hotplate at 56ºC (Figure 12) (model 35-D; IITC Life Science Instruments, Woodland Hill, CA). WRL is defined as the time elapsed from the onset of hotplate contact to withdrawal of the hindpaw (Figure 11) and measured with a stopwatch. Normal rats withdraw their paws from the hotplate within 4 seconds or less (18). The affected limbs were tested three times, with an interval of 2 minutes between consecutive tests to prevent sensitization, and the three latency times were averaged to obtain a final result (19; 20). The cut off time for heat stimulation was set at 12 seconds to avoid skin damage to the foot (3; 21).

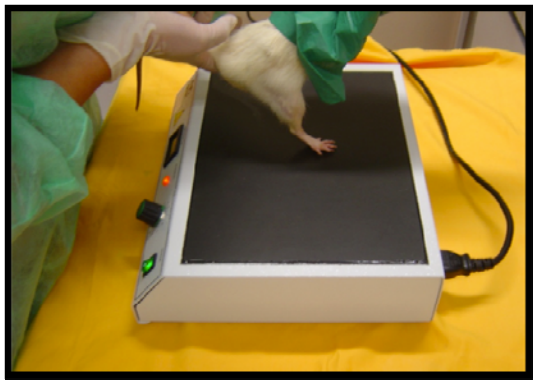

Figure 11 – WRL test (13)**.**

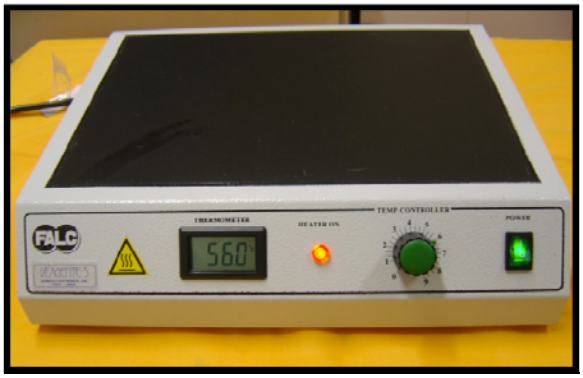

Figure 12 - Hotplate for WRL test (13)

4 Morphological Evaluation

Design-based quantitative morphology and electron microscopy

After the follow-up time, rats were anaesthetised and a 10-mm-long segment of the sciatic nerve that included the injured portion was collected, fixed, and prepared for morphological analysis and histomorphometry of myelinated nerve fibers. A 10-mm segment of uninjured sciatic nerve was also withdrawn from the control animals. Immediately after collecting the nerve, rats were euthanized through an intracardiac injection of 5% sodium pentobarbital (Eutasil®). Sciatic nerve samples were immersed immediately in a fixation solution, containing 2.5% purified glutaraldehyde and 0.5% saccarose in 0.1M Sorensen phosphate buffer for 6-8 hours. Specimens were then washed in a solution containing 1.5% saccarose in 0.1M Sorensen phosphate buffer, post-fixed in 2% osmium tetroxide, dehydrated and embedded in Glauerts' embedding mixture of resins consisting in equal parts of Araldite M and the Araldite Härter, HY 964 (Merck, Darmstad, Germany), to which was added 1-2% of the accelerator 964, DY 064 (Merck, Darmstad, Germany). The plasticizer dibutyl phthalate was added in a quantity of 0.5% (19; 20). Series of 2-µm thick semi-thin transverse sections were cut using a Leica Ultracut UCT ultramicrotome (Leica Microsystems, Wetzlar, Germany) and stained by Toluidine blue for 2-3 minutes for high resolution light microscopy examination. In each nerve, histomorphometry was conducted using a DM4000B microscope equipped with a DFC320 digital camera and an IM50 image manager system (Leica Microsystems, Wetzlar, Germany). This system reproduced microscopic images (obtained through a 100x oil-immersion objective) on the computer monitor at a magnification adjusted by a digital zoom. The final magnification was 6600x enabling accurate identification and morphometry analysis of myelinated nerve fibers. One semi-thin section from each nerve was randomly selected and used for the morpho-quantitative analysis. The total cross-sectional area of the nerve was measured and sampling fields were then randomly selected using a protocol previously described (3; 21). Briefly, cross-sectional area of the nerve is divided into various equal geometric fields (usually >15) and then each of these are divided into smaller fields. The first sampling field is randomly selected and then the selection of the next fields was defined through a systematic “jump” process. Possible "edge effects" (i.e. counting a fibre more than once, especially for larger fibres that appear in more than one sampling field) were compensated by employing a two-dimensional dissector procedure, which is based on sampling the "tops" of fibers (22). Briefly, considering a two-dimensional observational field where direction (North/South) is defined and the North top of each

fiber is marked. The top of each fiber represents the point of the shape of the fibre that first intersects the observational field, and since it appears only once, therefore it will be counted only once.

Mean fiber density was calculated by dividing the total number of nerve fibers within the sampling field by its area (N/mm^2). Total fibers number (N) was then estimated by multiplying the mean fiber density by the total cross-sectional area of the whole nerve cross section assuming a uniform distribution of nerve fibers across the entire section. Fiber and axon area were measured and the circle-fitting diameter of fiber (D) and axon (d) were calculated. These data were used to calculate myelin thickness [(D-d)/2], myelin thickness/axon diameter ratio [(D-d)/2d], and fiber/axon diameter ratio (D/d). The precision of the histomorphometry methods was evaluated by calculating the coefficient of error (CE). Regarding quantitative estimates of fiber number, the *CE(n)* was obtained as follows (23; 24):

$$CE(n) = \frac{1}{\sqrt{\Sigma Q'}}$$

Equation 4 - quantitative estimates of fiber number

Where $\Sigma Q'$ is the number of counted fibers in all dissectors.

For size estimates, the coefficient of error was estimated as follows (22):

$$CE(z) = \frac{SEM}{Mean}$$

Equation 5 - coefficient of error

Where SEM = standard error of the mean.

The sampling scheme was designed in order to keep the CE below 0.10, which assures enough accuracy for neuromorphological studies (23; 24).

Transmission electron microscopy

The immunohistochemical technique is based on the use of antibodies that bind specifically to certain cell antigen and thus became visible by fluorescence microscopy or confocal laser. For this it is necessary to use certain fluorophores or fluorescent probes to detect the antigen-antibody complexes. This technique allowed detection of the axon regeneration and possible migration of Schwann cells within the guide tubes or in biomaterials during the regeneration of peripheral nerve (26). By immunhistochemistry, the antibodies used are anti-NF-200kd (antiprotein 200kd neurofilament) and anti-GFAP (anti-glial protein). The first antibody will allow for tracing of regenerating axons and the second, the possible migration of Schwann cells within the guide tubes (27). Nowadays there are a number of antigens available, antigen-antibody affinity, antibody types and methods of assessment and detection. However, it

is necessary that the method is assessed for each particular situation. For optical microscopy, is usually used staining hematoxylin-eosin (28).

For transmission electron microscopy, ultra-thin sections were cut by means of the same ultramicrotome and stained with saturated aqueous solution of uranyl acetate and lead citrate. Ultra-thin sections were analyzed using a JEM-1010 transmission electron microscope (JEOL, Tokyo, Japan) equipped with a Mega-View-III digital camera and a Soft-Imaging-System (SIS, Münster, Germany) for the computerized acquisition of the images.

Scanning electron microscope analysis

The surface morphology of the chitosan membranes was observed under a scanning electron microscope (SEM; JEOL JSM 6301F) equipped with x-ray energy dispersive spectroscopy (EDX) microanalysis capability (Voyager XRMA System, Noran Instruments).

Cell culture, intracellular calcium concentration ($[Ca^{2+}]_i$) measurements and cell adherence assays

N1E-115 cell line is a clone of cells derived from mouse neuroblastoma C-1300 [58] and retains numerous biochemical, physiological, and morphological properties of differentiated neuronal cells in culture [59]. N1E-115 neuronal cells were cultured in poly-l-lisine coated Petri dishes (around 2 x 10^6 cells) on 2 x 2 cm chitosan fragments (chitosan type I, type II and type III) at 37ºC, 5% CO_2 in a humidified atmosphere (Nuaire). Maintenance medium was 89.8% Dulbecco's Modified Eagle's Medium (DMEM) supplemented with glutamine (GlutaMAX; Gibco), 10% fetal bovine serum (FBS, Sigma), and 0.1% penicillin/streptomycin (100000 U/ml penicillin, 10 mg/ml streptomycin; Sigma) and with 0.1% β-amphoterrycin (250 µg/ml, Sigma). The culture medium was changed every 48 hours and the cells were observed daily in an inverted microscope. Before surgery, once N1E-115 cell culture reached approximately 80% confluence, cells were supplied with differentiation medium containing DMSO. The differentiation medium was composed by 95.8% Dulbecco's Modified Eagle's Medium (DMEM) supplemented with glutamine (GlutaMAX; Gibco), 2.5% FBS, 0.1% penicillin/streptomycin (100000 U/ml penicillin, 10 mg/ml streptomycin; Sigma), 0.1% β-amphoterrycin (250 µg/ml, Sigma), and 1.5% DMSO (Sigma). Cell culture viability was assessed by measuring intracellular free calcium concentration ($[Ca^{2+}]_i$). The $[Ca^{2+}]_i$

was measured in Fura-2-AM-loaded cells, through dual wavelength spectrofluorometry as previously described (22; 26). $[Ca^{2+}]_i$ was determined in N1E-115 cell culture before differentiation and 24, 48 and 72 hours after the onset of DMSO-induced differentiation, in order to determine the best period of neural differentiation, before the $[Ca^{2+}]_i$ rise and the initiation of the apoptosis process.

REFERENCES

1. Luís AL, Amado S, Geuna S, Rodrigues JM, Simões MJ, Santos JD, et al. Long-term functional and morphological assessment of a standardized rat sciatic nerve crush injury with a non-serrated clamp. [Internet]. Journal of neuroscience methods. 2007 Jun ;163(1):92-104.
2. Luis AL, Rodrigues JM, Amado S, Veloso AP, Armada-Da-silva PAS, Raimondo S, et al. PLGA 90/10 and caprolactone biodegradable nerve guides for the reconstruction of the rat sciatic nerve [Internet]. Microsurgery. 2007 ;27(2):125–137.
3. Varejão ASP, Cabrita AM, Meek MF, Fornaro M, Geuna S, Giacobini-Robecchi MG. Morphology of nerve fiber regeneration along a biodegradable poly (DLLA-epsilon-CL) nerve guide filled with fresh skeletal muscle. [Internet]. Microsurgery. 2003 Jan ;23(4):338-45.
4. Varejão AS, Melo-Pinto P, Meek MF, Filipe VM, Bulas-Cruz J. Methods for the experimental functional assessment of rat sciatic nerve regeneration. [Internet]. Neurological research. 2004 Mar ;26(2):186-94.
5. Beer GM, Steurer J, Meyer VE. Standardizing nerve crushes with a non-serrated clamp. [Internet]. Journal of reconstructive microsurgery. 2001 Oct ;17(7):531-4.
6. Sporel-Ozakat RE, Edwards PM, Hepgul KT, Savas A, Gispen WH. A simple method for reducing autotomy in rats after peripheral nerve lesions. [Internet]. Journal of neuroscience methods. 1991 Feb ;36(2-3):263-5.
7. Kerns JM, Braverman B, Mathew A, Lucchinetti C, Ivankovich AD. A comparison of cryoprobe and crush lesions in the rat sciatic nerve. [Internet]. Pain. 1991 Oct ;47(1):31-9.
8. Varejão ASP, Cabrita AM, Patricio JA, Bulas-Cruz J, Gabriel RC, Melo-Pinto P, et al. Functional assessment of peripheral nerve recovery in the rat: gait kinematics [Internet]. Microsurgery. 2001 ;21(8):383–388.
9. Varejão ASP, Cabrita AM, Meek MF, Bulas-Cruz J, Filipe VM, Gabriel RC, et al. Ankle kinematics to evaluate functional recovery in crushed rat sciatic nerve [Internet]. Muscle & nerve. 2003 ;27(6):706–714.
10. Varejão ASP, Cabrita AM, Meek MF, Bulas-Cruz J, Gabriel RC, Filipe VM, et al. Motion of the foot and ankle during the stance phase in rats. [Internet]. Muscle & nerve. 2002 Nov ;26(5):630-5.
11. Dijkstra JR, Meek MF, Robinson PH, Gramsbergen A. Methods to evaluate functional nerve recovery in adult rats: walking track analysis, video analysis and

the withdrawal reflex. [Internet]. Journal of neuroscience methods. 2000 Mar ;96(2):89-96.

12. Winter DA. Biomechanics and Motor Control of Human Movement [Internet]. Wiley; 2004.
13. Luis AL. Reparação de lesões do nervo periférico. 2008 Doctoral Thesis; ICBAS-UP.
14. Bain JR, Mackinnon SE, Hunter DA. Functional evaluation of complete sciatic, peroneal, and posterior tibial nerve lesions in the rat. [Internet]. Plastic and reconstructive surgery. 1989 Jan ;83(1):129-38.
15. Bervar M. Video analysis of standing--an alternative footprint analysis to assess functional loss following injury to the rat sciatic nerve. [Internet]. Journal of neuroscience methods. 2000 Oct ;102(2):109-16.
16. Koka R, Hadlock TA. Quantification of functional recovery following rat sciatic nerve transection. [Internet]. Experimental neurology. 2001 Mar ;168(1):192-5.
17. Thalhammer JG, Vladimirova M, Bershadsky B, Strichartz GR. Neurologic Evaluation of the Rat during Sciatic Nerve Block with Lidocaine [Internet]. Anesthesiology. 1995 Apr ;82(4):1013-1025.
18. Hu D, Hu R, Berde CB. Neurologic evaluation of infant and adult rats before and after sciatic nerve blockade. [Internet]. Anesthesiology. 1997 Apr ;86(4):957-65.
19. Shir Y, Campbell JN, Raja SN, Seltzer Z. The correlation between dietary soy phytoestrogens and neuropathic pain behavior in rats after partial denervation. [Internet]. Anesthesia and analgesia. 2002 Feb ;94(2):421-6.
20. Campbell JN. Nerve lesions and the generation of pain. [Internet]. Muscle & nerve. 2001 Oct ;24(10):1261-73.
21. Varejão ASP, Cabrita AM, Geuna S, Patrício J a, Azevedo HR, Ferreira AJ, et al. Functional assessment of sciatic nerve recovery: biodegradable poly (DLLA-epsilon-CL) nerve guide filled with fresh skeletal muscle. [Internet]. Microsurgery. 2003 Jan ;23(4):346-53.
22. Geuna S, Tos P, Battiston B, Guglielmone R. Verification of the two-dimensional disector, a method for the unbiased estimation of density and number of myelinated nerve fibers in peripheral nerves. [Internet]. Annals of anatomy = Anatomischer Anzeiger : official organ of the Anatomische Gesellschaft. 2000 Jan ;182(1):23-34.
23. Geuna S, Gigo-Benato D, Rodrigues A de C. On sampling and sampling errors in histomorphometry of peripheral nerve fibers. [Internet]. Microsurgery. 2004 Jan ;24(1):72-6.

24. Schmitz C. Variation of fractionator estimates and its prediction. [Internet]. Anatomy and embryology. 1998 Nov ;198(5):371-97.
25. Di Scipio F, Raimondo S, Tos P, Geuna S. A simple protocol for paraffin-embedded myelin sheath staining with osmium tetroxide for light microscope observation. [Internet]. Microscopy research and technique. 2008 Jul ;71(7):497-502.
26. Geuna S, Tos P, Guglielmone R, Battiston B, Giacobini-Robecchi MG. Methodological issues in size estimation of myelinated nerve fibers in peripheral nerves. [Internet]. Anatomy and embryology. 2001 Jul ;204(1):1-10.
27. Raimondo S, Fornaro M, Di Scipio F, Ronchi G, Giacobini-Robecchi MG, Geuna S. Chapter 5: Methods and protocols in peripheral nerve regeneration experimental research: part II-morphological techniques. [Internet]. International review of neurobiology. 2009 Jan ;8781-103.
28. Luís AL, Rodrigues JM, Geuna S, Amado S, Simões MJ, Fregnan F, et al. Neural cell transplantation effects on sciatic nerve regeneration after a standardized crush injury in the rat. [Internet]. Microsurgery. 2008 Jan ;28(6):458-70.

Chapter 3 - Use of hybrid chitosan membranes and N1E-115 cells for promoting nerve regeneration in an axonotmesis rat model

Amado S, Simões MJ, Armada da Silva PAS, Luís AL, Shirosaki Y, Lopes MA, et al. Use of hybrid chitosan membranes and N1E-115 cells for promoting nerve regeneration in an axonotmesis rat model. [Internet]. Biomaterials. 2008 Nov; 29(33):4409-19 DOI: 10.1016/j.biomaterials.2008.07.043.

1 Introduction

Peripheral nerve injuries are a frequent pathology in today's society (1). Despite recent progress in peripheral nerve trauma management, recovery of functional parameters is usually far from normal, even for the most skilled surgeons, and thus much attention is being paid to nerve regeneration research (2; 3).

The experimental model based on the induction of a crush injury (axonotmesis) in the rat sciatic nerve provides a very realistic testing bench for lesions involving plurifascicular mixed nerves with axons of different size and type competing to reach and re-innervate distal targets (4; 5). After a lesion of axonotmesis, the distal nerve fragment undergoes a process named Wallerian degeneration, which leads to the degradation of axons and myelin sheaths and creates a favourable environment for nerve regeneration (6-9). Both macrophages and Schwann cells are locally recruited to eliminate axonal and myelin fragments. While distal stump degenerates, the proximal stump initiates the regeneration process - the axonal ends elongate in order to reach the distal stump and Schwann cells differentiate and multiply, being responsible for the ensheathing and myelination of the newly sprouted axons (6; 7; 9-12). This type of injury is thus appropriate to investigate the cellular and molecular mechanisms of peripheral nerve regeneration, to assess the role of different factors in the regeneration process (13) and to perform preliminary *in vivo* testing of biomaterials that will be useful in tube-guide fabrication for more serious injuries of the peripheral nerve, such as neurotmesis.

Autologous nerve grafting is the gold standard to reconstruct a large defect in a peripheral nerve, but with some important disadvantages, such as availability of the donor site and complications related to its sacrifice, inadequate recovery of function and aberrant regeneration (14-21). Nowadays, the use of entubulation has attempted to overcome these problems. A cylinder-shaped tube is placed between the nerve ends, not only allowing orientation of growing nerve fibres, but also enabling the incorporation of substances, either molecules or cells, that enhance nerve regeneration (16; 21; 22). Among the various materials than can be used in the composition of the tube guides, biodegradable substances offer two important advantages: one surgical step is saved, as they avoid the need to be removed as required for autologus tissue transplantation and it is possible to modulate the time of degradation according to the axonal regeneration time diminishing inflammation on the lesion site. Thus, a major challenge in tissue engineering is to create adequate scaffolds that are capable of replace the autografts techniques. As far as peripheral nerve regeneration is

concerned, a wide range of substances have been developed to meet this purpose (16; 21; 25; 26).

There are many properties required for desirable nerve guided conduit. They include permeability that prevents fibrous scar tissue invasion but allow nutrient and oxygen supply, revascularization to improve nutrient and oxygen supply, mechanical strengths to maintain a stable support structure for the nerve regeneration, immunological inertness with surrounding tissues, biodegradability to prevent chronic inflammatory response and pain by nerve compression, easy regulation of conduit diameter and wall thickness, and surgical amenability (26). The degradation rate of these biomaterials should be related to the axonal regeneration time. Among the various substances proposed for the fashioning of nerve conduits, chitosan has recently attracted particular attention because of its biocompatibility, biodegradability, low toxicity, low cost, enhancement of wound-healing and antibacterial effects(27). In addition, the potential usefulness of chitosan in nerve regeneration have been demonstrated both in vitro and in vivo (28-34). Chitosan is a partially deacetylated polymer of acetyl glucosamine obtained after the alkaline deacetylation of chitin (35). Chitosan matrices have been shown to have low mechanical strength under physiological conditions and to be unable to maintain a predefined shape for transplantation, which has limited their use as nerve guidance conduits in clinical applications. The improvement of their mechanical properties can be achieved by modifying chitosan with a silane agent. γ-glycidoxypropyltrimethoxysilane (GPTMS) is one of the silane-coupling agents, which has epoxy and methoxysilane groups. The epoxy group reacts with the amino groups of chitosan molecules, while the methoxysilane groups are hydrolyzed and form silanol groups, and the silanol groups are subjected to the construction of a siloxane network due to the condensation. Thus, the mechanical strength of chitosan can be improved by the crosslinking between chitosan and GPTMS and siloxane network. Chitosan and chitosan-based materials have been proven to promote adhesion, survival, and neurite outgrowth of neural cells (36; 37).

Together with scaffolds, neurotrophic factors have also been the target of intensive research - their role in nerve regeneration and the way they influence neural development, survival, outgrowth, and branching (20). Among neurotrophic factors, neurotrophins have been heavily investigated in nerve regeneration studies. They include the nerve growth factor (NGF), brain-derived neurotrophic factor (BDNF), neurotrophin-3 (NT-3), and neurotrophin-4/5 (NT-4/5)(38). Neurotrophic factors promote a variety of neural responses, including survival and outgrowth of the motor and sensory nerve fibers, and spinal cord regeneration (22; 39). However, *in vivo*

responses to neurotrophic factors can vary due to the method of their delivering. Therefore, the development and use of controlled delivery devices are required for the study of complex systems. N1E-115 cell line that undergoes neuronal differentiation in response to either dimethylsulfoxide (DMSO), adenosine 3’5’-cyclic monophosphate (cAMP) or serum withdrawal is an important cellular system to locally produce and deliver neurotrophic factors (40; 41).

Based on this premises, the aim of the study was to bring together two of the more promising recent trends in nerve regeneration research: 1) local enwrapping of the lesion site of axonotmesis by means of hybrid chitosan membranes; 2) application of a cell delivery system to improve local secretion of neurotrophic factors.

First, types I, II and III chitosan membranes were screened by an *in vitro* assay. Then, membranes were evaluated *in vivo* to assess their biocompatibility and their effects on nerve fiber regeneration and nerve recovery in a standardized rat sciatic nerve crush injury model (42; 43).

2 Materials and methods

2.1 Preparation of chitosan membranes

Chitosan (high molecular weight, Aldrich®, USA) was dissolved in 0.25M acetic acid aqueous solution to a concentration of 2% (w/v). To obtain type II and type III membranes, GPTMS (Aldrich®, USA) was also added to the chitosan solution and stirred at room temperature for 1h. The solutions for type I and II chitosan membranes were then poured into polypropylene containers with cover, and aged at 60°C for 2 days. The drying process for type III chitosan membrane was significantly different: the solutions were frozen for 24h at -20°C and then transferred to the freeze-dryer, where they were left 12h to complete dryness. The chitosan membranes (type I, II and III) were soaked in 0.25N sodium hydroxide aqueous solution to neutralize remaining acetic acid, washed well with distilled water, and dried again at 60°C for 2 days (type I and II) or freeze dried (type III). All membranes were sterilized with ethylene oxide gas, considered by some authors the most suitable method of sterilization for chitosan membranes (44). Prior to their use *in vivo*, membranes were kept during 1 week at room temperature in order to clear any ethylene oxide gas remnants.

Scanning electron microscope analysis

The surface morphology of the chitosan membranes was observed under a scanning electron microscope (SEM; JEOL JSM 6301F) equipped with x-ray energy dispersive spectroscopy (EDX) microanalysis capability (Voyager XRMA System, Noran Instruments).

Cell culture, intracellular calcium concentration ($[Ca^{2+}]_i$) measurements and cell adherence assays

N1E-115 is a clone of cells derived from mouse neuroblastoma C-1300 (45) and retains numerous biochemical, physiological, and morphological properties of differentiated neuronal cells in culture (46). N1E-115 neuronal cells were cultured in poly-l-lisine coated Petri dishes (around 2 x 106 cells) on 2 x 2 cm chitosan fragments (chitosan type I, type II and type III) at 37ºC, 5% CO2 in a humidified atmosphere (Nuaire). Maintenance medium was 89.8% Dulbecco's Modified Eagle's Medium (DMEM) supplemented with glutamine (GlutaMAX; Gibco), 10% fetal bovine serum (FBS, Sigma), 0.1% penicillin/streptomycin (100000 U/ml penicillin, 10 mg/ml

streptomycin; Sigma) and with 0.1% β-amphoterrycin (250 µg/ml, Sigma). The culture medium was changed every 48 hours and the cells were observed daily in an inverted microscope. Before surgery, once N1E-115 cell culture reached approximately 80% confluence, cells were supplied with differentiation medium containing DMSO. The differentiation medium was composed by 95.8% Dulbecco's Modified Eagle's Medium (DMEM) supplemented with glutamine (GlutaMAX; Gibco), 2.5% FBS, 0.1% penicillin/streptomycin (100000 U/ml penicillin, 10 mg/ml streptomycin; Sigma), 0.1% β-amphoterrycin (250 µg/ml, Sigma), and 1.5% DMSO (Sigma). Cell culture viability was assessed by measuring intracellular free calcium concentration ($[Ca^{2+}]_i$). The $[Ca^{2+}]_i$ was measured in Fura-2-AM-loaded cells, through dual wavelength spectrofluorometry as previously described (24). $[Ca^{2+}]_i$ was determined in N1E-115 cell culture before differentiation and 48 hours after the onset of DMSO-induced differentiation.

In vivo assays

All procedures were performed with the approval of the Veterinary Authorities of Portugal in accordance with the European Communities Council Directive of November 1986 (86/609/EEC).

Figure 13 - The picture shows the dorsal incisions made on the dorsal area of the four Wistar rats, to test the biocompatibility of the chitosan membranes: 1 (left cranial incision), type I chitosan membrane; 2 (mid-right incision), type II chitosan membrane; 3 (left caudal incision), type III chitosan membrane

Biocompatibility assay

Prior to their use on crushed sciatic nerves, the three types of chitosan membranes were tested *in vivo* to assess their biocompatibility: 4 adult female Wistar rats were used. On each one, under general anaesthesia, 3 longitudinal dorsal incisions, 3 cm-long, were made and 2 x 2 cm fragments were implanted (Figure 13). Animals were sacrificed on weeks one, two, four and eight. The membrane remnants were collected together with skin and subcutaneous tissues and were fixed in a 10% formaldehyde solution for later histological analysis. Throughout the 8-week follow-up time, all animals remained healthy, and none developed local or systemic signs of infection and/or inflammation.

Nerve regeneration assay

In vivo nerve regeneration assay was carried out in types II and III chitosan membranes only because of the higher elasticity which proved to facilitate surgery. A total of 36 adult female Wistar rats (Charles River Laboratories, Barcelona, Spain) weighing approximately 250g at the start of the experiment were used. The animals were divided by six experimental groups of six animals each. Animals were housed two animals per cage (Makrolon type 4, Tecniplast, VA, Italy), in a temperature and humidity controlled room with 12-12h light / dark cycles, and were allowed normal cage activities under standard laboratory conditions. The animals were fed with standard chow and water *ad libitum*. Adequate measures were taken to minimize pain and discomfort taking into account human endpoints for animal suffering and distress. Animals were housed for 2 weeks before entering the experiment. All procedures were performed with the approval from the Veterinary Authorities of Portugal, and in accordance with the European Communities Council Directive of 24 November 1986 (86/609/EEC). The experimental groups were set according to treatment after nerve sciatic crush injury. Therefore, in one group the animals recovered from the sciatic crush injury without any other intervention (*Crush*). In other two groups, the crushed sciatic nerve was encircled by a type II chitosan membrane either alone (*ChitosanII*) or covered with a monolayer of N1E-115 cells, differentiated *in vitro* (*ChitosanIICell*). In the remaining two groups, type III chitosan was used alone (*ChitosanIII*) or covered by N1E-115 cells (*ChitosanIIICell*). Finally, an additional group of unoperated animals was used as control for nerve histological analysis. The standardized crush injury was carried out with the animals placed prone under sterile conditions and the skin from the

clipped lateral right thigh scrubbed in a routine fashion with antiseptic solution. Under deep anaesthesia [ketamine (Imalgene 1000®) 9 mg/100 g; xylazine (Rompun®), 1.25 mg/100 g, atropine 0.025 mg/100 g body weight, IP], the right sciatic nerve was exposed unilaterally through a skin incision extending from the greater trochanter to the mid-thigh followed by a muscle splitting incision. After nerve mobilisation, a non-serrated clamp (Institute of Industrial Electronic and Material Sciences, University of Technology, Vienna, Austria) exerting a constant force of 54 N, was used for a period of 30 seconds to create a 3-mm-long crush injury, 10 mm above the bifurcation into tibial and common peroneal nerves (16; 20). The starting diameter of the sciatic nerve was about 1 mm, flattening during the crush to 2 mm, giving a final pressure of *p*9 MPa. The nerves were kept moist with 37ºC sterile saline solution throughout the surgical intervention. Muscle and skin were then closed with 4/0 resorbable sutures. The surgical procedure was performed with the aid of an M-650 operating microscope (Leica Microsystems, Wetzlar, Germany). To prevent autotomy, a deterrent substance was applied to rats' right foot (21; 25). The animals were intensively examined for signs of autotomy and contracture and none presented severe wounds (absence of a part of the foot or severe infection) or contractures during the study.

2.2 Functional Assessment of Reinnervation

Motor performance and nociceptive function

All animals were tested preoperatively (week 0), and every week until week 8 and then every two weeks until the end of the 12-week follow-up time. Animals were gently handled, and tested in a quiet environment to minimize stress levels. Motor performance and nociceptive function were evaluated by measuring extensor postural thrust (EPT) and withdrawal reflex latency (WRL), respectively. For EPT test, the entire body of the rat, except the hindlimbs, was wrapped in a surgical towel and supported by the thorax. The affected hindlimb was then lowered towards the platform of a digital balance (model PLS 510-3, Kern & Sohn GmbH, Kern, Germany) to elicit the EPT. As the animal was lowered over the platform, it extended the hindlimb, anticipating the contact made by the distal metatarsus and digits. The force in grams applied to the digital platform balance was recorded (digital scale range 0-500 g). The same procedure was applied to the contra-lateral, unaffected limb. The affected and normal limbs were tested 3 times, with an interval of 2 minutes between consecutive tests, and the three values were averaged to obtain a final result. The normal (unaffected limb) EPT (NEPT) and experimental EPT (EEPT) values were incorporated into an equation

Equation 3) to derive the percentage of functional deficit, as described in the literature (27):

% Motor deficit = [(NEPT – EEPT)/NEPT] x 100

Equation 3 – EPT formula

The nociceptive withdrawal reflex (WRL) was adapted from the hotplate test as described by Masters et al. (47). The rat was wrapped in a surgical towel above its waist and then positioned to stand with the affected hindpaw on a hotplate at 56ºC (model 35-D; IITC Life Science Instruments, Woodland Hill, CA). WRL is defined as the time elapsed from the onset of hotplate contact to withdrawal of the hindpaw and measured with a stopwatch. Normal rats withdraw their paws from the hotplate within 4 seconds or less (28). The affected limbs were tested three times, with an interval of 2 minutes between consecutive tests to prevent sensitization, and the three latency times were averaged to obtain a final result (22). The cut off time for heat stimulation was set at 12 seconds to avoid skin damage to the foot (28).

Sciatic Functional Index (SFI) and Static Sciatic Index (SSI)

For SFI, animals were tested in a confined walkway measuring 42-cm-long and 8.2-cm-wide, with a dark shelter at the end. A white paper was placed on the floor of the rat walking corridor. The hindpaws of the rats were pressed down onto a finger paint-soaked sponge, and they were then allowed to walk down the corridor leaving its hind footprints on the paper. Often, several walks were required to obtain clear print marks of both feet. Prior to any surgical procedure, all rats were trained to walk in the corridor, and a baseline walking track was recorded. Subsequently, walking tracks were recorded every week until the week-8 postoperatively and then on weeks 10 and 12. Several measurements were taken from the footprints: (I) distance from the heel to the third toe, the print length (PL); (II) distance from the first to the fifth toe, the toe spread (TS); and (III) distance from the second to the fourth toe, the intermediary toe spread (ITS). For both dynamic (SFI) and static assessment (SSI), all measurements were taken from the experimental (E) and normal (N) sides. Prints for measurements were chosen at the time of walking based on clarity and completeness at a point when the rat was walking briskly. The mean distances of three measurements were used to calculate the following factors (dynamic and static):

Toe spread factor (TSF) = (ETS – NTS)/NTS

Intermediate toe spread factor (ITSF) = (EITS – NITS)/NITS

Print length factor (PLF) = (EPL – NPL)/NPL

Where the capital letters E and N indicate injured (experimental) and non-injured side (normal), respectively.

SFI was calculated as described by Bain et al. (30) according to the following equation Equation 4):

SFI = -38.3 (EPL – NPL)/NPL + 109.5(ETS-NTS)/NTS + 13.3(EIT-NIT)/NIT – 8.8 = (-38.3 x PLF) + (109.5 x TSF) + (13.3 x ITSF) – 8.8

Equation 4- SFI formula

Static footprints were obtained at least during four occasional rest periods. For the sciatic static index (SSI) only the parameters TS and ITS, were measured (31):

SSI = [(108.44 x TSF) + (31.85 x ITSF)] - 5.49

Equation 5 –SSI formula

For both SFI and SSI, an index score of 0 is considered normal and an index of -100 indicates total impairment. When no footprints were measurable, the index score of -100 was given (32). Reproducible walking tracks could be measured from all rats. In each walking track three footprints were analysed by a single observer, and the average of the measurements was used in SFI calculations.

Kinematic analysis

Ankle kinematics and stance duration analysis were carried out prior to nerve injury and on weeks one, four, eight and twelve of recovery. Animals walked on a perspex track with length, width and height of respectively 120, 12, and 15 cm. In order to ensure locomotion in a straight direction, the width of the apparatus was adjusted to the size of the rats during the experiments, and a darkened cage was connected at the end of the corridor to attract the animals. The rats' gait was video recorded at a rate of 100 Hz images per second (JVC GR-DVL9800, New Jersey, USA). The camera was positioned at the track half length where gait velocity was steady, and 1 m distant from the track obtaining a visualization field of 14 cm wide. Only walking trials with stance phases lasting between 150 and 400 ms were considered for analysis, since this corresponds to the normal walking velocity of the rat (20–60 cm/s) (33; 34; 48). The video images were stored in a computer hard disk for latter analysis using an appropriate software APAS® (Ariel Performance Analysis System, Ariel Dynamics, San Diego, USA). 2-D biomechanical analysis (sagittal plan) was carried out applying a two-segment model of the ankle joint, adopted from the model firstly developed by Varejão

et al. (48). Skin landmarks were tattooed at 3 points: the proximal edge of the tibia, the lateral malleolus and, the fifth metatarsal head. The rats' ankle angle was determined using the scalar product between a vector representing the foot and a vector representing the lower leg. Four complete walking cycles were analysed per rat. With this model, positive and negative values of position of the ankle joint indicate dorsiflexion and plantarflexion, respectively. For each stance phase the following time points were identified: initial contact (IC), opposite toe-off (OT), heel-rise (HR) and toe-off (TO) (34; 48), and were time normalized for 100% of the stance phase. The normalized temporal parameters were averaged over all recorded trials. Angular ankle's velocity was also determined (negative values correspond to dorsiflexion).

2.3 Design-based quantitative morphology and electron microscopy

After the 12-week follow-up time, rats were anaesthetised and a 10-mm-long segment of the sciatic nerve that included the injured portion was collected, fixed, and prepared for morphological analysis and histomorphometry of myelinated nerve fibers. A 10-mm segment of uninjured sciatic nerve was also withdrawn from the 6 control animals. Immediately after collecting the nerve, rats were euthanized through an intracardiac injection of 5% sodium pentobarbital (Eutasil®). Sciatic nerve samples were immersed immediately in a fixation solution, containing 2.5% purified glutaraldehyde and 0.5% saccarose in 0.1M Sorensen phosphate buffer for 6-8 hours. Specimens were then washed in a solution containing 1.5% saccarose in 0.1M Sorensen phosphate buffer, post-fixed in 2% osmium tetroxide, dehydrated and embedded in Glauerts' embedding mixture of resins consisting in equal parts of Araldite M and the Araldite Härter, HY 964 (Merck, Darmstad, Germany), to which was added 1-2% of the accelerator 964, DY 064 (Merck, Darmstad, Germany). The plasticizer dibutyl phthalate was added in a quantity of 0.5% [75]. Series of 2-µm thick semi-thin transverse sections were cut using a Leica Ultracut UCT ultramicrotome (Leica Microsystems, Wetzlar, Germany) and stained by Toluidine blue for 2-3 minutes for high resolution light microscopy examination. In each nerve, histomorphometry was conducted using a DM4000B microscope equipped with a DFC320 digital camera and an IM50 image manager system (Leica Microsystems, Wetzlar, Germany). This system reproduced microscopic images (obtained through a 100x oil-immersion objective) on the computer monitor at a magnification adjusted by a digital zoom. The final magnification was 6600x enabling

accurate identification and morphometry analysis of myelinated nerve fibers. One semi-thin section from each nerve was randomly selected and used for the morpho-quantitative analysis. The total cross-sectional area of the nerve was measured and sampling fields were then randomly selected using a protocol previously described (37). Possible "edge effects" were compensated by employing a two-dimensional dissector procedure which is based on sampling the "tops" of fibers (37). Mean fiber density was calculated by dividing the total number of nerve fibers within the sampling field by its area (N/mm^2). Total fibers number (N) was then estimated by multiplying the mean fiber density by the total cross-sectional area of the whole nerve cross section assuming a uniform distribution of nerve fibers across the entire section. Fiber and axon area were measured and the circle-fitting diameter of fiber (D) and axon (d) were calculated. These data were used to calculate myelin thickness [(D-d)/2], myelin thickness/axon diameter ratio [(D-d)/2d], and fiber/axon diameter ratio (D/d). The precision of the histomorphometry methods was evaluated by calculating the coefficient of error (CE). Regarding quantitative estimates of fiber number, the *CE(n)* was obtained as follows in Equation 6 (37):

$$CE(n) = \frac{1}{\sqrt{\Sigma Q'}}$$

Equation 6 - quantitative estimates of fiber number

Where $\Sigma Q'$ is the number of counted fibers in all dissectors.

For size estimates, the coefficient of error was estimated as follows in Equation 7 (36):

$$CE(z) = \frac{SEM}{Mean}$$

Equation 7 - coefficient of error

Where SEM = standard error of the mean.

The sampling scheme was designed in order to keep the CE below 0.10, which assures enough accuracy for neuromorphological studies (49).

For transmission electron microscopy, ultra-thin sections were cut by means of the same ultramicrotome and stained with saturated aqueous solution of uranyl acetate and lead citrate. Ultra-thin sections were analyzed using a JEM-1010 transmission electron microscope (JEOL, Tokyo, Japan) equipped with a Mega-View-III digital camera and a Soft-Imaging-System (SIS, Münster, Germany) for the computerized acquisition of the images.

3 Statistics

Two-way mixed factorial ANOVA was used to test for the effect of time (within subjects effect) and group (between subjects effect). Sphericity was evaluated by the Mauchly's test and when this assumption was not satisfied, the degrees of freedom were corrected by using the more conservative Greenhouse-Geiser's epsilon. Differences between pre-surgery results and those obtained throughout the 12-week recovery period were systematically assessed by applying planned contrasts (General Linear Model, simple contrasts). The effect of the chitosan membrane alone or associated to N1E-115 differentiated cells was then evaluated through two way mixed factorial ANOVA. For histomorphometry, statistical comparisons of quantitative data were subjected to one-way ANOVA test. MANOVA analysis was employed to assess differences in functional recovery between the experimental groups. Statistical significance was established as $p<0.05$. All statistical procedures were performed by using the statistical package SPSS (version 14.0, SPSS, Inc) except histomorphometry data that was analysed using the software "Statistica per discipline bio-mediche" (McGraw-Hill, Milan, Italy). All data in this study is presented as mean ± standard error of the mean (SEM).

4 Results

4.1 *In vitro* results and SEM analysis of chitosan membranes

Results obtained from epifluorescence technique are referred to measurements from non-differentiated N1E-115 cells and after 48h of differentiation in the presence of 1.5% DMSO. The mean value of $[Ca^{2+}]_i$ in non-differentiated N1E-115 cells (N = number of cells submitted to $[Ca^{2+}]_i$ measurement) was 39.9 ± 3.4 nM (N = 15), 35.9 ± 3.2 nM (N = 15) and 40.2 ± 2.9 nM (N = 15), for cultures over chitosan membranes, type I,II and III, respectively. Values of $[Ca^{2+}]_i$ for N1E-115 cells after 48h of differentiation in the presence of 1.5% DMSO were 42.9 ± 5.1 nM (N = 15), 44.3 ± 4.8 nM (N = 15) and 41.6 ± 4.3 nM (N = 15), for cultures over chitosan membranes, type I,II and III, respectively. All these values are not statistically different for $p<0.05$, and correspond to $[Ca^{2+}]_i$ from cells that did not begin the apoptosis process besides the evident neural differentiation. According to this fact, it is reasonable to conclude that chitosan membranes, previously presented as type I, II and III, were a viable substrate for N1E-115 neuronal cell line adhesion, multiplication and differentiation.

Figure 14 shows the SEM microstructure of type II Figure 14A) and type III (Figure 14B) chitosan membranes, respectively. The drying techniques employed to prepare the membranes were freeze-drying (type III) and the conventional thermal drying (type I and type II), which led to extremely dissimilar microstructural and mechanical properties. In this study, the chitosan membranes type III have about 110 μm pores and about 90% of porosity.

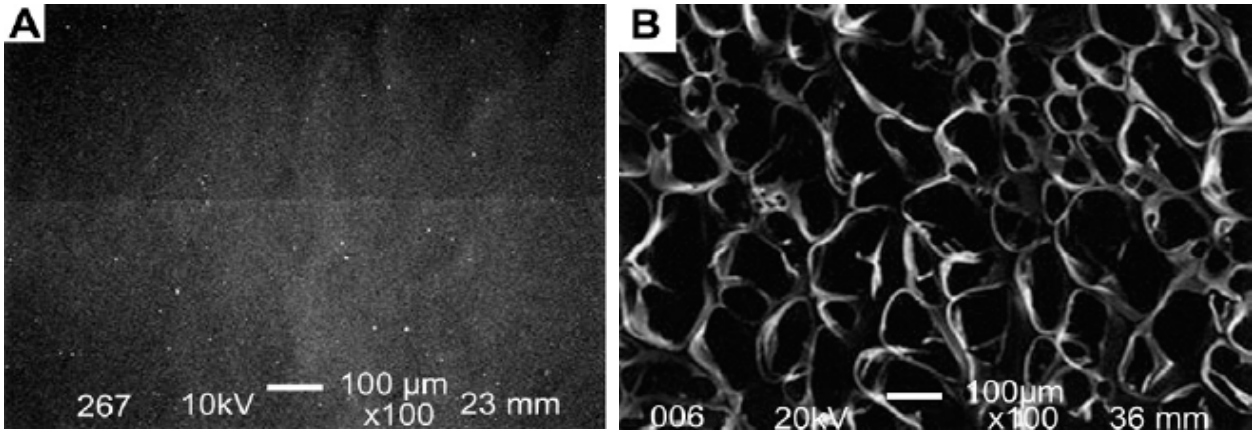

Figure 14 - Scanning electron microscopy microstructure of chitosan membranes. (A) Type II chitosan membrane. (B) Type III chitosan membrane, showing a more porous microstructure, when compared to Type II chitosan membrane

4.2 *In vivo* biocompatibility results

Despite the same composition, type II and type III membranes presented a distinct behavior: the latter elicited an exuberant cellular infiltrate composed in a large extent by multinucleated giant cells and some mast cells, whereas type II chitosan elicited a mild fibrous capsule and a discrete inflammatory reaction. Type III chitosan membranes underwent a completely different aging process, the so called freeze drying. This lyophilisation procedure resulted in highly porous membranes: after freezing and lyophilisation, the spaces formerly occupied by the solvent were left emptied so these porous membranes presented a superior surface/volume ratio, when compared to the type I and type II chitosan membranes. As surface/volume ratio increases, there is a higher contact surface with the host's immune system, which could explain the resulting exuberant cellular component. In fact, this study demonstrated that the three chitosan membranes tested *in vitro* and *in vivo* were biocompatible and therefore an important scaffold for the reconstruction of peripheral nerve, after axonotmesis or neurotmesis injury, associated or not to neurotrophic factors cellular producing systems. Types II and III chitosan membranes showed higher elasticity in comparison to type I chitosan membrane, a feature which would facilitate the surgical manipulation. Therefore, we decided to carry out *in vivo* testing with chitosan types II and III only.

4.3 Functional Assessment of Reinnervation

Immediately after the acute compression injury, the crushed areas of all sciatic nerves were flattened but nerve continuity was preserved. Complete flaccid paralysis of the operative foot was observed following crush injury. All rats survived, with no wound infection or automutilation.

Withdrawal reflex latency (WRL)

The results obtained, performing Withdrawal Reflex Latency (WRL) test to evaluate the nociceptive function are shown in Figure 15. Two way ANOVA shows that the WRL were significantly affected after the sciatic nerve crush [$F_{(10,250)}$=82,884; p<0,000]. Contrast analysis indicates that the WRL values were affected up to week 8. Beyond this time point, WRL values, the experimental groups pooled together, were similar to those preoperatively. A significant effect of group was found for WRL data [$F_{(4,25)}$=12,018; p<0,000], and post hoc analysis showed that differences were significant between *ChitosanII* group from one side and *ChitosanIICell*, *ChitosanIII* and

ChitosanIIICell groups on the other side (p<0,05). These results are suggestive of a slower rate of recovery in WRL with the use of type II chitosan.

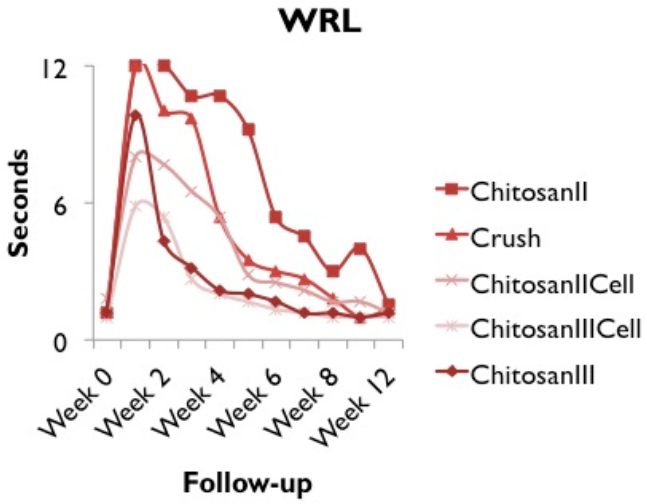

Figure 15 - WRL results

Motor Deficit (EPT)

The EPT values obtained during the healing period of 12 weeks are represented in Figure 16. EPT values were significantly affected by the crush injury [$F_{(10,250)}$=1497,366; p<0,000] and contrast analysis shows that at week 12, EPT had still not recovered to baseline values. There were significant differences in EPT values between the experimental groups [$F_{(4,25)}$=12,018; p<0,000] and post hoc analysis shows that the EPT values from the *Crush* group were significantly different from those of the *ChitosanIICell* and *ChitosanIIICell* (p<0,05), suggesting a negative effect of the N1E 115-differentiated cells on motor recovery after sciatic crush injury.

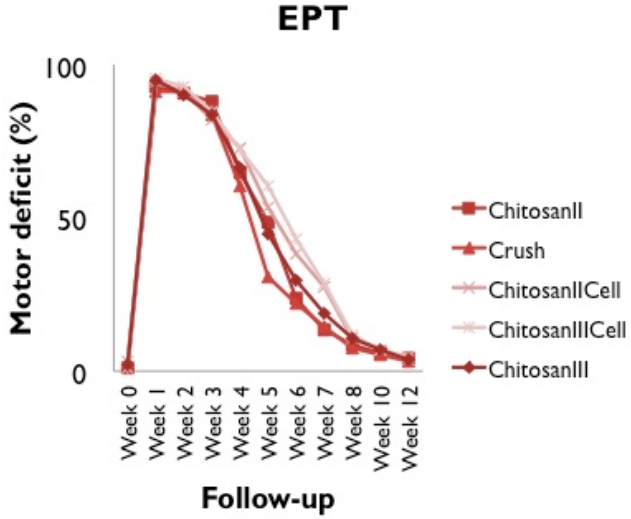

Figure 16 - EPT results

Sciatic functional index (SFI) and Static Sciatic Index (SSI)

SFI and SSI results are depicted in Figure 17 and Figure 18, respectively. Two way ANOVA shows that SFI values changed significantly after the crush injury [$F_{(10,250)}$=488,931; p<0,000]. Contrast analysis shows that SFI values were different from baseline until week 7 of recovery. A significant effect of group was observed for SFI values [$F_{(4,25)}$=144,125; p=0,01] with post hoc analysis indicating that values from *ChitosanIICell* group were different from those of the *ChitosanII* and *ChitosanIII* groups. Two way ANOVA analysis on SSI data was similar to that of the just reported SFI results. However, post hoc analysis shows that SSI results from the *ChitosanIIICell* group were different from those of the *Crush*, *ChitosanII* and *ChitosanIICell* groups.

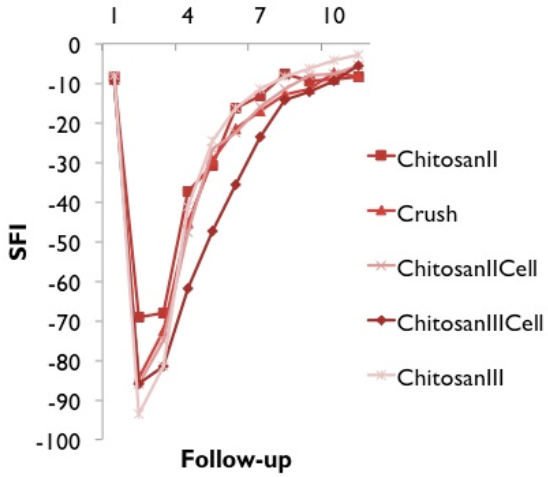

Figure 17 - SFI results

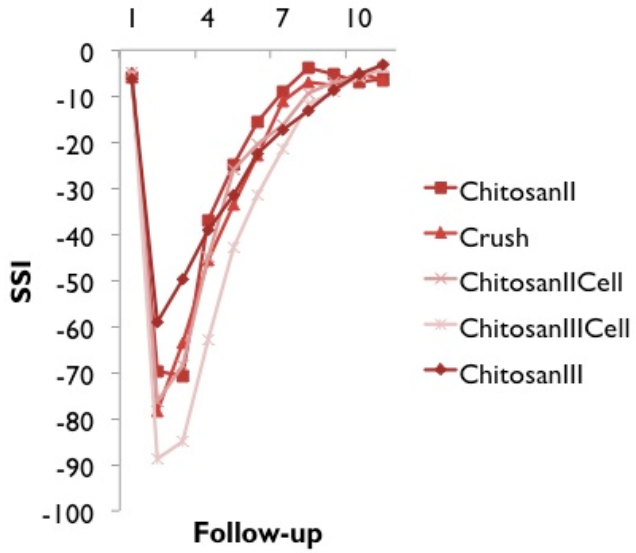

Figure 18 - SSI results

Ankle joint Kinematics

Video recordings of the rats' gait were undertaken at week 0 (pre-operatively) and at post-surgery at weeks 0, 2, 4, 8 and 12, so the amount of time points for statistical analysis was reduced to only five (see Methods). Figure 19 and Figure 20 represent the values of ankle joint angle and the values of ankle joint velocity at IC, OT, HR and TO, respectively, obtained by kinematic analysis during the healing period of 12 weeks.

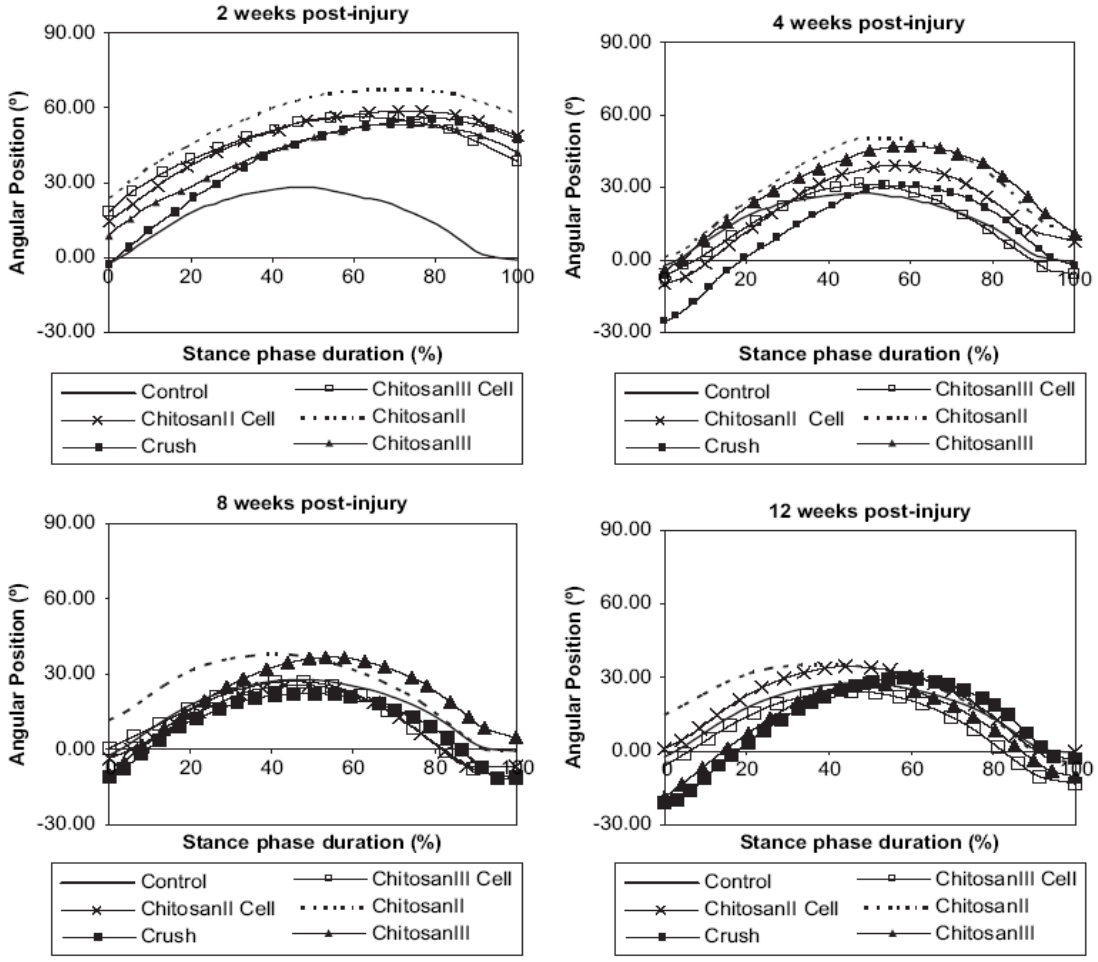

Figure 19 - Curves representing ankle joint angle in the sagittal plane during the stance phase of walking. Note the absence of plantarflexion at push off in all sciatic crushed groups at week 2 post-injury. The normal ankle motion pattern is progressively regained during the 12-weeks recovery period. The mean of each group is plotted: (solid line) Control Group; (■) Axonotmesis Group (Crush); (dashed line) Axonotmesis involved with chitosan II membrane (ChitosanII); (▲) Axonotmesis involved with chitosan III membrane (ChitosanIII); (x) Axonotemesis involved with chitosan type II membrane covered with the cellular system (ChitosanIICell); (□) Axonotemesis involved with chitosan type III membrane covered with the cellular system (ChitosanIIICell).

Initial Contact (IC)

The ankle joint angle at IC changed significantly after the sciatic crush [$F_{(4, 100)}$=28,705; p<0,000]. Such changes were transient and by week 4 ankle joint angle at IC was indistinguishable from baseline, as indicated by contrast analysis. Two way ANOVA revealed group differences [$F_{(4,25)}$=10,671; p<0,000] and post hoc analysis shows that *ChitosanII* group was different from all the other four groups.

Opposite toe off (OT)

Ankle joint angle at OT was significantly affected after the crush injury [$F_{(4,100)}$=13,464; p<0,000] but by week 4 of recovery joint position at this point of stance had recovered to normal values. Two way ANOVA revealed a significant group effect [$F_{(4,25)}$=4,150; p=0,01] and post hoc analysis showed that ankle joint angles at OT in the *ChitosanII* group throughout the study were significantly different from *Crush* and *ChitosanIII* groups (Figure 19).

Ankle joint velocity at OT was significantly affected after the crush injury [$F_{(4,100)}$=8,582; p<0,000] and returned to preoperative values at week 4 (p<0,05). There were significant differences between the groups for ankle joint velocity at OT [$F_{(4,25)}$=3,164; p<0,031] with post hoc analysis showing significant differences between *ChitosanII* and *ChitosanIICell* groups (p<0,05) (Figure 20).

Heel Raise (HR)

Ankle joint angle at HR was significantly altered after the sciatic nerve injury [$F_{(4,100)}$=34,151; p<0,000] until week 12 (p<0,05). A significant effect of group was found for this variable [$F_{(4,25)}$=3,456; p<0,022]. Post hoc tests found significant differences in ankle joint angle at HR between *ChitosanII* and the *Crush* and *ChitosanIIICell* groups (Figure 19).

Instantaneous ankle's joint velocity at HR was significantly affected after axonotmesis [$F_{(4,100)}$=42,384; p<0,000] with contrast analysis showing that differences in ankle's joint velocity were significantly different from normal values until week 4 of recovery. A significant effect of group was registered [$F_{(4,25)}$=3,766; p<0,016], and post hoc tests showed significant differences between *ChitosanII* and *ChistosanIICell* groups (Figure 20).

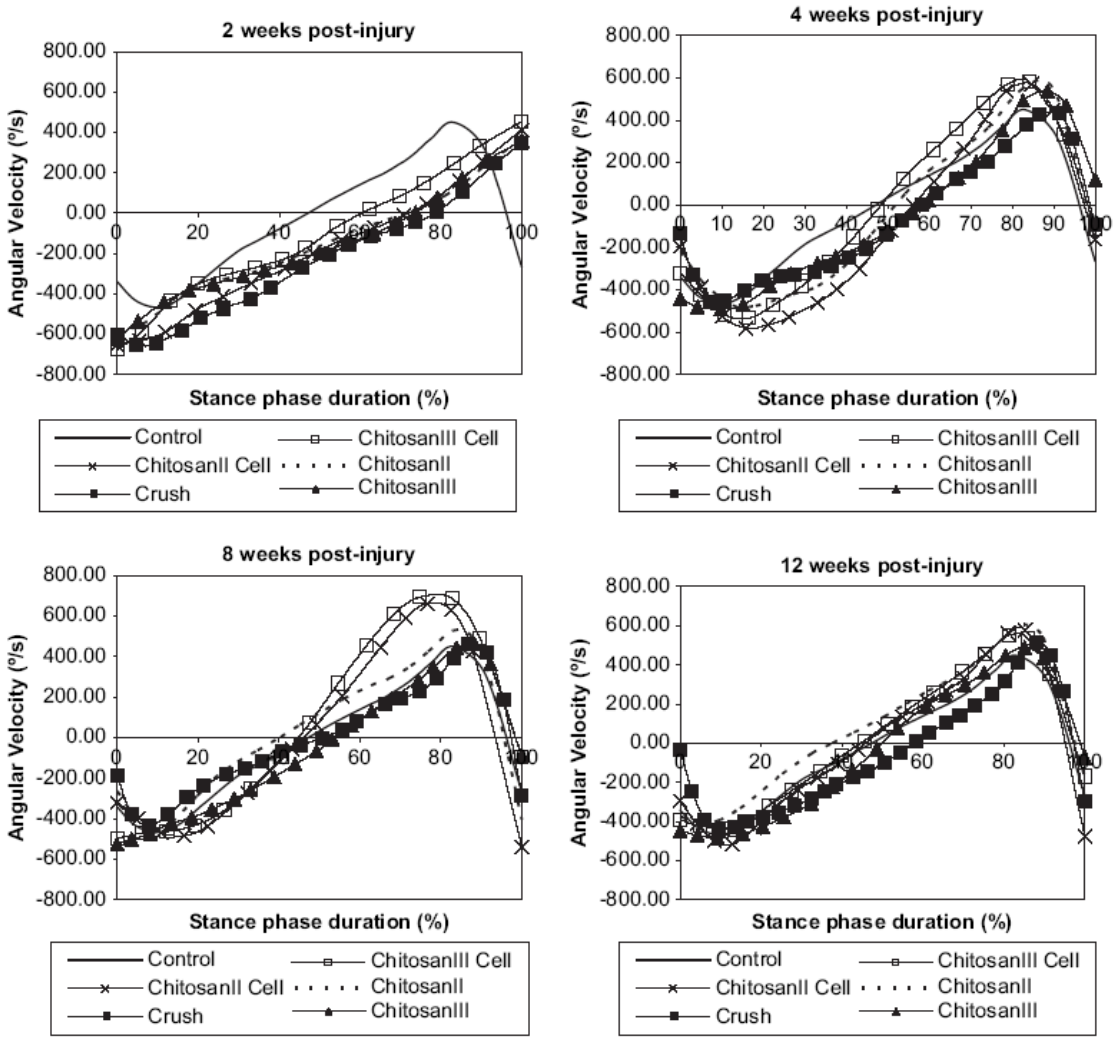

Figure 20 - Curves represent ankle joint angular velocity in the sagittal plane during the stance phase of walking. Note the loss of the normal ankle joint angular velocity biphasic response in all sciatic crushed groups at week 2 post-injury. The normal ankle velocity pattern is progressively regained during the 12-weeks recovery period. The mean of each group is plotted: (solid line) Control Group; (■)Axonotmesis Group (Crush); (dashed line) Axonotmesis involved with chitosan II membrane (ChitosanII); (▲) Axonotmesis involved with chitosan III membrane (ChitosanIII); (x) Axonotemesis involved with chitosan type II membrane covered with the cellular system (ChitosanIICell); (□)Axonotemesis involved with chitosan type III membrane covered with the cellular system (ChitosanIIICell).

Toe off (TO)

Ankle joint angle at TO was significantly altered after the sciatic nerve injury [$F_{(4,100)}$=181,588; p<0,000]. Contrast analysis showed that at week 12 ankle's joint angle mean value at TO was similar to that registered before the sciatic nerve injury. A significant effect of group was found for this variable [$F_{(4,25)}$=3,409; p<0,023]. Post hoc tests found significant differences in ankle's joint angle at TO between *ChitosanII* and *ChitosanIIICell* groups (Figure 19). Ankle's joint velocity at TO was significantly affected after the crush injury [$F_{(4,100)}$=103,331; p<0,000] with contrast analysis showing that ankle's joint velocity did not recovered completely within the 12-weeks follow up time. A significant effect of group was registered [$F_{(4,25)}$=9,689; p<0,000], and post hoc tests showed significant differences between *ChitosanIICell*, from one hand and *Crush*, *ChitosanIII* and *ChistosanIIICell* groups, on the other hand (Figure 20).

MANOVA analysis was employed to further compare the results of the walk kinematic analysis of the experimental groups, using values of week 12 only. A significant effect of the experimental group was observed (Pillai's Trace 3,709; p<0,000). Multivariate contrast analysis (K matrix) showed that *ChitosanIII* was the group differing from *Crush* group in a less number of variables. This indicates that at the end of the recovery period animals in *ChitosanIII* group presented a degree of functional recovery similar to that registered in the *Crush* group.

4.4 Morphological and histomorphometrical analysis

Figure 21 shows the histological appearance of control normal sciatic nerve cross sections (Figure 21A) in comparison to cross sections of the regenerated nerve fibers with and without cell delivery (Figure 21B-F). As expected, regenerated nerve fibers in all five experimental groups were organized in microfascicles and were smaller than control nerve fibers. In the two experimental groups in which cell delivery was carried out (Figure 21B,D,F), the presence of unusual cell profiles, interpretable as the transplanted cells, were detectable at the periphery of the nerves. This was seldom observed in inner parts of the nerve (Figure 21F) suggesting that only few transplanted cells colonized the inner nerve interstice.

Electron microscopy confirms that a good regeneration pattern of both unmyelinated and myelinated nerve fibers occurred in all experimental groups, irrespectively of the enrichment with neural stem cells (Figure 23A,B and Figure 24A,B). The border zone of the nerve still shows the presence of some chitosan debris integrated with the collagen fibers of the epineurium (Figure 23C,D). Moreover, in the two experimental groups in which cell delivery was carried out (Figure 24), it was possible to find some of

transplanted cells localized in the border zone of the regenerated nerve (Figure 24C,D).

Results of the design-based morphoquantitative analysis of regenerated myelinated nerve fibers permitted to quantitatively compare the different experimental groups. As expected, fiber density was significantly ($p<0.05$) higher in all experimental groups in comparison to control sciatic nerves, while mean axon and fiber diameter and myelin thickness were significantly ($p<0.05$) lower.

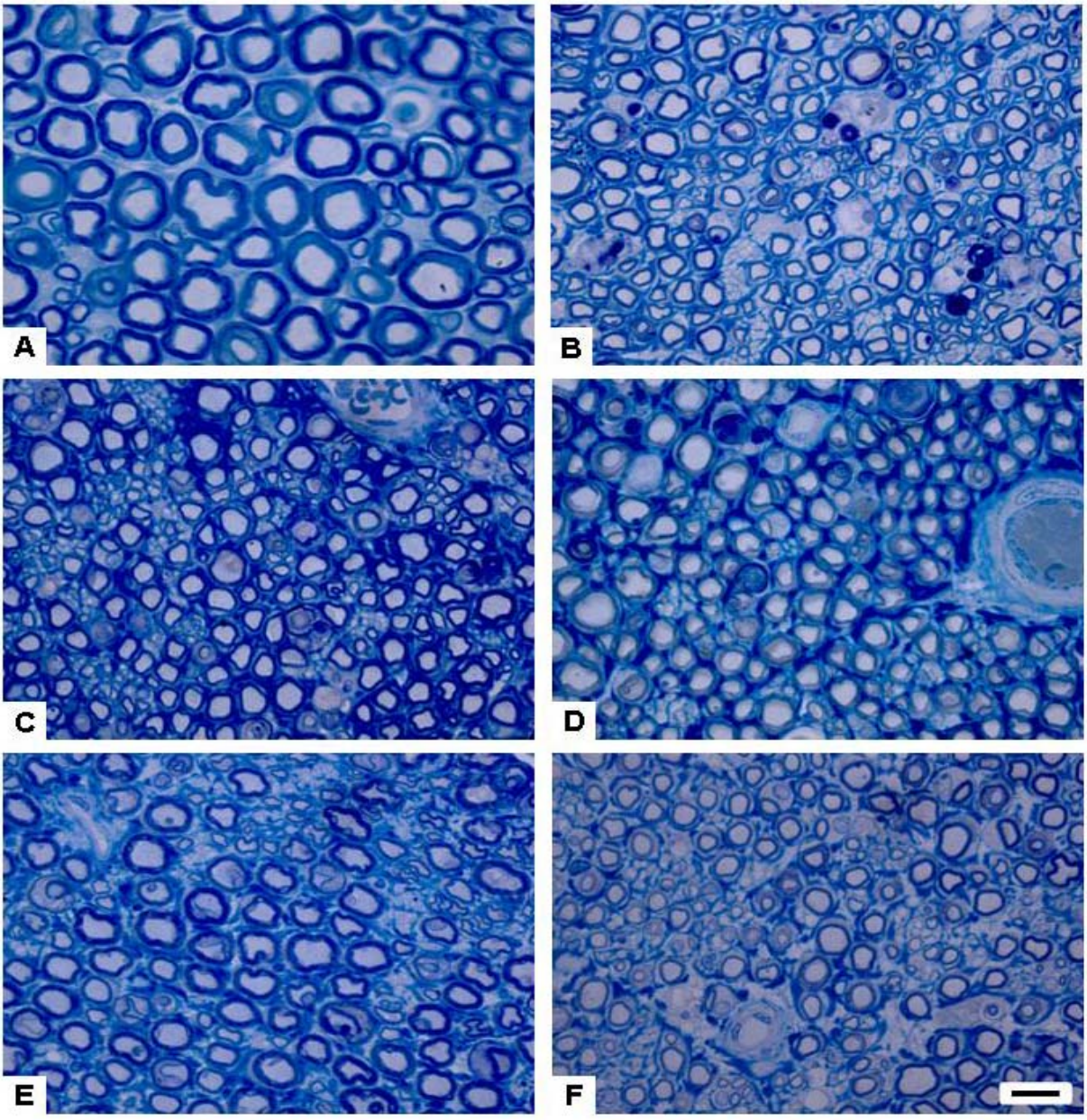

Figure 21 - High resolution photomicrographs of nerve fibers from control and regenerated rat sciatic nerves. (A) Control group; (B) Crush group; (C) ChitosanII group; (D) ChitosanIICell group; (E) ChitosanIII group. (F) ChitosanIIICell group. Original magnification: 1000x

As regards the number of regenerated myelinated nerve fibers, this parameter was found to be significantly higher ($p<0.05$) in comparison to controls in four out of the five experimental groups only; in fact, *ChitosanIII* group showed a number of fibers not significantly ($p<0.05$) different in comparison to normal control nerves.

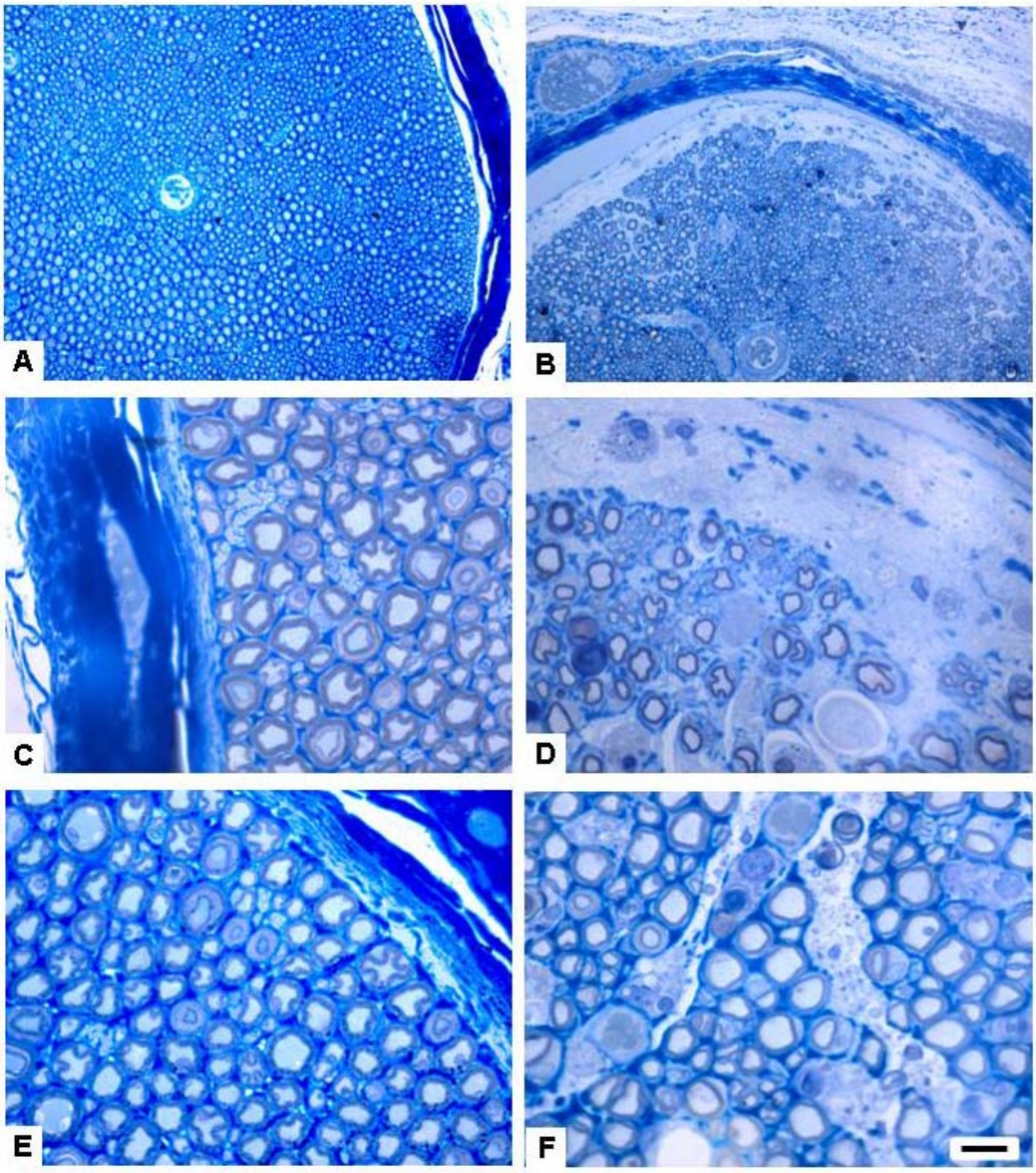

Figure 22 - High resolution photomicrographs comparing ChitosanIII (A, C, E) and ChitosanIIICell (B, D, F) groups. The presence of transplanted cells is clearly identifiable at the periphery of the nerve (D) and, seldom, also in the inner nerve areas (F). Original magnification: A, B: = 200x; C-F=1000x

The peculiarity of the experimental group characterized by type III chitosan membrane enwrapment, was also confirmed by statistical analysis of inter-group variability among experimental groups which demonstrated that *ChitosanIII* group has a significantly ($p<0.05$) higher mean fiber and axon diameter and myelin thickness in comparison with all other experimental crush groups.

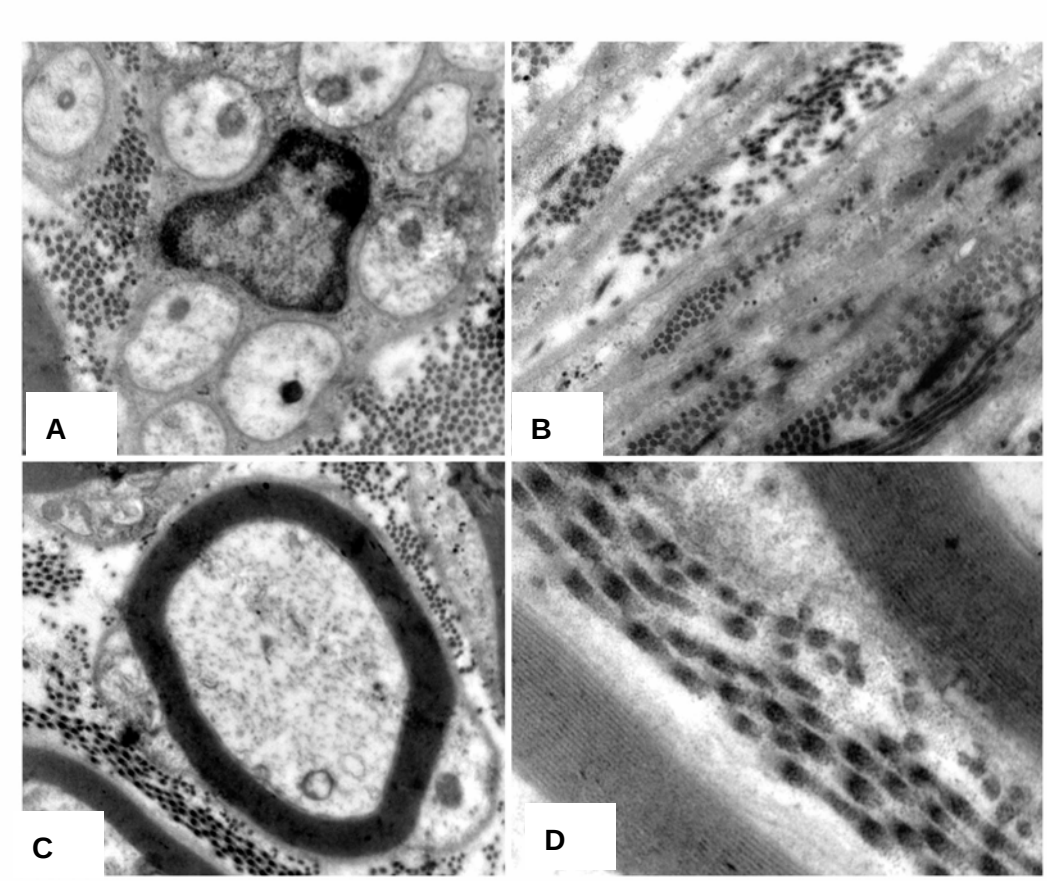

Figure 23 - Electron microscopy regenerated nerve fibers in ChitosanIII experimental group. In panels A and B, the ultrastructural appearance of unmyelinated (A) and myelinated (B) nerve fibers can be appreciated. In panels C and D, the presence of chitosan debris mingled with epineurial connective tissue can be still detected. Original magnification: A = 40,000x; B = 30,000x; C = 50,000x; D = 150,000x.

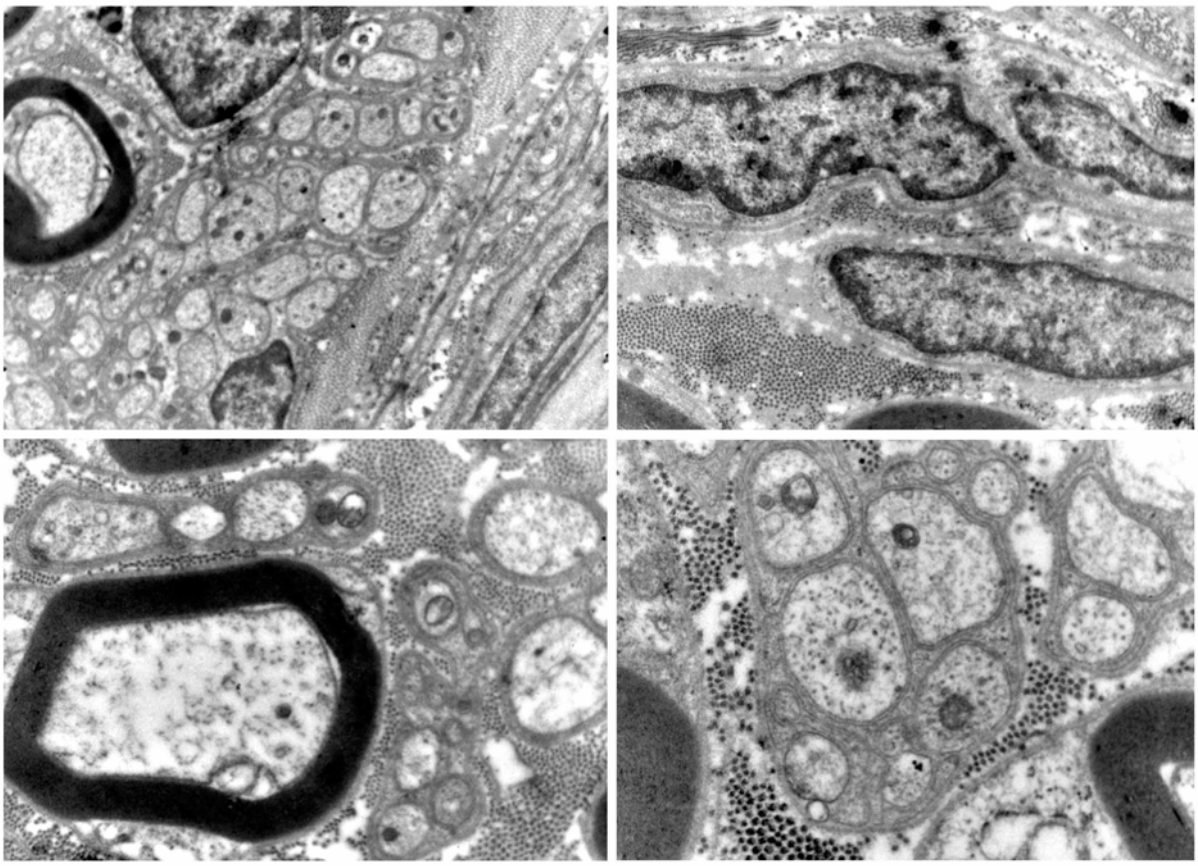

Figure 24 - Electron microscopy regenerated nerve fibers in ChitosanIIICell experimental group. In panels A and B, the ultrastructural appearance of unmyelinated (A) and myelinated (B) nerve fibers can be appreciated. In panels C and D, the presence of elongated transplanted cells mingled with chitosan debris and epineurial connective tissue can be still detected. Original magnification: A = 40,000x; B = 25,000x; C = 10,000x; D = 15,000x.

5 Discussion

To find out effective strategies for promoting peripheral nerve regeneration is a challenging issue in Regenerative Medicine (1-3; 19; 38; 50-52). The study of new materials for promoting nerve regeneration is usually carried out in axonotmesis nerve lesion models (20). Although nerve fibers always regenerate after experimental axonotmesis, there are considerable differences in the extent and rate of recovery between studies which probably reflect the different techniques used to induce the injury (20; 21; 38). To cope with this limitation, in this study we used a standardized clamping procedure that was described in details in previous works (20; 21; 49; 53), for investigating the effects of enwrapping the axonotmesis site with type II and type III chitosan membranes. In two experimental groups, chitosan membranes were covered with *in vitro* differentiated N1E-115 cells before implanting them *in vivo*. In neuronal cells the regulation of the intracellular free calcium concentration $[Ca^{2+}]_i$ plays an important role in physiological processes such as growth and differentiation, controlling important cell functions like the release of neurotransmitters and the membrane's excitability. The mechanisms that control $[Ca^{2+}]_i$ are of crucial importance for normal homeostasis, and its deregulation has been associated to cellular changes and even cell death, when $[Ca^{2+}]_i$ reaches values above 105 nM (42). The measurements of $[Ca^{2+}]_i$ of the N1E-115 cells *in vitro* differentiated by the addition of DMSO indicated that these cells did not begin the apoptosis process although the evident neural differentiation supporting the hypothesis that chitosan membranes type I, II and III, were a viable substrate for N1E-115 neuronal cell line adhesion, multiplication and differentiation. The *in vivo* biocompatibility studies also corroborated that the three types of chitosan membranes were biocompatible and therefore an important scaffold for the reconstruction of peripheral nerve, after axonotmesis or neurotmesis injury, associated or not to cellular systems producing neurotrophic factors. The higher elasticity observed in type II and III chitosan membranes, when compared to type I, that facilitates surgery, induced us to carry out the *in vivo* testing on the rat sciatic nerve regeneration, with these GPTMS hybrid membranes only, abandoning type I membranes. As a matter of fact, the GPTMS hybrid membranes provide a suitable scaffolding environment for neural tissue engineering, making this material a potential candidate for scaffolds in neural tissue engineering.

The *in vivo* study on crushed rat sciatic nerve experimental model showed that morphological predictors of nerve regeneration (number of fibers, axon and fiber size and myelin thickness) were significantly improved in *ChitosanIII* group in comparison to

all other experimental crush groups, thus suggesting that type III chitosan is a suitable biomaterial to be used in reconstructive peripheral nerve surgery. Functional assessment partially supported the morphometric results since results of the WRL, EPT, SFI and SSI tests suggest that chitosan type II and the N1E-115 cells have a reduced degree of functional recovery which is in line with results of histomorphometric analysis.

Results of both morphological and functional predictors of nerve regeneration also showed that enrichment of chitosan membranes with N1E-115 neural cells did not have any positive effect on nerve regeneration in comparison to crush controls and, in case of type III chitosan membrane, the presence of transplanted cells seemed to prevent the positive effect of the membrane wrapping alone on nerve regeneration. These results are in agreement with previous investigation that showed that N1E-115 cell population does not have significant effect in promoting axon regeneration and, when N1E-115 cells were cultured inside a PLGA scaffold used to bridge a nerve defect, they can even exert negative effects on nerve fiber regeneration (21; 53). Thus N1E-115 cells did not prove to be a potential candidate therapeutic agent for treatment of nerve injury and their utilization is just limited to research purposes, mainly as a basic scientific step in the investigation of the potentiality for nerve regeneration promotion of cell transplantation delivery systems that permit that transplanted cells are able to secrete neurotrophic factors in the site of injury without being directly in contact with regenerating axons.

Chitosan type II and chitosan type III were developed as a hybrid of chitosan by the addition of GPTMS. Wettability of material surfaces is one of the key factors for protein adsorption, cell attachment and migration (39). The addition of GPTMS improves the wettability of chitosan surfaces (41), and therefore chitosan type II and chitosan type III are expected to be more hydrophilic than the original chitosan (41). Chitosan type III was developed to be more porous, with a larger surface to volume ratio but preserving mechanical strength and the ability to adapt to different shapes. Significant differences in water uptake between commonly used chitosan and our hybrid chitosan type III were previously reported due to the difference in the ability of the matrix to hold water (13). In fact, hybrid chitosan-based membranes may retain about two times as much biological liquid fluid as chitosan (13). A synergetic effect of a more favourable porous microstructure and physicochemical properties (more wettable and higher water uptake level) of chitosan type III compared to chitosan type II, and the presence of silica ions may be responsible for the good results obtained in this study for the former in the nerve regeneration process.

The observation that significant improvement of axonal regeneration was obtained in crushed sciatic nerves surrounded by chitosan type III membranes alone suggests that this material may not just work as a simple mechanical scaffold but instead may work as an inducer of nerve regeneration. The regenerative property of chitosan type III might be explained by the action on Schwann cell proliferation and axon elongation and myelination (9; 13). Yet, the expression of established myelin genes such as PMP22, PO and MBP (40) may be influenced by the presence of silica ions which exert an effect on several glycoprotein expression (13; 43).

6 Conclusions

Enwrapment of the site of a nerve crush lesion with a chitosan type III membrane significantly improves nerve regeneration in the rat, whereas enrichment of chitosan membranes with N1E-115 neural cells does have positive effects. Whereas translation of animal studies to patients should always be dealt with caution, the results obtained in this experimental study open interesting perspectives for the clinical employment of hybrid chitosan membranes in peripheral nerve reconstruction.

REFERENCES

1. Schlosshauer B, Dreesmann L, Schaller H-E, Sinis N. Synthetic nerve guide implants in humans: a comprehensive survey. [Internet]. Neurosurgery. 2006 Oct;59(4):740-7; discussion 747-8.

2. Samii M, Carvalho GA, Nikkhah G, Penkert G. Surgical reconstruction of the musculocutaneous nerve in traumatic brachial plexus injuries. [Internet]. Journal of neurosurgery. 1997 Dec;87(6):881-6.[

3. Höke A. Mechanisms of Disease: what factors limit the success of peripheral nerve regeneration in humans? [Internet]. Nature clinical practice. Neurology. 2006 Aug;2(8):448-54.

4. Lee JM, Tos P, Raimondo S, Fornaro M, Papalia I, Geuna S, et al. Lack of topographic specificity in nerve fiber regeneration of rat forelimb mixed nerves. [Internet]. Neuroscience. 2007 Feb;144(3):985-90. 1

5. Tos P, Battiston B, Nicolino S, Raimondo S, Fornaro M, Lee JM, et al. Comparison of fresh and predegenerated muscle-vein-combined guides for the repair of rat median nerve. [Internet]. Microsurgery. 2007 Jan;27(1):48-55.

6. Chen G, Ushida T, Tateishi T. Preparation of poly(L-lactic acid) and poly(DL-lactic-co-glycolic acid) foams by use of ice microparticulates. [Internet]. Biomaterials. 2001 Sep;22(18):2563-7.

7. Chandy T, Sharma CP. Chitosan--as a biomaterial. [Internet]. Biomaterials, artificial cells, and artificial organs. 1990 Jan;18(1):1-24.

8. Yamaguchi I, Itoh S, Suzuki M, Osaka A, Tanaka J. The chitosan prepared from crab tendons: II. The chitosan/apatite composites and their application to nerve regeneration. [Internet]. Biomaterials. 2003 Aug;24(19):3285-92.

9. Yuan Y, Zhang P, Yang Y, Wang X, Gu X. The interaction of Schwann cells with chitosan membranes and fibers in vitro. [Internet]. Biomaterials. 2004 Aug;25(18):4273-8.

10. Ishikawa N, Suzuki Y, Ohta M, Cho H, Suzuki S, Dezawa M, et al. Peripheral nerve regeneration through the space formed by a chitosan gel sponge. [Internet]. Journal of biomedical materials research. Part A. 2007 Oct ;83(1):3340.

11. Wang W, Itoh S, Matsuda A, Ichinose S, Shinomiya K, Hata Y, et al. Influences of mechanical properties and permeability on chitosan nano/microfiber mesh

tubes as a scaffold for nerve regeneration. [Internet]. Journal of biomechanical materials research. Part A. 2008;84(2):557-66.

12. Senel S, McClure SJ. Potential applications of chitosan in veterinary medicine. [Internet]. Advanced drug delivery reviews. 2004 Jun;56(10):1467-80.

13. Shirosaki Y, Tsuru K, Hayakawa S, Osaka A, Lopes MA, Santos JD, et al. In vitro cytocompatibility of MG63 cells on chitosan-organosiloxane hybrid membranes. [Internet]. Biomaterials. 2005 Feb;26(5):485-93.

14. Amano T, Richelson E, Nirenberg M. Neurotransmitter synthesis by neuroblastoma clones (neuroblast differentiation-cell culture-choline acetyltransferase-acetylcholinesterase-tyrosine hydroxylase-axons-dendrites). [Internet]. Proceedings of the National Academy of Sciences of the United States of America. 1972 Jan;69(1):258-63.

15. Marreco PR, Luz Moreira P da, Genari SC, Moraes AM. Effects of different sterilization methods on the morphology, mechanical properties, and cytotoxicity of chitosan membranes used as wound dressings. [Internet]. Journal of biomedical materials research. Part B, Applied biomaterials. 2004 Nov;71(2):268-77. 9

16. Beer GM, Steurer J, Meyer VE. Standardizing nerve crushes with a non-serrated clamp. [Internet]. Journal of reconstructive microsurgery. 2001 Oct;17(7):531-4.

17. Kimhi Y, Palfrey C, Spector I, Barak Y, Littauer UZ. Maturation of neuroblastoma cells in the presence of dimethylsulfoxide. [Internet]. Proceedings of the National Academy of Sciences of the United States of America. 1976 Feb;73(2):462-6.

18. Schmidt CE, Leach JB. Neural tissue engineering: strategies for repair and regeneration. [Internet]. Annual review of biomedical engineering. 2003 Jan;5293-347.

19. Lundborg G, Dahlin L, Danielsen N, Zhao Q. Trophism, tropism, and specificity in nerve regeneration. [Internet]. Journal of reconstructive microsurgery. 1994 Sep;10(5):345-54.

20. Varejão AS, Melo-Pinto P, Meek MF, Filipe VM, Bulas-Cruz J. Methods for the experimental functional assessment of rat sciatic nerve regeneration. [Internet]. Neurological research. 2004 Mar;26(2):186-94.

21. Luís AL, Amado S, Geuna S, Rodrigues JM, Simões MJ, Santos JD, et al. Long-term functional and morphological assessment of a standardized rat sciatic

nerve crush injury with a non-serrated clamp. [Internet]. Journal of neuroscience methods. 2007 Jun;163(1):92-104.

22. Varejão ASP, Cabrita AM, Meek MF, Bulas-Cruz J, Melo-Pinto P, Raimondo S, et al. Functional and morphological assessment of a standardized rat sciatic nerve crush injury with a non-serrated clamp. [Internet]. Journal of neurotrauma. 2004 Nov;21(11):1652-70.

23. Tuttle JB, Richelson E. Phenytoin action on the excitable membrane of mouse neuroblastoma. [Internet]. The Journal of pharmacology and experimental therapeutics. 1979 Dec;211(3):632-7.

24. Fisher SK, Domask LM, Roland RM. Muscarinic receptor regulation of cytoplasmic Ca2+ concentrations in human SK-N-SH neuroblastoma cells: Ca2+ requirements for phospholipase C activation. [Internet]. Molecular pharmacology. 1989 Feb;35(2):195-204.

25. Sporel-Ozakat RE, Edwards PM, Hepgul KT, Savas A, Gispen WH. A simple method for reducing autotomy in rats after peripheral nerve lesions. [Internet]. Journal of neuroscience methods. 1991 Feb;36(2-3):263-5.

26. Luís AL, Rodrigues JM, Geuna S, Amado S, Simões MJ, Fregnan F, et al. Neural cell transplantation effects on sciatic nerve regeneration after a standardized crush injury in the rat. [Internet]. Microsurgery. 2008 Jan;28(6):458-70.[cited 2011 Mar 15]

27. Koka R, Hadlock TA. Quantification of functional recovery following rat sciatic nerve transection. [Internet]. Experimental neurology. 2001 Mar;168(1):192-5.[cited 2010 Dec 7]

28. Hu D, Hu R, Berde CB. Neurologic evaluation of infant and adult rats before and after sciatic nerve blockade. [Internet]. Anesthesiology. 1997 Apr;86(4):957-65.

29. Varejão ASP, Cabrita AM, Geuna S, Patrício J a, Azevedo HR, Ferreira AJ, et al. Functional assessment of sciatic nerve recovery: biodegradable poly (DLLA-epsilon-CL) nerve guide filled with fresh skeletal muscle. [Internet]. Microsurgery. 2003 Jan;23(4):346-53.

30. Bain JR, Mackinnon SE, Hunter DA. Functional evaluation of complete sciatic, peroneal, and posterior tibial nerve lesions in the rat. [Internet]. Plastic and reconstructive surgery. 1989 Jan;83(1):129-38.

31. Bervar M. Video analysis of standing--an alternative footprint analysis to assess functional loss following injury to the rat sciatic nerve. [Internet]. Journal of neuroscience methods. 2000 Oct;102(2):109-16.

32. Dijkstra JR, Meek MF, Robinson PH, Gramsbergen A. Methods to evaluate functional nerve recovery in adult rats: walking track analysis, video analysis and the withdrawal reflex. [Internet]. Journal of neuroscience methods. 2000 Mar;96(2):89-96.

33. Clarke KA, Parker AJ. A quantitative study of normal locomotion in the rat. [Internet]. Physiology & behavior. 1986 Jan;38(3):345-51.[

34. Varejão ASP, Cabrita AM, Meek MF, Bulas-Cruz J, Gabriel RC, Filipe VM, et al. Motion of the foot and ankle during the stance phase in rats. [Internet]. Muscle & nerve. 2002 Nov;26(5):630-5.

35. Di Scipio F, Raimondo S, Tos P, Geuna S. A simple protocol for paraffin-embedded myelin sheath staining with osmium tetroxide for light microscope observation. [Internet]. Microscopy research and technique. 2008 Jul;71(7):497-502.

36. Schmitz C. Variation of fractionator estimates and its prediction. [Internet]. Anatomy and embryology. 1998 Nov;198(5):371-97.

37. Geuna S, Gigo-Benato D, Rodrigues A de C. On sampling and sampling errors in histomorphometry of peripheral nerve fibers. [Internet]. Microsurgery. 2004 Jan;24(1):72-6.

38. Mackinnon SE, Dellon AL, O'Brien JP. Changes in nerve fiber numbers distal to a nerve repair in the rat sciatic nerve model. [Internet]. Muscle & nerve. 1991 Nov;14(11):1116-22.

39. Hench L. Biomaterials: An Interfacial Approach (Biophysics and bioengineering series) [Internet]. Academic Pr; 1982.

40. Kuhn G, Lie A, Wilms S, Müller HW. Coexpression of PMP22 gene with MBP and P0 during de novo myelination and nerve repair. [Internet]. Glia. 1993 Aug;8(4):256-64.

41. Tateishi T, Chen G, Ushida T. Biodegradable porous scaffolds for tissue engineering [Internet]. Journal of Artificial Organs. 2002 Jun;5(2):77-83.

42. Trump BF, Berezesky IK. Calcium-mediated cell injury and cell death. [Internet]. The FASEB journal: official publication of the Federation of American Societies for Experimental Biology. 1995 Feb;9(2):219-28.

43. Pietak AM, Reid JW, Stott MJ, Sayer M. Silicon substitution in the calcium phosphate bioceramics. [Internet]. Biomaterials. 2007 Oct ;28(28):4023-32.

44. Wenling C, Duohui J, Jiamou L, Yandao G, Nanming Z, Xiufang Z. Effects of the degree of deacetylation on the physicochemical properties and Schwann cell affinity of chitosan films. [Internet]. Journal of biomaterials applications. 2005 Oct;20(2):157-77.

45. Rodrigues JM, Luís AL, Lobato JV, Pinto MV, Faustino A, Hussain NS, et al. Intracellular Ca2+ concentration in the N1E-115 neuronal cell line and its use for peripheric nerve regeneration. [Internet]. Acta médica portuguesa. 2005;18(5):323-8.

46. Rodrigues JM, Luís AL, Lobato JV, Pinto MV, Lopes MA, Freitas M, et al. Determination of the intracellular Ca2+ concentration in the N1E-115 neuronal cell line in perspective of its use for peripheric nerve regeneration. [Internet]. Biomedical materials and engineering. 2005 Jan;15(6):455-65.

47. Masters DB, Berde CB, Dutta SK, Griggs CT, Hu D, Kupsky W, et al. Prolonged regional nerve blockade by controlled release of local anesthetic from a biodegradable polymer matrix. [Internet]. Anesthesiology. 1993 Aug;79(2):340-6.

48. Varejão ASP, Cabrita AM, Meek MF, Bulas-Cruz J, Filipe VM, Gabriel RC, et al. Ankle kinematics to evaluate functional recovery in crushed rat sciatic nerve [Internet]. Muscle & nerve. 2003;27(6):706–714. l

49. Varejão ASP, Cabrita AM, Meek MF, Fornaro M, Geuna S, Giacobini-Robecchi MG. Morphology of nerve fiber regeneration along a biodegradable poly (DLLA-epsilon-CL) nerve guide filled with fresh skeletal muscle. [Internet]. Microsurgery. 2003 Jan;23(4):338-45.

50. Geuna S, Papalia I, Tos P. End-to-side (terminolateral) nerve regeneration: a challenge for neuroscientists coming from an intriguing nerve repair concept. [Internet]. Brain research reviews. 2006 Sep;52(2):381-8.

51. Battiston B, Geuna S, Ferrero M, Tos P. Nerve repair by means of tubulization: literature review and personal clinical experience comparing biological and synthetic conduits for sensory nerve repair. [Internet]. Microsurgery. 2005 Jan;25(4):258-67.

52. Meek MF, Robinson PH, Stokroos I, Blaauw EH, Kors G, Dunnen WF den. Electronmicroscopical evaluation of short-term nerve regeneration through a thin-walled biodegradable poly(DLLA-epsilon-CL) nerve guide filled with modified denatured muscle tissue. [Internet]. Biomaterials. 2001 May;22(10):1177-85.

53. Luis AL, Rodrigues JM, Amado S, Veloso AP, Armada-Da-silva PAS, Raimondo S, et al. PLGA 90/10 and caprolactone biodegradable nerve guides for the reconstruction of the rat sciatic nerve [Internet]. Microsurgery. 2007;27(2):125–137.

Chapter 4 - Effects of Collagen Membranes Enriched with in Vitro-Differentiated N1E-115 Cells on Rat Sciatic Nerve Regeneration after End-to-End Repair

Amado S, Rodrigues JM, Luís AL, Armada-da-Silva P a S, Vieira M, Gartner A, et al. Effects of collagen membranes enriched with in vitro-differentiated N1E-115 cells on rat sciatic nerve regeneration after end-to-end repair. [Internet]. Journal of neuroengineering and rehabilitation. 2010 Jan;7:7.

5 Introduction

Nerve regeneration is a complex biological phenomenon. In the peripheral nervous system, nerves can spontaneously regenerate without any treatment if nerve continuity is maintained (axonotmesis) whereas more severe type of injuries must be surgically treated by direct end-to-end surgical reconnection of the damaged nerve ends (1-3). Unfortunately, the functional outcomes of nerve repair are in many cases unsatisfactory (4-10) thus calling for research in order to reveal more effective strategies for improving nerve regeneration. However, recent advances in neuroscience, cell culture, genetic techniques, and biomaterials provide optimism for new treatments for nerve injuries (1; 9-20).

The use of materials of natural origin has several advantages in tissue engineering. Natural materials are more likely to be biocompatible than artificial materials. Also, they are less toxic and provide a good support to cell adhesion and migration due to the presence of a variety of surface molecules. Drawbacks of natural materials include potential difficulties in their isolation and controlled scale-up (6-10). In addition to the use of intact natural tissues, a great deal of research has focused on the use of purified natural extracellular matrix (ECM) molecules, which can be modified to serve as appropriate scaffolding (16). ECM molecules, such as laminin, fibronectin and collagen have also been shown to play a significant role in axonal development and regeneration (8; 21; 22). For example, silicone tubes filled with laminin, fibronectin, and collagen led to a better regeneration over a 10 mm rat sciatic nerve gap compared to empty silicone controls (14). Collagen filaments have also been used to guide regenerating axons across 20–30 mm defects in rats (23-26). Further studies have shown that oriented fibers of collagen within gels, aligned using magnetic fields, provide an improved template for neurite extension compared to randomly oriented collagen fibers (22; 27). Finally, rates of regeneration comparable to those using a nerve autograft have been achieved using collagen tubes containing a porous collagen-glycosaminoglycan matrix (28-30). Nerve regeneration requires a complex interplay between cells, ECM, and growth factors. The local presence of growth factors plays an important role in controlling survival, migration, proliferation, and differentiation of the various cell types involved in nerve regeneration (8-10; 31). Therefore, therapies with relevant growth factors received increasing attention in recent years although growth factor therapy is a difficult task because of the high biological activity (in pico- to nanomolar range), pleiotrophic effects (acting on a variety of targets), and short

biological half-life (few minutes to hours) (32). Thus, growth factors should be administered locally to achieve an adequate therapeutic effect with little adverse reactions and the short biological half-life of growth factors demands for a delivery system that slowly releases locally the molecules over a prolonged period of time. Employment of biodegradable membranes enriched with a cellular system producing neurotrophic factors has been suggested to be a rational approach for improving nerve regeneration after neurotmesis (16).

The aim of this study was thus to verify if rat sciatic nerve regeneration after end-to-end reconstruction can be improved by seeding *in vitro* differentiated N1E-115 neural cells on a type III equine collagen membrane and enwrap the membrane around the lesion site. The N1E-115 cell line has been established from a mouse neuroblastoma (33) and have already been used with conflicting results as a cellular system to locally produce and deliver neurotrophic factors (6-10). *In vitro*, the N1E-115 cells undergo neuronal differentiation in response to dimethylsulfoxide (DMSO), adenosine 3', 5'-cyclic monophosphate (cAMP), or serum withdrawal (4-10). Upon induction of differentiation, proliferation of N1E-115 cells ceases, extensive neurite outgrowth is observed and the membranes become highly excitable (4-10). The interval period of 48 hours of differentiation was previously determined by measurement of the intracellular calcium concentration ($[Ca^{2+}]i$). At this time point, the N1E-115 cells present already the morphological characteristics of neuronal cells but cell death due to increased $[Ca^{2+}]i$ is not yet occurring as described elsewhere (4-10).

6 Methods

6.1 Cell culture

The N1E-115 cells, clones of cells derived from the mouse neuroblastoma C-130035 retain numerous biochemical, physiological, and morphological properties of neuronal cells in culture (4-10). N1E-115 neuronal cells were cultured in Petri dishes (around 2 x 10^6 cells) over collagen type III membranes (Gentafleece®, Resorba Wundversorgung GmbH + Co. KG, Baxter AG) at 37ºC, 5% CO_2 in a humidified atmosphere with 90% Dulbecco's Modified Eagle's Medium (DMEM; Gibco) supplemented with 10% fetal bovine serum (FBS, Gibco), 100 U/ml penicillin, and 100 µg/ml streptomycin (Gibco). The culture medium was changed every 48 hours and the Petri dishes were observed daily. The cells were passed or were supplied with differentiating medium containing 1.5% of DMSO once they reached approximately 80% confluence, mostly 48 hours after plating (and before the rats' surgery). The differentiating medium was composed of 96% DMEM supplemented with 2.5 % of FBS, 100 U/ml penicillin, 100 µg/ml streptomycin and 1.5% of DMSO (6-10).

6.2 Surgical procedure

Adult male Sasco Sprague Dawley rats (Charles River Laboratories, Barcelona, Spain) weighing 300-350 g, were randomly divided in 3 groups of 6 or 7 animals each. All animals were housed in a temperature and humidity controlled room with 12-12 hours light / dark cycles, two animals per cage (Makrolon type 4, Tecniplast, VA, Italy), and were allowed normal cage activities under standard laboratory conditions. The animals were fed with standard chow and water ad libitum. Adequate measures were taken to minimize pain and discomfort taking in account human endpoints for animal suffering and distress. Animals were housed for two weeks before entering the experiment. For surgery, rats were placed prone under sterile conditions and the skin from the clipped lateral right thigh scrubbed in a routine fashion with antiseptic solution. The surgeries were performed under an M-650 operating microscope (Leica Microsystems, Wetzlar, Germany). Under deep anaesthesia (ketamine 90 mg/Kg; xylazine 12.5 mg/Kg, atropine 0.25 mg/Kg i.m.), the right sciatic nerve was exposed through a skin incision extending from the greater trochanter to the mid-thigh distally followed by a muscle splitting incision. After nerve mobilisation, a transection injury was performed (neurotmesis) immediately above the terminal nerve ramification using straight

microsurgical scissors. Rats were then randomly assigned to three experimental groups. In one group (End-to-End), immediate cooptation with 7/0 monofilament nylon epineurial sutures of the 2 transected nerve endings was performed, in a second group (End-to-EndMemb) nerve transection was reconstructed by end-to-end suture, like in the first group, and then enveloped by a membrane of equine collagen type III. In a third group (End-to-EndMembCell) animals received the same treatment as the previous group but with equine collagen type III membranes covered with neural cells differentiated in vitro. Sciatic nerves from the contralateral site were left intact in all groups and served as controls. To prevent autotomy, a deterrent substance was applied to rats' right foot (34; 35). The animals were intensively examined for signs of autotomy and contracture during the postoperative and none presented severe wounds, infections or contractures. All procedures were performed with the approval of the Veterinary Authorities of Portugal in accordance with the European Communities Council Directive of November 1986 (86/609/EEC).

6.3 Functional assessment

Evaluation of motor performance (EPT) and nociceptive function (WRL)

Motor performance and nociceptive function were evaluated by measuring extensor postural thrust (EPT) and withdrawal reflex latency (WRL), respectively. The animals were tested pre-operatively (week-0), at weeks 1, 2, and every two weeks thereafter until week-20. The animals were gently handled, and tested in a quiet environment to minimize stress levels. The EPT was originally proposed by Thalhammer and collaborators, in 1995 (36) as a part of the neurological recovery evaluation in the rat after sciatic nerve injury. For this test, the entire body of the rat, excepting the hind-limbs, was wrapped in a surgical towel. Supporting the animal by the thorax and lowering the affected hind-limb towards the platform of a digital balance, elicits the EPT. As the animal is lowered to the platform, it extends the hind-limb, anticipating the contact made by the distal metatarsus and digits. The force in grams (g) applied to the digital platform balance (model TM 560; Gibertini, Milan, Italy) was recorded. The same procedure was applied to the contralateral, unaffected limb. Each EPT test was repeated 3 times and the average result was considered. The normal (unaffected limb) EPT (NEPT) and experimental EPT (EEPT) values were incorporated into an equation (Equation 8) to derive the functional deficit (varying between 0 and 1), as described by Koka and Hadlock, in 2001 (37).

Motor Deficit = (NEPT – EEPT) / NEPT

Equation 8 EPT formula

To assess the nociceptive withdrawal reflex (WRL), the hotplate test was modified as described by Masters and collaborators (38). The rat was wrapped in a surgical towel above its waist and then positioned to stand with the affected hind paw on a hot plate at 56ºC (model 35-D, IITC Life Science Instruments, Woodland Hill, CA). WRL is defined as the time elapsed from the onset of hotplate contact to withdrawal of the hind paw and measured with a stopwatch. Normal rats withdraw their paws from the hotplate within 4.3 s or less (39). The affected limbs were tested 3 times, with an interval of 2 min between consecutive tests to prevent sensitization, and the three latencies were averaged to obtain a final result (40; 41). If there was no paw withdrawal after 12 s, the heat stimulus was removed to prevent tissue damage, and the animal was assigned the maximal WRL of 12 s (42).

Kinematic Analysis

Ankle kinematics during the stance phase of the rat walk was recorded prior nerve injury (week-0), at week-2 and every 4 weeks during the 20-week follow-up time. Animals walked on a Perspex track with length, width and height of respectively 120, 12, and 15 cm. In order to ensure locomotion in a straight direction, the width of the apparatus was adjusted to the size of the rats during the experiments, and a darkened cage was placed at the end of the corridor to attract the animals. The rats gait was video recorded at a rate of 100 images per second (JVC GR-DVL9800, New Jersey, USA). The camera was positioned perpendicular to the mid-point of the corridor length at a 1-m distance thus obtaining a visualization field of 14-cm wide. Only walking trials with stance phases lasting between 150 and 400 ms were considered for analysis, since this corresponds to the normal walking velocity of the rat (20–60 cm/s) (42-44). The video images were stored in a computer hard disk for latter analysis using an appropriate software APAS® (Ariel Performance Analysis System, Ariel Dynamics, San Diego, USA). 2-D biomechanical analysis (sagittal plan) was carried out applying a two-segment model of the ankle joint, adopted from the model firstly developed by Varejão and collaborators (8; 42-44). Skin landmarks were tattooed at points in the proximal edge of the tibia, in the lateral malleolus and, in the fifth metatarsal head. The rats' ankle angle was determined using the scalar product between a vector representing the foot and a vector representing the lower leg. With this model, positive and negative values of position of the ankle joint indicate dorsiflexion and plantarflexion, respectively. For each stance phase the following time points were identified: initial contact (IC),

opposite toe-off (OT), heel-rise (HR) and toe-off (TO) (8; 42-44), and were time normalized for 100% of the stance phase. The normalized temporal parameters were averaged over all recorded trials. Angular velocity of the ankle joint was also determined where negative values correspond to dorsiflexion. Four steps were analysed for each animal (8).

Histological and Stereological analysis

A 10-mm-long segment of the sciatic nerve distal to the site of lesion was removed, fixed, and prepared for quantitative morphometry of myelinated nerve fibers. A 10-mm segment of uninjured sciatic nerve was also withdrawn from control animals (N=6). The harvested nerve segments were immersed immediately in a fixation solution containing 2.5% purified glutaraldehyde and 0.5% saccarose in 0.1M Sorensen phosphate buffer for 6-8 hours. Specimens were processed for resin embedding as described in details elsewhere (45; 46). Series of 2-µm thick semi-thin transverse sections were cut using a Leica Ultracut UCT ultramicrotome (Leica Microsystems, Wetzlar, Germany) and stained by Toluidine blue for stereological analysis of regenerated nerve fibers. The slides were observed with a DM4000B microscope equipped with a DFC320 digital camera and an IM50 image manager system (Leica Microsystems, Wetzlar, Germany). One semi-thin section from each nerve was randomly selected and used for the morpho-quantitative analysis. The total cross-sectional area of the nerve was measured and sampling fields were then randomly selected using a protocol previously described (46-48). Bias arising from the "edge effect" was coped with the employment of a two-dimensional disector procedure which is based on sampling the "tops" of fibers (49; 50). Mean fiber density in each disector was then calculated by dividing the number of nerve fibers counted by the disector's area (N/mm^2). Finally, total fiber number (N) in the nerve was estimated by multiplying the mean fiber density by the total cross-sectional area of the whole nerve. Two-dimensional disector probes were also used for the unbiased selection of a representative sample of myelinated nerve fibers for estimating circle-fitting diameter and myelin thickness. Precision and accuracy of the estimates were evaluated by calculating the coefficient of variation (CV=SD/mean) and coefficient of error (CE=SEM/mean) (46-48).

7 Statistical analysis

Two-way mixed factorial ANOVA was used to test for the effect of time in the *End-to-End* group (within subjects effect; 12 time points) and experimental groups (between subjects effect, 3 groups). The sphericity assumption was evaluated by the Mauchly's test and when this test could not be computed or when sphericity assumption was violated, adjustment of the degrees of freedom was done with the Greenhouse-Geiser's epsilon. When time main effect was significant (within subjects factor), simple planned contrasts (General Linear Model, simple contrasts) were used to compare pooled data across the three experimental groups along the recovery with data at week-0. When a significant main effect of treatment existed (between subjects factor), pairwise comparisions were carried out using the Tukey's HSD test. At week-0, kinematic data was recorded only from the *End-to-End* group so the main effect of time was evaluated only in this group. Evaluation of the main effect of treatment on ankle motion variables used only data after nerve injury. In this case, and when appropriate, pairwise comparisons were made using the Tukey's HSD test. Statistical comparisons of stereological morpho-quantitative data on nerve fibers were accomplished with one-way ANOVA test. Statistical significance was established as $p<0.05$. All statistical procedures were performed by using the statistical package SPSS (version 14.0, SPSS, Inc) except stereological data that were analysed using the software "*Statistica per discipline bio-mediche*" (McGraw-Hill, Milan, Italy). All data in this study is presented as mean ± standard error of the mean (SEM).

8 Results

8.1 Motor deficit and Nociception function

Motor deficit (EPT)

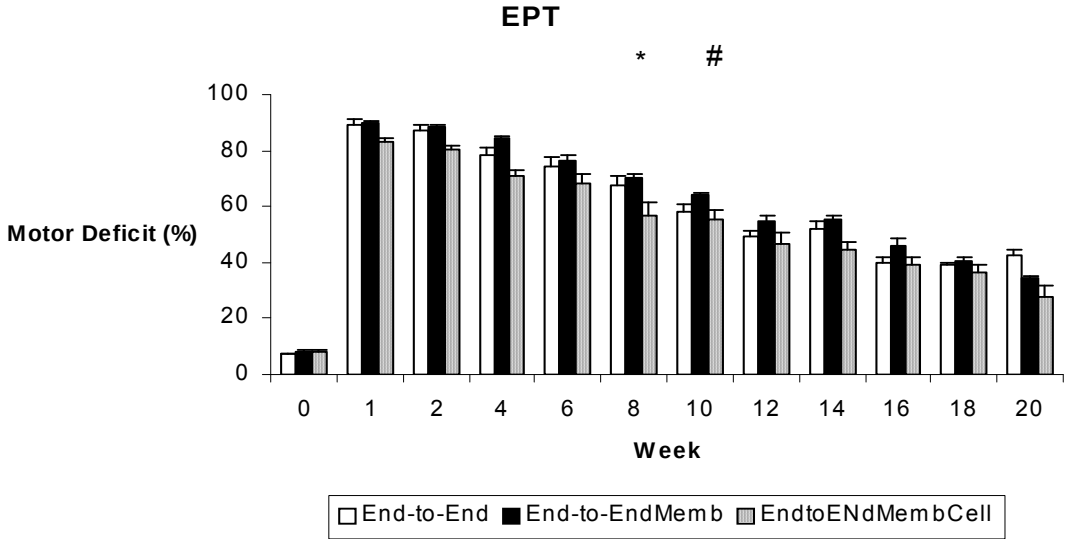

Figure 25 - Weekly values of the percentage of motor deficit obtained by the Extensor Postural Thrust (EPT) test. * Significantly different from week-0 all groups pooled together (p < 0.05). # Group End-to-EndMembCell significantly different from the other groups (p < 0.05). Results are presented as mean and standard error of the mean (SEM).

Before sciatic injury, EPT was similar in both hindlimbs in all experimental groups (Figure 25). In the first week after sciatic nerve transection, near total EPT loss was observed in the operated hindlimb, leading to a motor deficit ranging between 83 to 90%. The EPT response steadily improved during recovery but at week-20 the EPT values of the injured side were still significantly lower compared to values at week-0 ($p<0.05$). A significant main effect for treatment was found [$F(2,17) = 14.202$; $p=0.000$], with pairwise comparisons showing significantly better recovery of the EPT response in the End-to-EndMembCell group when compared to the other two experimental groups ($p<0.05$). At week-20, motor deficit decreased to 27% in the End-to-EndMembCell and to 34% and 42% in the End-to-End and End-to-EndMemb groups, respectively (Figure 25).

Nociception function (WRL)

In the week after sciatic transection, all the animals presented a severe loss of sensory and nociception function acutely after sciatic nerve transection and the WRL test has to be interrupted at the 12 s-cutoff time (Figure 26). During the following weeks there was recovery in paw nociception which was more clearly seen between weeks 6 and 8 post-surgery. At week-6, half of the animals still had no withdrawal response to the noxious thermal stimulus in the operated side, which is in contrast with week-8, when all animals presented a consistent, although delayed, response. Despite such improvement in WRL response, contrast analysis showed persistence of sensory deficit in all groups by the end of the 20-weeks recovery time ($p<0.05$). No differences between the groups was observed in the level of WRL impairment after the sciatic nerve transection [$F_{(2,17)} = 1.563$; $p=0.238$].

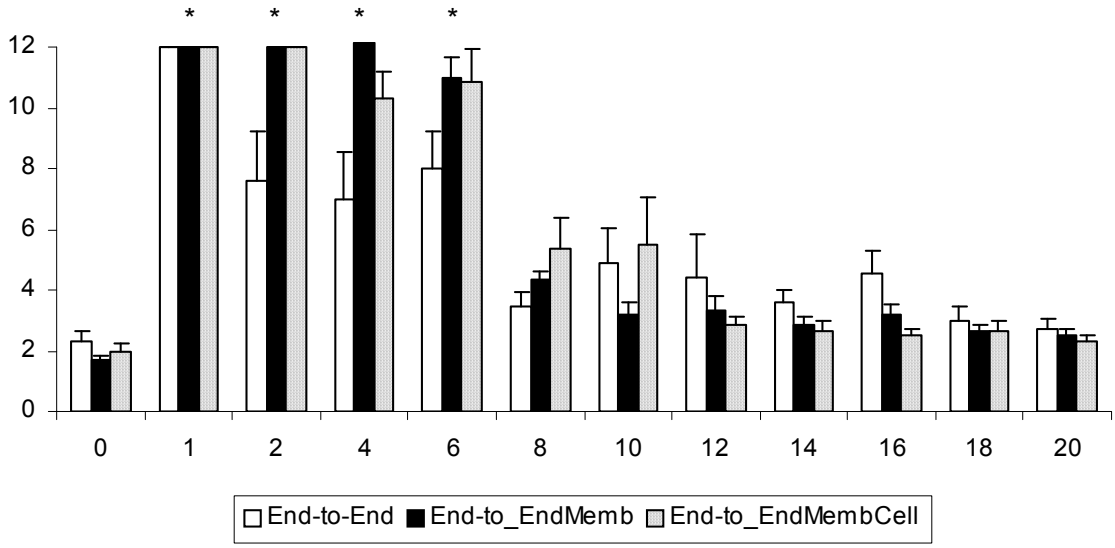

Figure 26 - Weekly values of the withdrawal reflex latency test. At week-1 all animals failed in responding to the noxious thermal stimulus within the 12 sec cut-off time. No differences between the percentages of motor deficit obtained by the Extensor Postural Thrust (EPT) test. * Significantly different from week-0 all groups pooled together ($p < 0.05$). Results are presented as mean and standard error of the mean (SEM).

Kinematics Analysis

Figure 27 and Figure 28 display the mean plots, respectively for ankle joint angle and ankle joint velocity during the stance phase of the rat walk. Comparisons to the normal ankle motion can only be draw for the *End-to-End* group for reasons explained in the Methods section. In the weeks following sciatic nerve transection, ankle joint motion became severely abnormal, particularly throughout the second half of stance corresponding to the push-off sub-phase. In clear contrast to the normal pattern of ankle movement, at week-2 post-injury animals were unable to extend this joint and dorsiflexion continued increasing during the entire stance, which is explained by the paralysis of plantarflexor muscles. The pattern of the ankle joint motion seemed to have improved only slightly during recovery. Contrast analysis was performed for each of the kinematic parameters (Table 1 and Table 2) with somewhat different results. For OT velocity and HR angle no differences existed before and after sciatic nerve transection, whereas for OT angle differences from pre-injury values were significant only at weeks 2 and 16 of recovery ($p<0.05$). The angle at IC showed a unique pattern of changes, being unaffected at week-2 post-injury and altered from normal in the following weeks of recovery. Probably the most consistent results are those of HR velocity, TO angle and TO velocity. These parameters were affected immediately after the nerve injury and remained abnormal along the entire 20-weeks recovery period ($p<0.05$). The effect of the different tissue engineering strategies was assessed comparing the kinematic data of the experimental groups only during the recovery period (see Methods). Statistical analysis demonstrated that the collagen membrane and the cells had no or little effect on ankle motion pattern recovery. Generally, no differences in the kinematic parameters were found between the groups. Exceptions were IC velocity in the *End-to-EndMembCell* group, which was different from the other two groups ($p<0.05$), and OT angle in the *End-to-EndMemb* group that was also different from the other two groups ($p<0.05$).

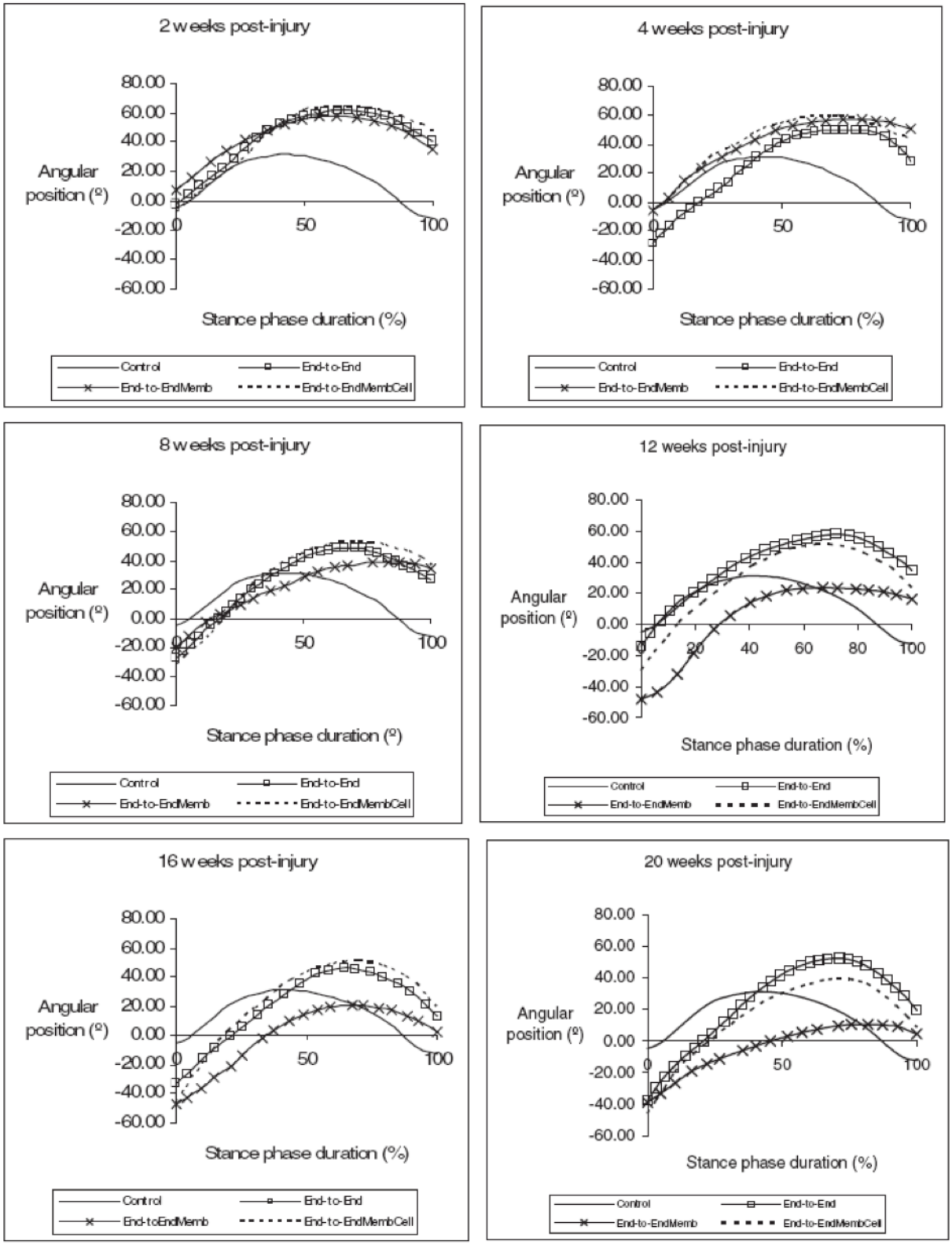

Figure 27- Kinematics plots in the sagittal plane for the angular position (°) of the ankle as it moves through the stance phase, during the healing period of 20 weeks. The mean of each group is plotted

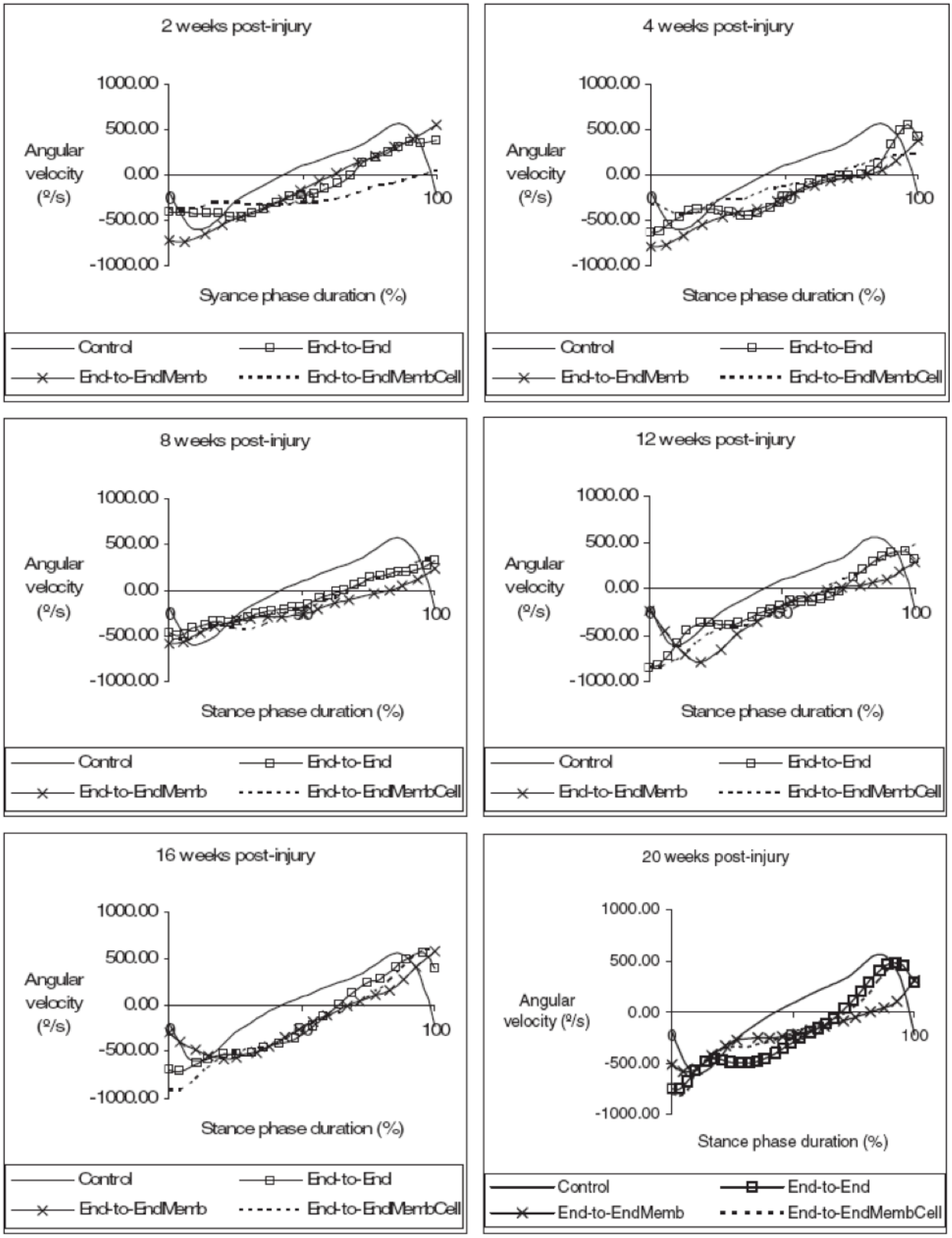

Figure 28 - Kinematics plots in the sagittal plane for the angular velocity (°/s) of the ankle as it moves through the stance phase, during the healing period of 20 weeks. The mean of each group is plotted.

Table 1- Ankle kinematics and stance duration analysis were carried out prior to nerve injury (week-0), at week-2, and every 4 weeks during the 20-week follow-up period.

Temporal Parameter		Week 0	Week 2	Week 4	Week 8	Week 12	Week 16	Week 20
IC	End-to-End	-4.84 ± 3.00	2.70 ± 1.29	-30.11 ± 5.38	-20.88 ± 4.22	-28.36 ± 3.84	-38.92 ± 4.82	-52.83 ± 6.46
	End-to-EndMemb		7.19 ± 2.94	-6.25 ± -2.55	-19.65 ± -8.02	-48.15 ± -19.66	-46.87 ± -19.13	-39.03 ± -15.93
	End-to-EndMembCell		4.95 ± 0.68	-31.59 ± 12.98	-23.79 ± 2.47	-29.57 ± 5.74	-42.25 ± 11.38	-46.04 ± 9.29
OT	End-to-End	25.65 ± 1.08	36.74 ± 4.71	18.75 ± 2.81	25.58 ± 8.88	24.79 ± 2.62	4.71 ± 4.35	16.61 ± 3.96
	End-to-EndMemb		20.37 ± 4.61	21.54 ± 9.92	9.78 ± 18.75	4.26 ± 18.44	-19.51 ± 16.74	-18.70 ± 20.74
	End-to-EndMembCell		33.15 ± 2.98	25.08 ± 4.86	28.15 ± 8.57	24.54 ± 8.91	21.75 ± 5.76	16.47 ± 6.73
HR	End-to-End	30.67 ± 2.44	51.20 ± 4.50	40.03 ± 2.21	36.82 ± 5.96	34.01 ± 5.87	34.30 ± 3.35	40.37 ± 4.75
	End-to-EndMemb		52.46 ± 2.16	48.04 ± 5.49	29.65 ± 22.49	20.89 ± 21.10	11.57 ± 20.18	4.16 ± 26.71
	End-to-EndMembCell		54.80 ± 2.44	44.16 ± 3.90	46.41 ± 6.68	43.69 ± 6.09	41.53 ± 6.66	29.08 ± 7.55
TO	End-to-End	-12.27 ± 7.01	41.49 ± 3.23	39.33 ± 3.03	27.28 ± 1.38	28.04 ± 3.11	15.02 ± 3.78	12.16 ± 3.43
	End-to-EndMemb		35.56 ± 1.69	50.77 ± 4.41	34.64 ± 21.86	16.36 ± 20.87	2.12 ± 18.58	4.60 ± 25.45
	End-to-EndMembCell		48.10 ± 1.60	44.76 ± 4.17	36.40 ± 6.11	23.37 ± 4.02	18.64 ± 5.76	8.71 ± 4.20

Values of the ankle angular position (°) at initial contact (IC); opposite toe-off (OT); heel-rise (HR); toe-off (TO) of the stance phase. Results are presented as mean and standard error of the mean (SEM). N corresponds to the number of rats within the experimental group.

Table 2- Ankle kinematics and stance duration analysis were carried out prior to nerve injury (wek-0), at week-2, and every 4 weeks during the 20-week follow-up period.

Temporal Parameter		Week 0	Week 2	Week 4	Week 8	Week 12	Week 16	Week 20
IC	End-to-End	-194.15 ± 44.35	-448.33 ± 66.25	-604.86 ± 66.95	-351.64 ± 73.81	-639.43 ± 120.70	-809.90 ± 88.67	-647.63 ± 81.94
	End-to-EndMemb		-728.48 ± -297.40	-785.62 ± -320.73	-593.43 ± -242.26	-234.56 ± -95.76	-302.06 ± -123.31	-514.54 ± -210.06
	End-to-EndMembCell		-557.10 ± 224.85	-505.97 ± 108.58	-845.50 ± 160.47	-933.63 ± 57.41	-914.05 ± 80.10	-903.24 ± 74.55
OT	End-to-End	-270.35 ± 19.65	-273.97 ± 47.92	-385.24 ± 37.99	-399.28 ± 34.85	-530.42 ± 68.29	-460.90 ± 66.08	-414.22 ± 35.18
	End-to-EndMemb		-641.95 ± -262.08	-528.60 ± -215.80	-321.92 ± -131.42	-449.49 ± -183.50	-582.66 ± -237.87	-411.32 ± -167.92
	End-to-EndMembCell		-357.80 ± 43.21	-495.68 ± 82.13	-372.17 ± 33.65	-467.31 ± 76.14	-471.29 ± 20.94	-278.67 ± 20.71
HR	End-to-End	53.25 ± 40.58	-177.64 ± 41.45	-246.61 ± 11.49	-333.55 ± 16.41	-280.20 ± 24.32	-322.47 ± 18.46	-322.86 ± 23.80
	End-to-EndMemb		-265.19 ± 28.15	-301.10 ± 65.99	-268.48 ± 64.92	-114.06 ± 82.52	-327.76 ± 86.17	-222.91 ± 51.33
	End-to-EndMembCell		-353.02 ± 24.39	-285.60 ± 21.13	-190.41 ± 9.69	-286.61 ± 57.54	-283.54 ± 12.24	-216.29 ± 21.36
TO	End-to-End	-221.38 ± 91.28	322.87 ± 109.64	327.44 ± 31.23	399.79 ± 82.70	403.59 ± 57.88	444.05 ± 78.95	193.03 ± 130.15
	End-to-EndMemb		554.31 ± 69.27	384.52 ± 66.65	227.17 ± 123.13	281.98 ± 79.91	577.14 ± 155.51	311.14 ± 197.88
	End-to-EndMembCell		248.78 ± 30.40	420.52 ± 28.58	355.25 ± 43.90	466.17 ± 43.54	551.88 ± 43.74	460.01 ± 51.01

Values of the ankle angular velocity (°/sec) at initial contact (IC); opposite toe-off (OT); heel-rise (HR); toe-off (TO) of the stance phase. Results are presented as mean and standard error of the mean (SEM). N corresponds to the number of rats within the experimental group.

8.2 Histological and Stereological Analysis

Table 3- Stereological quantitative assessment density, total number, diameter and myelin thickness of regenerated sciatic nerve fibers at week-20 after neurotmesis. Values are presented as mean ± SEM.

	N/mm^2 Density	N Number	D Fiber diameter (µm)
EndtoEnd	20,612 ± 1,607	14,624 ± 1,642	4.06 ± 0.30
EndtoEndMemb	23,575 ± 1,018	15,101 ± 1,172	3.87 ± 0.18
EndtoEndMembCell	22,394 ± 1,750	14,467 ± 1,524	3.96 ± 0.21
Control	15,905 ± 287	7,666 ± 190	6.66 ± 0.12

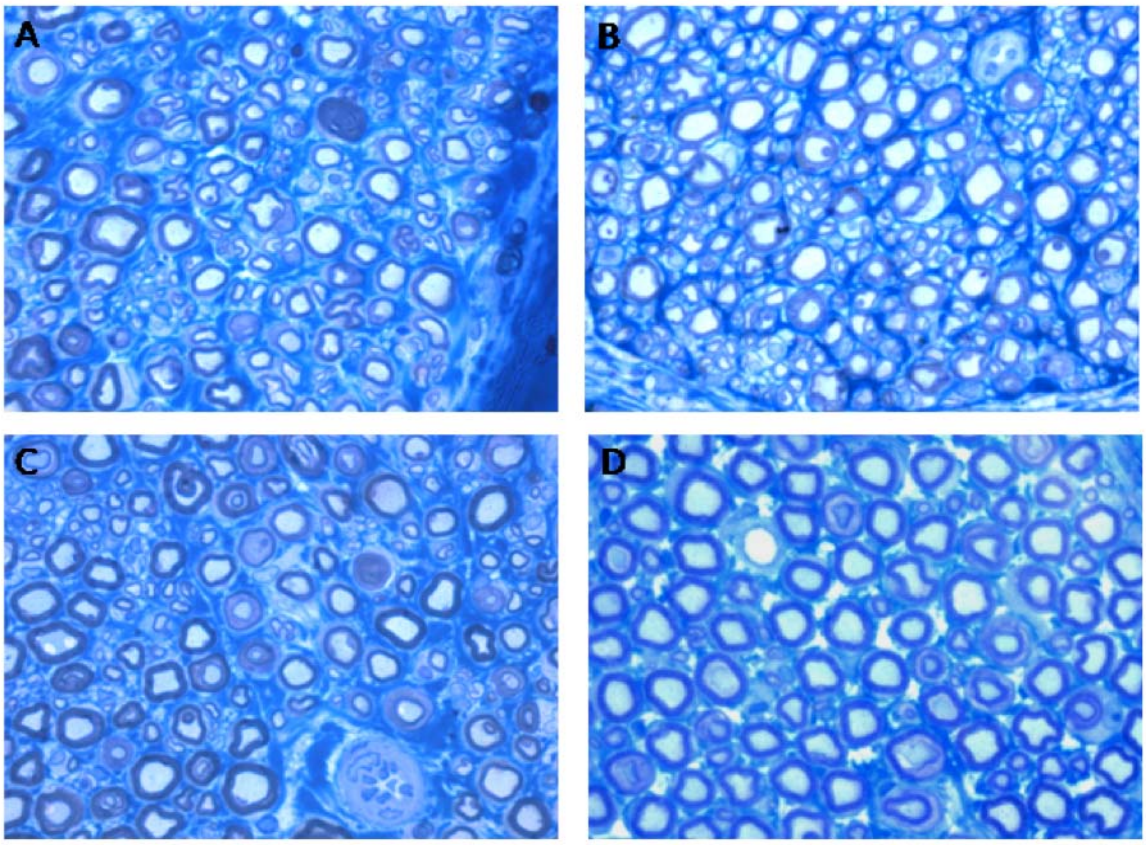

Figure 29 - Representative high resolution photomicrographs of nerve fibers form regenerated (A-C) and normal (D) rat sciatic nerves. A: End-to-End. B:End-to-EndMemb. C:End-to-EndMembCell. Magnification = × 1,500.

Figure 29 shows representative light micrographs of the regenerated sciatic nerves of the three groups (Figure 29A-C) and control sciatic normal nerves (Figure 29D). As expected, regeneration of axons was organized in many smaller fascicles in comparison to controls. The results of the stereological analysis of myelinated nerve fibers are reported in Table 3. Statistical analysis by ANOVA test revealed no significant ($p>0.05$) difference regarding any of the morphological parameters investigated in the regenerated axons from the three experimental groups. On the other hand, comparison between regenerated and control nerves showed, as expected, the presence of a significantly ($p<0.05$) higher density and total number of myelinated axons in experimental groups accompanied by a significantly ($p<0.05$) lower fiber diameter.

9 DISCUSSION

Transected peripheral nerves can regenerate provided that a connection is available between the proximal and distal severed stumps and, when no substance loss occurred; surgical treatment consists in direct end-to-end suturing of the nerve ends (2; 3). However, in spite of the progress of microsurgical nerve repair, the outcome of nerve reconstruction is still far from being optimal (51). Since during regeneration axons require neurotrophic support, they could benefit from the presence of a growth factors delivery cell system capable of responding to stimuli of the local environment during axonal regeneration.

In the present study, we aimed at investigating the effects of enwrapping the site of end-to-end rat sciatic nerve repair with equine type III collagen nerve membranes either alone or enriched with N1E-115 pre-differentiated into neural cells in the presence of 1.5% of DMSO. The rationale for the utilization of the N1E-115 cells was to take advantages of the properties of these cells as a neural-like cellular source of neurotrophic factors (6-10).

Results showed that enwrapment with a collagen membrane, with or without neural cell enrichment, did not lead to any significant improvement in most of functional and stereological predictors of nerve regeneration that we have assessed. The only exception was represented by motor deficit recovery which was significantly improved after lesion site enwrapment with membrane enriched with neural cells pre-differentiated from N1E-115 cell line.

Natural tissues possess several advantages when compared to synthetic materials, when use to reconstruct peripheral nerves after injury. Natural materials are more likely to be biocompatible than artificial materials, are less toxic, and provide a support structure to promote cell adhesion and migration. Drawbacks, on the other hand, include potential difficulties with isolation and controlled scale-up. In addition to intact acellular tissues, a great deal of research has focused on the use of purified natural ECM proteins and glycosaminoglycans, which can be modified to serve as appropriate scaffolding. ECM molecules, such as laminin, collagen, and fibronectin, have been shown to play a significant role in axonal development and repair in the body (24; 52). There are a number of examples in which the ECM proteins laminin, fibronectin, and collagen have been used for nerve repair applications (21; 23-25; 52-56). For example, silicone tubes filled with laminin, fibronectin, and collagen show improved regeneration over a 10 mm rat sciatic nerve gap compared to empty silicone controls (14). Collagen

filaments have also been used to guide regenerating axons across 20–30 mm defects in rats (25; 26; 57). Further studies have shown that oriented fibers of collagen within gels, aligned using magnetic fields, provide an improved template for neurite extension compared to randomly oriented collagen fibers (22; 27). Rates of regeneration after neurotmesis comparable to those using a nerve autograft have been achieved using collagen tubes containing a porous collagen-glycosaminoglycan matrix (29; 30).

Results of this study contribute to the lively debate about the employment of cell transplantation for improving post-traumatic nerve regeneration (58; 59). Actually, a great enthusiasm among researchers and especially the public opinion has risen over the last years about cell-based therapies in Regenerative Medicine (60-62) and there seems to be widespread conviction that this type of therapy is not only effective but also very safe in comparison to other pharmacological or surgical therapeutic approaches. By contrast, recent studies showed that cell-based therapy might be ineffective for improving nerve regeneration [66-69], and results of the present study are in line with these observations. Recently, it has even been shown that N1E-115 cell transplantation can also have negative results by hindering the nerve regeneration process after tubulisation repair (17). Of course, the choice of the cell type to be used for transplantation is very important for the therapeutic success and use of another cell type could have led to better results, especially when the cellular system of choice is derived from autologous or heterologous stem cells1 (17-20; 58; 63). Moreover, the construction of more appropriate tube-guides with integrated growth factor delivery systems and/or cellular components could improve the effectiveness of nerve tissue engineering. In fact, single-molded tube guides may not give sufficient control over both the mechanical properties and the delivery of bioactive agents. More complex devices will be needed, such as multilayered tube guides where growth factors are entrapped in polymer layers with varying physicochemical properties or tissue engineered tube guides containing viable stem cells (17-20; 58; 63). The combination of two or more growth factors will likely exert a synergistic effect on nerve regeneration, especially when the growth factors belong to different families and act via different mechanisms. Combinations of growth factors can be expected to enhance further nerve regeneration, particularly when each of them is delivered at individually tailored kinetics (16-20; 58; 63). The determination and control of suitable delivery kinetics for each of several growth factors will constitute a major hurdle both technically and biologically with the biological hurdle lying in the compliance with the naturally occurring cross talk between growth factors and cells. A solution to this problem may be the use of

autologous stem cells because they can synthesize several growth factors and differentiate into Schwann cells which are critical for very long gaps (16-20; 58; 63).
Previous work already published by other research groups, point out a very interesting source of stem cells for nerve regeneration of peripheral nerve and spinal cord. They developed hair follicle pluripotent stem cells (hfPS) and have shown that these cells can differentiate to neurons, glial cells *in vitro*, and other cell types, and can promote nerve and spinal cord regeneration *in vivo*. These cells are located above the hair follicle bulge (hfPS cell area) and are nestin and CD34 positive, and keratin 15 negative (64-67). The mouse hfPS cells were implanted into the gap region of the severed sciatic and tibial nerve of mice. These cells, after 6-8 weeks, transdifferentiated largely into Schwann cells. Also, blood vessels formed a network around the joined sciatic and tibial nerve. Function of the rejoined sciatic and tibial nerve was confirmed by contraction of the gastrocnemius muscle upon electrical stimulation and by walking track analysis (64-66). hfPS cells can promote axonal growth and functional recovery after peripheral nerve injury, offering an important opportunity for future clinical application. These hfPS cells, in contrast to Embrionic stem cells, N1E-115 cells after *in vitro* differentiation and induced pluripotent stem cells, do not require any genetic manipulation, are readily accessible from any patient, and lack the ethical issues, do not form tumors.

References

1. Lundborg G. Alternatives to autologous nerve grafts. [Internet]. Handchirurgie, Mikrochirurgie, plastische Chirurgie. 2004 Feb ;36(1):1-7.
2. Matsuyama T, Mackay M, Midha R. Peripheral nerve repair and grafting techniques: a review [Internet]. Neurologia medico-chirurgica. 2000 ;40(4):187–199.
3. Siemionow M, Brzezicki G. Chapter 8: Current techniques and concepts in peripheral nerve repair. [Internet]. International review of neurobiology. 2009 Jan ;87141-72.
4. Kimhi Y, Palfrey C, Spector I, Barak Y, Littauer UZ. Maturation of neuroblastoma cells in the presence of dimethylsulfoxide. [Internet]. Proceedings of the National Academy of Sciences of the United States of America. 1976 Feb ;73(2):462-6.
5. Prasad KN, Kentroti S, Edwards-Prasad J, Vernadakis A, Imam M, Carvalho E, et al. Modification of the expression of adenosine 3',5'-cyclic monophosphate-induced differentiated functions in neuroblastoma cells by beta-carotene and D-alpha-tocopheryl succinate. [Internet]. Journal of the American College of Nutrition. 1994 Jun ;13(3):298-303.
6. Rodrigues JM, Luís AL, Lobato JV, Pinto MV, Faustino A, Hussain NS, et al. Intracellular Ca2+ concentration in the N1E-115 neuronal cell line and its use for peripheric nerve regeneration. [Internet]. Acta médica portuguesa. 2005 ;18(5):323-8.
7. Rodrigues JM, Luís AL, Lobato JV, Pinto MV, Lopes MA, Freitas M, et al. Determination of the intracellular Ca2+ concentration in the N1E-115 neuronal cell line in perspective of its use for peripheric nerve regeneration. [Internet]. Bio-medical materials and engineering. 2005 Jan ;15(6):455-65.
8. Luís AL, Amado S, Geuna S, Rodrigues JM, Simões MJ, Santos JD, et al. Long-term functional and morphological assessment of a standardized rat sciatic nerve crush injury with a non-serrated clamp. [Internet]. Journal of neuroscience methods. 2007 Jun ;163(1):92-104.
9. Luís AL, Rodrigues JM, Geuna S, Amado S, Simões MJ, Fregnan F, et al. Neural cell transplantation effects on sciatic nerve regeneration after a standardized crush injury in the rat. [Internet]. Microsurgery. 2008 Jan ;28(6):458-70.

10. Amado S, Simões MJ, Armada da Silva PAS, Luís AL, Shirosaki Y, Lopes MA, et al. Use of hybrid chitosan membranes and N1E-115 cells for promoting nerve regeneration in an axonotmesis rat model. [Internet]. Biomaterials. 2008 Nov ;29(33):4409-19.
11. Doolabh VB, Hertl MC, Mackinnon SE. The role of conduits in nerve repair: a review. [Internet]. Reviews in the neurosciences. 7(1):47-84.
12. Jensen JN, Tung THH, Mackinnon SE, Brenner MJ, Hunter DA. Use of anti-CD40 ligand monoclonal antibody as antirejection therapy in a murine peripheral nerve allograft model. [Internet]. Microsurgery. 2004 Jan ;24(4):309-15.
13. Geuna S, Papalia I, Tos P. End-to-side (terminolateral) nerve regeneration: a challenge for neuroscientists coming from an intriguing nerve repair concept. [Internet]. Brain research reviews. 2006 Sep ;52(2):381-8.
14. Chen YS, Hsieh CL, Tsai CC, Chen TH, Cheng WC, Hu CL, et al. Peripheral nerve regeneration using silicone rubber chambers filled with collagen, laminin and fibronectin. [Internet]. Biomaterials. 2000 Aug ;21(15):1541-7.
15. Dunnen WF den, Robinson PH, Wessel R van, Pennings AJ, Leeuwen MB van, Schakenraad JM. Long-term evaluation of degradation and foreign-body reaction of subcutaneously implanted poly(DL-lactide-epsilon-caprolactone). [Internet]. Journal of biomedical materials research. 1997 Sep ;36(3):337-46.
16. Schmidt CE, Leach JB. Neural tissue engineering: strategies for repair and regeneration. [Internet]. Annual review of biomedical engineering. 2003 Jan ;5293-347.
17. Luís AL, Rodrigues JM, Geuna S, Amado S, Shirosaki Y, Lee JM, et al. Use of PLGA 90:10 scaffolds enriched with in vitro-differentiated neural cells for repairing rat sciatic nerve defects. [Internet]. Tissue engineering. Part A. 2008 Jun ;14(6):979-93.
18. Battiston B, Raimondo S, Tos P, Gaidano V, Audisio C, Scevola A, et al. Chapter 11: Tissue engineering of peripheral nerves [Internet]. Elsevier; 2009.
19. Zacchigna S, Giacca M. Chapter 20: Gene therapy perspectives for nerve repair. [Internet]. International review of neurobiology. 2009 Jan ;87381-92.
20. Karagoz H, Ulkur E, Uygur F, Senol MG, Yapar M, Turan P, et al. Comparison of regeneration results of prefabricated nerve graft, autogenous nerve graft, and vein graft in repair of nerve defects. [Internet]. Microsurgery. 2009 Jan ;29(2):138-43.

21. Kauppila T, Jyväsjärvi E, Huopaniemi T, Hujanen E, Liesi P. A laminin graft replaces neurorrhaphy in the restorative surgery of the rat sciatic nerve. [Internet]. Experimental neurology. 1993 Oct ;123(2):181-91.
22. Ceballos D, Navarro X, Dubey N, Wendelschafer-Crabb G, Kennedy WR, Tranquillo RT. Magnetically aligned collagen gel filling a collagen nerve guide improves peripheral nerve regeneration. [Internet]. Experimental neurology. 1999 Aug ;158(2):290-300.
23. Toba T, Nakamura T, Lynn AK, Matsumoto K, Fukuda S, Yoshitani M, et al. Evaluation of peripheral nerve regeneration across an 80-mm gap using a polyglycolic acid (PGA)--collagen nerve conduit filled with laminin-soaked collagen sponge in dogs. [Internet]. The International journal of artificial organs. 2002 Mar ;25(3):230-7.
24. Grimpe B, Silver J. The extracellular matrix in axon regeneration. [Internet]. Progress in brain research. 2002 Jan ;137333-49.
25. Yoshii S, Oka M. Peripheral nerve regeneration along collagen filaments. [Internet]. Brain research. 2001 Jan ;888(1):158-162.
26. Itoh S, Takakuda K, Kawabata S, Aso Y, Kasai K, Itoh H, et al. Evaluation of cross-linking procedures of collagen tubes used in peripheral nerve repair. [Internet]. Biomaterials. 2002 Dec ;23(23):4475-81.
27. Dubey N, Letourneau PC, Tranquillo RT. Guided neurite elongation and schwann cell invasion into magnetically aligned collagen in simulated peripheral nerve regeneration. [Internet]. Experimental neurology. 1999 Aug ;158(2):338-50.
28. Archibald SJ, Shefner J, Krarup C, Madison RD. Monkey median nerve repaired by nerve graft or collagen nerve guide tube. [Internet]. The Journal of neuroscience : the official journal of the Society for Neuroscience. 1995 May ;15(5 Pt 2):4109-23.
29. Chamberlain LJ, Yannas IV, Hsu HP, Strichartz G, Spector M. Collagen-GAG substrate enhances the quality of nerve regeneration through collagen tubes up to level of autograft. [Internet]. Experimental neurology. 1998 Dec ;154(2):315-29.
30. Chamberlain LJ, Yannas IV, Hsu HP, Strichartz GR, Spector M. Near-terminus axonal structure and function following rat sciatic nerve regeneration through a collagen-GAG matrix in a ten-millimeter gap. [Internet]. Journal of neuroscience research. 2000 Jun ;60(5):666-77.

31. Fu Y. Contributing Factors to Poor Functional Nerve Repair : Prolonged Denervation Recovery after Delayed. 1995 ;15(May):3886-3895.
32. Tria MA, Fusco M, Vantini G, Mariot R. Pharmacokinetics of nerve growth factor (NGF) following different routes of administration to adult rats. [Internet]. Experimental neurology. 1994 Jun ;127(2):178-83.
33. Amano T, Richelson E, Nirenberg M. Neurotransmitter synthesis by neuroblastoma clones (neuroblast differentiation-cell culture-choline acetyltransferase-acetylcholinesterase-tyrosine hydroxylase-axons-dendrites). [Internet]. Proceedings of the National Academy of Sciences of the United States of America. 1972 Jan ;69(1):258-63.
34. Kerns JM, Braverman B, Mathew A, Lucchinetti C, Ivankovich AD. A comparison of cryoprobe and crush lesions in the rat sciatic nerve. [Internet]. Pain. 1991 Oct ;47(1):31-9.
35. Sporel-Ozakat RE, Edwards PM, Hepgul KT, Savas A, Gispen WH. A simple method for reducing autotomy in rats after peripheral nerve lesions. [Internet]. Journal of neuroscience methods. 1991 Feb ;36(2-3):263-5.
36. Thalhammer JG, Vladimirova M, Bershadsky B, Strichartz GR. Neurologic Evaluation of the Rat during Sciatic Nerve Block with Lidocaine [Internet]. Anesthesiology. 1995 Apr ;82(4):1013-1025.
37. Koka R, Hadlock TA. Quantification of functional recovery following rat sciatic nerve transection. [Internet]. Experimental neurology. 2001 Mar ;168(1):192-5.
38. Masters DB, Berde CB, Dutta SK, Griggs CT, Hu D, Kupsky W, et al. Prolonged regional nerve blockade by controlled release of local anesthetic from a biodegradable polymer matrix. [Internet]. Anesthesiology. 1993 Aug ;79(2):340-6.
39. Hu D, Hu R, Berde CB. Neurologic evaluation of infant and adult rats before and after sciatic nerve blockade. [Internet]. Anesthesiology. 1997 Apr ;86(4):957-65.
40. Campbell JN. Nerve lesions and the generation of pain. [Internet]. Muscle & nerve. 2001 Oct ;24(10):1261-73.
41. Shir Y, Campbell JN, Raja SN, Seltzer Z. The correlation between dietary soy phytoestrogens and neuropathic pain behavior in rats after partial denervation. [Internet]. Anesthesia and analgesia. 2002 Feb ;94(2):421-6.
42. Varejão ASP, Cabrita AM, Meek MF, Bulas-Cruz J, Filipe VM, Gabriel RC, et al. Ankle kinematics to evaluate functional recovery in crushed rat sciatic nerve [Internet]. Muscle & nerve. 2003 ;27(6):706–714.

43. Varejão ASP, Cabrita AM, Geuna S, Patrício J a, Azevedo HR, Ferreira AJ, et al. Functional assessment of sciatic nerve recovery: biodegradable poly (DLLA-epsilon-CL) nerve guide filled with fresh skeletal muscle. [Internet]. Microsurgery. 2003 Jan ;23(4):346-53.
44. Varejão ASP, Cabrita AM, Meek MF, Bulas-Cruz J, Gabriel RC, Filipe VM, et al. Motion of the foot and ankle during the stance phase in rats. [Internet]. Muscle & nerve. 2002 Nov ;26(5):630-5.
45. Di Scipio F, Raimondo S, Tos P, Geuna S. A simple protocol for paraffin-embedded myelin sheath staining with osmium tetroxide for light microscope observation. [Internet]. Microscopy research and technique. 2008 Jul ;71(7):497-502.
46. Raimondo S, Fornaro M, Di Scipio F, Ronchi G, Giacobini-Robecchi MG, Geuna S. Chapter 5: Methods and protocols in peripheral nerve regeneration experimental research: part II-morphological techniques. [Internet]. International review of neurobiology. 2009 Jan ;8781-103.
47. Geuna S, Tos P, Battiston B, Guglielmone R. Verification of the two-dimensional disector, a method for the unbiased estimation of density and number of myelinated nerve fibers in peripheral nerves. [Internet]. Annals of anatomy. 2000 Jan ;182(1):23-34.
48. Geuna S, Tos P, Guglielmone R, Battiston B, Giacobini-Robecchi MG. Methodological issues in size estimation of myelinated nerve fibers in peripheral nerves. [Internet]. Anatomy and embryology. 2001 Jul ;204(1):1-10.
49. Geuna S, Gigo-Benato D, Rodrigues A de C. On sampling and sampling errors in histomorphometry of peripheral nerve fibers. [Internet]. Microsurgery. 2004 Jan ;24(1):72-6.
50. Geuna S. The revolution of counting "tops": two decades of the disector principle in morphological research. [Internet]. Microscopy research and technique. 2005 Apr ;66(5):270-4.
51. Gordon T, Sulaiman O, Boyd JG. Experimental strategies to promote functional recovery after peripheral nerve injuries. [Internet]. Journal of the peripheral nervous system : JPNS. 2003 Dec ;8(4):236-50.
52. Rutishauser U. Adhesion molecules of the nervous system. [Internet]. Current opinion in neurobiology. 1993 Oct ;3(5):709-15.
53. Luis AL, Rodrigues JM, Amado S, Veloso AP, Armada-Da-silva PAS, Raimondo S, et al. PLGA 90/10 and caprolactone biodegradable nerve guides for the

reconstruction of the rat sciatic nerve [Internet]. Microsurgery. 2007 ;27(2):125–137.

54. Tong XJ, Hirai K, Shimada H, Mizutani Y, Izumi T, Toda N, et al. Sciatic nerve regeneration navigated by laminin-fibronectin double coated biodegradable collagen grafts in rats. [Internet]. Brain research. 1994 Nov ;663(1):155-62.
55. Whitworth IH, Brown RA, Doré C, Green CJ, Terenghi G. Orientated mats of fibronectin as a conduit material for use in peripheral nerve repair. [Internet]. Journal of hand surgery (Edinburgh, Scotland). 1995 Aug ;20(4):429-36.
56. Ahmed Z, Brown RA. Adhesion, alignment, and migration of cultured Schwann cells on ultrathin fibronectin fibres. [Internet]. Cell motility and the cytoskeleton. 1999 Jan ;42(4):331-43.
57. Yoshii S, Oka M, Shima M, Taniguchi A, Akagi M. 30 mm regeneration of rat sciatic nerve along collagen filaments. [Internet]. Brain research. 2002 Sep ;949(1-2):202-8.
58. Terenghi G, Wiberg M, Kingham PJ. Chapter 21: Use of stem cells for improving nerve regeneration. [Internet]. International review of neurobiology. 2009 Jan ;87393-403.
59. Lundborg G. Enhancing posttraumatic nerve regeneration. [Internet]. Journal of the peripheral nervous system : JPNS. 2002 Oct ;7(3):139-40.[cited 2011 Mar 31] Available from: http://www.ncbi.nlm.nih.gov/pubmed/12365560
60. Tohill M, Terenghi G. Stem-cell plasticity and therapy for injuries of the peripheral nervous system. [Internet]. Biotechnology and applied biochemistry. 2004 Aug ;40(Pt 1):17-24.
61. Pfister LA, Papaloïzos M, Merkle HP, Gander B. Nerve conduits and growth factor delivery in peripheral nerve repair. [Internet]. Journal of the peripheral nervous system : JPNS. 2007 Jul ;12(2):65-82.
62. Chalfoun CT, Wirth GA, Evans GRD. Tissue engineered nerve constructs: where do we stand? [Internet]. Journal of cellular and molecular medicine. 10(2):309-17.
63. Dahlin L, Johansson F, Lindwall C, Kanje M. Chapter 28: Future perspective in peripheral nerve reconstruction. [Internet]. Elsevier; 2009. [cited 2010 Nov 22] Available from: http://www.ncbi.nlm.nih.gov/pubmed/19682657
64. Amoh Y, Kanoh M, Niiyama S, Hamada Y, Kawahara K, Sato Y, et al. Human hair follicle pluripotent stem (hfPS) cells promote regeneration of peripheral-nerve injury: an advantageous alternative to ES and iPS cells. [Internet]. Journal of cellular biochemistry. 2009 Aug ;107(5):1016-20.

65. Amoh Y, Li L, Campillo R, Kawahara K, Katsuoka K, Penman S, et al. Implanted hair follicle stem cells form Schwann cells that support repair of severed peripheral nerves. [Internet]. Proceedings of the National Academy of Sciences of the United States of America. 2005 Dec ;102(49):17734-8.

66. Amoh Y, Li L, Katsuoka K, Penman S, Hoffman RM. Multipotent nestin-positive, keratin-negative hair-follicle bulge stem cells can form neurons. [Internet]. Proceedings of the National Academy of Sciences of the United States of America. 2005 May ;102(15):5530-4.

67. Li L, Mignone J, Yang M, Matic M, Penman S, Enikolopov G, et al. Nestin expression in hair follicle sheath progenitor cells. [Internet]. Proceedings of the National Academy of Sciences of the United States of America. 2003 Aug ;100(17):9958-61.

Chapter 5 - The sensitivity of two-dimensional hindlimb joints kinematics analysis in assessing function in rats after sciatic nerve crush

Amado S, Armada-da-Silva P, João F, Mauricio AC, Luis AL, Simões MJ, et al. The sensitivity of two-dimensional hindlimb joints kinematics analysis in assessing function in rats after sciatic nerve crush. Behavioural brain research. 2011; *submitted*.

1 Introduction

Injury of peripheral nerves is generally followed by abnormal nerve regeneration, axonal misrouting, and incorrect reinnervation of the target organs (1; 2). Intense investigation exists trying to develop new nerve treatments and neurorehabilitation strategies, including alternative surgical techniques (3; 4), the use of biomaterial and cellular systems (5-7), nerve electrical stimulation (8) and different modalities of exercise (9; 10).

The evaluation of the effectiveness of peripheral nerve treating strategies, however, requires accurate assessment of functional recovery, since the latter is the major goal of peripheral nerve treatment and the most important outcome when translating experimental treatment approaches to humans. Notwithstanding, functional assessment in animal models of peripheral nerve injury is a challenging task. The rat sciatic nerve is a widely used model of peripheral nerve injury. In this case, computer-assisted biomechanical analysis of joint motion during walking using video recordings and focusing on ankle joint motion as been shown to be a valid and reliable method to evaluate functional recovery and the reestablishment of proper reinnervation (11-13). When compared to other functional tests, in particular the standard sciatic functional index test, analysis of ankle motion pattern during walking in sciatic-injured rats demonstrates higher sensitivity to motion deficits and shows better relationship with the degree of nerve regeneration (13). Also, recent studies demonstrate that measures of two-dimensional (2D) ankle joint motion during rat walking present good day-to-day and inter-observer reliabilities and are capable of identifying animals carrying injuries to the sciatic, tibial or common peroneal nerves (14).

Joint kinematics during a given movement, such as walking, is usually represented by a trajectory in an angle versus time space. Specific kinematic parameters are then extracted from such trajectories considering particular events that can be unambiguously defined (12; 14; 15). This can result in a varied number of variables that may be used to measure changes in the normal pattern of joint motion. In the case of experimental injury to the sciatic nerve of the rat, authors have focused on the ankle joint kinematics during walking, based on the fact this nerve innervates the muscles crossing this joint (11; 12; 14-16). Some studies limited their walking analyses only to the stance phase, based on the argument that muscles are particularly active during the stance phase in order to support the load of body weight and to generate the power needed to accelerate the body forwardly (5; 11; 12; 17). However, more recent studies have choose to analyze ankle motion during both the stance and swing phases of

walking (14; 18), thus raising the ability to unveil motion deficits of the ankle joint after sciatic nerve injury since this nerve supplies both dorsiflexor and plantarflexor muscles. Also, 2D video analysis of ankle joint motion in the two walking phases is important to distinguish between injuries to the sciatic, tibial or common peroneal nerves (18).

In previous studies we also conducted video recordings of the rat walk in the sagittal plane pre and post sciatic crush injury, measured ankle joint angles at given time points during the stance phase and calculated the angular velocities at these instants of time (5; 11). The angular velocity of the ankle joint motion was used as an attempt to improve the accuracy of ankle kinematic analysis to detect walking dysfunction. In fact, there are cases where results of ankle joint angles are difficult to interpret, raising concerns about their validity as a functional assessment. For example in our previous study (11), we reported in sciatic nerve-crushed rats unchanged ankle angle at the instant of opposite toe off in the early paralytic stage (two weeks post-injury) and altered ankle angle at this time point thereafter and until the end of the twelve weeks follow-up time. Inconsistent results were found also for other ankle kinematics parameters in this study (11), as well as in other studies (14; 19). These suggest that not all ankle kinematic parameters are sensitive to severe functional deficit caused by complete sciatic nerve denervation and therefore are not a valid functional test. Importantly, the use of inaccurate kinematic parameters blurs the results and may become an obstacle to draw sound conclusions.

Sciatic nerve crush is also likely to affect the kinematics of hindlimb joints other than the ankle joint. Motion changes at the hip and knee joints might accompany ankle joint dysfunction during walking either to compensate for the abnormal movement of the ankle joint or else due to higher-level reorganization of the whole hindlimb action in response to long-lasting motor and proprioceptive deficits of the muscles supplied by the sciatic nerve (20). Therefore, it is possible that screening hip and knee motion will enhance the sensitivity and specificity of kinematic analysis of walking in the rat sciatic nerve model. To our knowledge a walking analysis that includes a description of the hip, knee and ankle joint kinematics after sciatic nerve injury has never been performed.

The sensitivity (i.e. the true positive rate) and specificity (i.e. the true negative rate) are two key properties of diagnostic and screening tests. These test properties can be evaluated using linear discriminant analysis particularly if we are talking of multivariate tests that combine several parameters (21). Discriminant analysis simply addresses classification or discrimination in which objects or patterns are classified into one of several distinct populations using a predictive model developed on a set of

independent variables (22). The number of subjects that are correctly classified by the discriminant model provides a measure of the sensitivity of the set of testing variables used in its building. Conversely, the number of subjects misclassified is a measure of the specificity of the test variables. Additionally, discriminant analysis gives information about the relative importance of each of the independent variables in their classification role, yielding a sound basis for discarding variables with little contribution in separating the groups. Therefore, discriminant analysis may be used to identify which are the best walking joint kinematic parameters to assess functional recovery after sciatic nerve injury in the rat.

In this study we conduct a detailed 2D biomechanical analysis of the hip, knee and ankle joints in the rat and employed linear discriminant analysis to assess the sensitivity and specificity of a large set of spatiotemporal and joint kinematic variables as a test of movement dysfunction after sciatic nerve injury. Sciatic nerve-crushed rats in the denervated (one week post injury) and in the reinnervated (twelve weeks post injury) phases were used as they may serve as a model of animals with severe and minor walking deficits, respectively. Sham-operated controls were used as the normal walking group.

2 Methods and Materials

Twenty four male Sprague-Dawley rats (Harlan Laboratories, Udine, Italy) were randomly assigned to one of three groups. A crush injury to the right sciatic nerve was induced in animals in two of the groups, while animals of the third group underwent a sham surgery (Sham). Walking tests were performed one week after sciatic nerve injury, corresponding to a period of complete denervation and paralysis of sciatic-innervated muscles (DEN group) (23), and twelve weeks after either sciatic nerve crush (REINN group) or sham surgery (Sham group). After twelve weeks from a sciatic nerve crush, muscle reinnervation has occurred and functional recovery based on the standard sciatic functional index is complete (11; 24; 25). As a result of the longer follow up time, mean (±SD) weight was higher in the REINN (454.1±15.8 g) and Sham (435.5±17.6) groups, compared to the DEN group (351±5.1 g). All procedures were performed with the approval of the Veterinary Authorities of Portugal in accordance with the European Communities Council Directive of November 1986 (86/609/EEC).
The sciatic crush injury procedure was described in detail elsewhere (11). Briefly, under deep anaesthesia (ketamine 9 mg/100 g; xylazine 1.25 mg/100 g, i.p.), the right sciatic nerve was exposed by skin incision and by splitting the fascia and muscles overlying the nerve. The right sciatic nerve was crushed in the gluteal region, well before its trifurcation point, by applying pressure for 30 s using a non-serrated clamp (25; 26). The muscle, fascia, and skin were closed with 4/0 resorbable sutures. To prevent autotomy, a deterrent substance was applied to the rats' right hindleg and foot [(27; 28). The animals were intensively examined for signs of autotomy and contracture and none of the animals presented severe wounds (absence of a part of the foot or severe infection) or contractures during the study. In sham-operated animals, skin and muscle incisions were performed and the sciatic nerve exposed and mobilized, but no injury was induced to this nerve. All animals were left to recover in their cages with no other measures taken that could enhance nerve regeneration and/or functional recovery.

2.1 Kinematic analysis

An optoelectronic system of six infrared cameras (Oqus-300, Qualisys, Sweden) operating at a frame rate of 200Hz was used to record the motion of the right hindlimb. After shaving, seven reflective markers with 2mm diameter were attached to the skin of the right hindlimb at the following bony prominences: (1) tip of fourth finger, (2) head of

fifth metatarsal, (3) lateral malleolus, (4) lateral knee joint, (5) trochanter major, (6) anterior superior iliac spine, and (7) ischial tuberosity. All markers were placed by the same person. Animals walked on a Perspex track with length, width and height of respectively 120, 12 and 15cm with two darkened cages placed at both ends of the corridor to attract the animals and facilitate walking. Before data collection, all animals performed two or three conditioning trials to be familiarized with the corridor. Cameras were positioned to minimize light reflection artifacts and to allow recording 4 to 5 consecutive walking cycles, defined as the time between two consecutive initial ground contacts (IC) of the right fourth finger. The motion capture space was calibrated regularly using a fixed set of markers and a wand of known length (20 cm) moved across the recorded field. Calibration was accepted when the standard deviation of the wand's length measures was below 0.4 mm. Planar motion in the sagittal plane of the hip, knee and ankle joint was calculated with Visual 3D software (C-Motion, Inc, Germantown, USA) by a computational procedure implementing the dot product between the skeletal segments articulated by these joints. Joint velocity was also calculated using the first derivative of joint angle motion. The trajectory of the reflective markers was smoothed using a Butterworth low-pass filter with a 6 Hz cut-off. Data were obtained by averaging six walking cycles. Each walking cycle was time normalized by interpolation using the longest trial. Our angles convention was: 1) decreasing hip angle value – hip flexion; 2) decreasing knee angle value – knee flexion; 3) positive ankle angle value – dorsiflexion. Positive angular velocity indicates increasing angle values. This also applies to the ankle joint: positive angular velocity signifies increasing dorsiflexion. Joint angle and angular velocity values were measured at the instants of initial ground contact (IC), defined as the time point where horizontal velocity of the toe reflective marker becomes zero, midstance (MSt), the point of fifty per cent duration of the stance phase, toe-off (TO), defined as the instant the horizontal velocity of the toe's reflective marker increases from zero, and midswing (MSw), defined as the point of fifty per cent duration of the swing phase. Additional kinematics parameters recorded included peak angles and angular velocities during both phases of the walking cycle.

Spatiotemporal parameters, including walking velocity, walking cycle duration, stride length, stance duration, and swing duration, were directly given by Visual 3D software based on horizontal displacement of the reflective markers.

Interjoint coordination shape patterns were studied by using cyclograms or else designated angle-angle plots. The angle-angle plots included those of hip-knee, knee-ankle and hip-ankle. Cyclograms perimeters were measured using the euclidean distance between each two consecutive points.

3 Statistical analysis and modelling

Univariate ANOVA was used to test for differences between the groups. Further pairwise comparisons were performed using the Tukey's HSD test.

Linear disciriminant analysis was used to predict walking function and to classify animals after sciatic nerve crush and controls. Four models were tested utilizing spatiotemporal data and joint kinematics data of the hip, knee and ankle joints, separately. For each subset all parameters were employed, meaning using both joint angle and angular velocity in the cases of joint kinematics. Peak angles and angular velocities were excluded from this analysis. The stepwise method was selected to input the criterion variables with the Wilk's Lambda choose as the method for inclusion or rejection of the predictive variables. The leave-one-method was implemented for further model cross-validation. This method is particularly useful when using small samples and when a training sub-sample is not available for unbiased model development. This method operates by having each subject classified by a discriminant model constructed on the basis of data pertaining to the remaining subjects. Data are presented as mean and standard deviation (SD). Statistical analysis was performed using SPSS software package (version 17, SPSS Inc). Statistical significance was accepted at $p<0.05$.

4 Results

4.1 Spatiotemporal parameters

Spatiotemporal data are presented in Table 4. The DEN group had a lower walking velocity and a shorter stride length compared to the Sham group (p=0.005 and p=0.007, for walking velocity and stride length, respectively) but not to the REINN group (p=0.058 and p=0.145, for walking velocity and stride length, respectively). The walking cycle time was longer in the DEN group, again only compared to the Sham group (p=0.046, Sham group; p=0.131, REINN group). The DEN group also showed a significantly longer swing duration, compared to both REINN (p=0.000) and Sham (p=0.000) groups. No differences in spatiotemporal measures were observed between the REINN and the Sham groups.

Table 4 - Mean values for spatiotemporal data for each experimental group; eight animals per group

Groups	Walking velocity (ms^{-1})	Cycle duration (s)	Stride length (m)	Stance time (s)	Swing time (s)
DEN	0.161±0.029[b]	0.852±0.057[b]	0.133±0.003[b]	0.238±0.030	0.175±0.009[a]
REINN	0.210±0.016	0.730±0.035	0.148±0.006	0.258±0.010	0.123±0.002
Sham	0.231±0.014	0.697±0.030	0.160±0.005	0.248±0.015	0.125±0.002

[a]Significantly different from REINN and Sham; p<0.05;

[#b]Significantly different from Sham only; p<0.05

4.2 Joint kinematics

Plots of mean ankle, hip and knee joint angle and angular velocity are shown in Figure 30 with the parameter measures reported in Table 5, Table 6 and Table 7

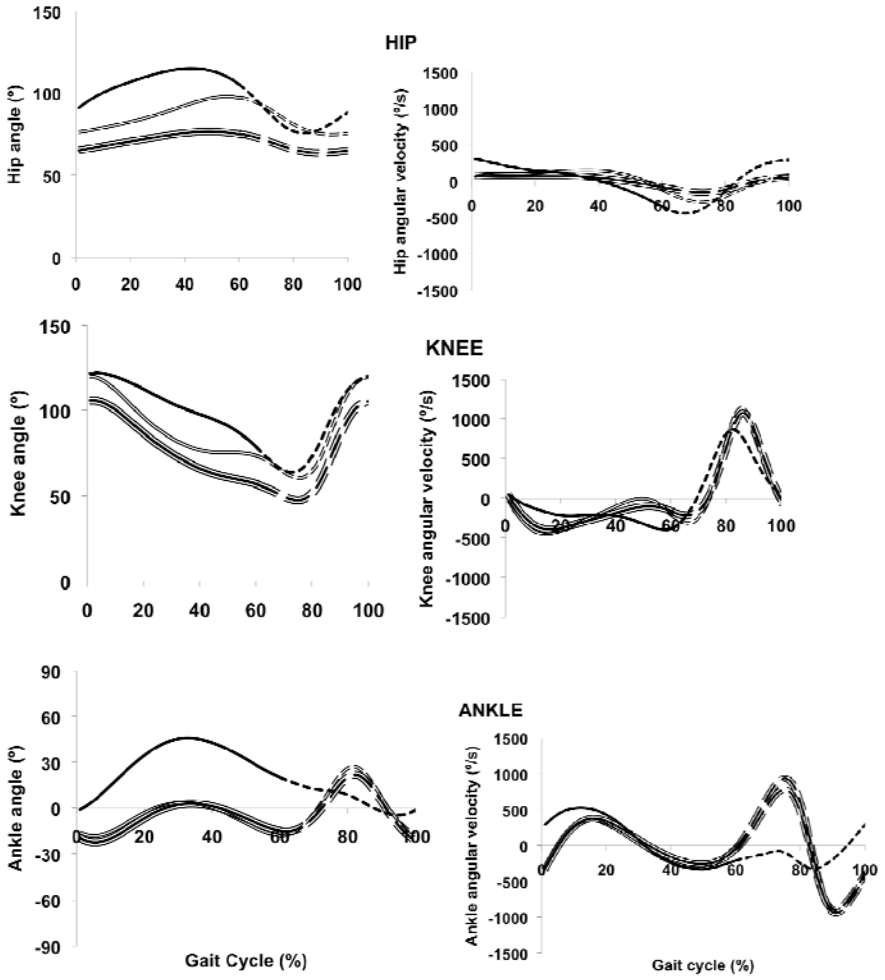

Figure 30 - Mean trajectories for hip (upper graphs), knee (middle graphs) and ankle (lower graphs) joint angle (left hand graphs) and angular velocity (right hand graphs) during the rat's walking cycle. Full lines correspond to the stance phase and dashed lines correspond to the swing phase of the walking cycle. In the hip joint angle, increased extension during the stance phase is visible in the DEN group (single line) as well as the increased flexion in the REINN group (triple line). Also evident, the deep altered ankle kinematics in both stance and swing phases in the DEN group and similar trajectories of ankle angle and angular velocity between the REINN and Sham groups. All groups n=8.

The ankle was the most affected joint after sciatic nerve injury. During the stance phase, the most evident ankle motion change is the higher overall dorsiflexion angle in

the DEN group. In this group, ankle motion is also severely affected across the swing phase, and the characteristic movement of fast dorsiflexion followed by plantarflexion that can be seen in REINN and Sham groups is absent in the DEN group. Accordingly, changes in ankle angular velocity in the DEN group occur mostly during the swing phase and not during the stance phase. In both REINN and Sham groups, ankle's maximal dorsiflexion and plantarflexion angular velocities are recorded during the swing phase, that obviously correspond to a large range of movement of the ankle performed in a short time interval. In the DEN group, these two peak angular velocities are no longer observed and in replace of a large amplitude movement, the ankle performs a slow and small amplitude plantarflexion movement along the entire swing phase. This ankle motion pattern is consistent with total paralysis of the hindleg muscles and loss of contractile force of both the dorsiflexor and plantarflexor muscles caused by complete injury of the motoneuron axons in the sciatic nerve.

Reflecting the deep ankle kinematics changes in the DEN group, ANOVA reveals significant differences between the groups for all ankle kinematics parameters, excepting ankle's angular velocity at MSw ($p=0.192$, Table 5). Pairwise tests showed significant differences in ankle angles and angular velocities between the DEN group and both REINN and Sham groups, excepting for ankle angle at MSw, where the differences were significant only between DEN and Sham groups (11.4±11.3º and 28.1±13.9º, for DEN and Sham groups, respectively, $p<0.05$). Peak dorsiflexion angle during the stance phase was increased in the DEN group comparing with the other two groups (47.42±7.82º, 3.60±14.19º, 4.53±15.19º, DEN, REINN, Sham groups, respectively; both pairwise comparisons, $p=0.000$). No clear peak plantarflexion angle could be identified in animals of the DEN group, either in the stance or in the swing phase. Ankle peak angles and angular velocities during the swing phase in REINN and Sham groups were similar (Table 5).

Hip joint motion was also affected by sciatic nerve crush (Figure 30 and Table 6). Hip joint excursion during walking was considerably increased in the DEN group. This increased range of motion was due to a larger hip extension during the stance phase while hip flexion during the swing phase remained relatively unaffected (Figure 30). Accordingly, hip angular velocity was also higher in the DEN group, than in the REINN and Sham groups (Figure 30). In the DEN group, hip angle at IC, TO, and MSt were significantly different compared to the Sham group ($p<0.05$). Hip joint angle and angular velocity at MSt were different between the REINN and Sham groups ($p=0.046$ and $p=0.034$ for hip angle and velocity, respectively). Hip's peak extension angle occurred at around TO and therefore it was not computed. In the swing phase, a distinct hip flexion peak angle could be noticed only in the DEN group. However, its

value was similar to maximum hip flexion angle in the other groups for the same walking phase (Figure 30). Hip peak flexion and extension velocities were increased in DEN group compared to both REINN and Sham groups.

The changes in knee joint motion with denervation (DEN group) were less pronounced than those registered in ankle and hip joints (Figure 30). The most evident knee angle change in the denervated group is increased knee angle extension, particularly during the stance phase (Table 7). The increased knee extension in the DEN group is likely a compensation for the augmented ankle dorsiflexion and a strategy to maintain the whole limb length. Knee angle changes were also noticed in the REINN group. This group showed increased knee flexion at TO (50.29±15.09º), compared to both Sham (72.50±11.26º, p=0.037) and DEN (79.40±13.55º, p=0.001) groups. Also, peak knee flexion angle during the swing phase was increased in REINN group, compared to the DEN group (p=0.047). This reflected a global increase in knee flexion throughout the entire walking cycle in the REINN group compared to knee motion in sham-control animals (Figure 30). No differences in knee angle at IC and MSw were found between the groups. Knee angular velocity in the DEN group was different from either the Sham or REINN groups at MSt, TO, and MSw. No differences in knee angular velocity were found between REINN and Sham groups. Knee peak flexion velocity during the swing phase was similar in all groups.

Table 5 - Mean values for ankle joint angle and angular velocity for each experimental group; eight animals per group

		Ankle joint							
	Groups	IC	MSt	Peak value extension (plantarflexion)	Peak value flexion (dorsiflexion)	TO	Peak value extension (plantarflexion)	Peak value flexion (dorsiflexion)	MSw
Angle (°)	DEN	-0.6± 12.9[a]	46.2± 8.4[a]	-0.81± 13.26	47.42± 7.82[a]	17.1± 9.4[a]	-5.31± 12.65[b]	17.50± 9.57	11.4± 11.3[b]
	REINN	-20.1± 12.5	4.2± 14.1	-22.45± 13.08	3.60± 14.19	-14.6± 13.6	-20.86± 12.69	22.63± 14.89	23.1± 15.1
	Sham	-16.4± 9.6	4.7± 15.1	-18.55± 11.15	4.53± 15.19	-17.0± 11.0	-17.34± 9.97	28.66± 14.49	29.1± 13.9
Velocity (°/s)	DEN	321.8± 145.8[a]	200.3± 91.6[a]	573.93± 64.71	-447.97± 100.00	-361.4± 237.8[a]	42.13± 122.98	-407.78± 156.76	-228.0± 256.1
	REINN	-313.4± 100.7	1.4± 56.2	386.26± 43.01	-297.82± 49.87	431.4± 113.6	846.71± 100.51	-912.5± 140.87	-402.3± 91.2
	Sham	-280.9± 127.4	-52.2± 81.8	359.45± 87.23	-359.57± 68.31	486.8± 104.1	1025.51± 198.15	-967.05± 189.79	-383.1± 220.6

[a] Significantly different from REINN and Sham; $p < 0.05$; [b] Significantly different from Sham only; $p < 0.05$

Table 6 - Mean values for hip joint angle and angular velocity for each experimental group; eight animals per group

		Hip joint							
	Groups	IC	MSt	Peak value extension	Peak value flexion	TO	Peak value extension	Peak value flexion	MSw
Angle (°)	DEN	90.51± 14.84[b]	112.50± 8.70[b]	116.58± 11.07	91.25± 14.46[a]	109.42± 13.51[b]	104.45± 14.30[b]	74.77± 15.54	75.38± 15.71
	REINN	65.44± 10.20	74.76± 13.11[b]	77.27± 14.38	65.30± 10.04	71.06± 14.41	74.90± 15.53	63.30± 10.84	63.94± 11.47
	Sham	76.42± 10.15	89.01± 11.16	98.50± 14.40	76.44± 10.19	93.40± 14.80	97.42± 15.48	74.38± 9.79	77.26± 10.80
Velocity (°/s)	DEN	294.67± 85.80[a]	125.43± 83.40	116.70± 86.56	-372.18± 168.03	-347.56± 116.73[a]	302.19± 82.24[a]	-471.49± 155.71[a]	-138.63± 86.07
	REINN	62.52± 32.64	73.92± 48.24[b]	109.15± 34.03	-70.02± 68.37	-155.40± 49.02	71.27± 26.05	-164.38± 64.76	-30.01± 78.72
	Sham	71.42± 29.92	157.03± 44.71	163.95± 32.73	-89.67± 82.09	-236.47± 55.28	86.56± 18.40	-299.45± 62.17	-144.23± 107.46

[a]Significantly different from REINN and Sham; $p < 0.05$; [b]Significantly different from Sham only; $p < 0.05$

Table 7 - Mean values for knee joint angle and angular velocity for each experimental group; eight animals per group

		Knee joint							
	Groups	IC	MSt	Peak value extension	Peak value flexion	TO	Peak value extension	Peak value flexion	MSw
Angle (°)	DEN	121.08± 14.46	105.33± 16.04[a]	123.34± 14.88	77.33± 7.83	79.40± 13.55	120.07± 14.91	62.24± 14.10[b]	72.13± 17.87
	REINN	105.54± 14.30	69.66± 13.70	105.92± 14.71	56.29± 15.09[c]	50.70± 13.34[c]	105.73± 14.11	46.62± 11.92	64.75± 12.20
	Sham	119.69± 11.78	80.06± 7.41	120.11± 11.90	72.50± 11.26	68.25± 12.65	119.78± 11.86	59.86± 10.39	76.72± 10.27
Velocity (°/s)	DEN	26.49± 69.29	-161.26± 84.53[a]	-40.14± 64.96	-270.98± 44.66	-621.61± 137.42[a]	959.80± 189.25	-452.17± 144.97	872.07± 230.25[a]
	REINN	9.01± 82.35	-255.12± 28.54	-125.40± 77.40	-390.89± 56.54	-265.91± 65.89	1101.70± 105.38	-237.73± 66.86	1073.30± 101.82
	Sham	-58.44± 54.69	-213.98± 69.05	17.96± 112.34	-447.77± 84.79	-363.16± 87.63	1173.84± 139.00	-339.01± 110.13	1100.27± 173.29

[a] Significantly different from REINN and Sham; $p < 0.05$; [b] Significantly different from REINN only; $p < 0.05$ [c] significantly different from DEN and Sham; $p < 0.05$

4.3 CYCLOGRAMS

The cyclograms in Figure 31 display the interjoint coordination for hip-knee, hip-ankle and knee-ankle during the rat walking cycle. Our cyclograms of Sham group are comparable to thoe observed in non-injured rats during level walking (29).

In line with hip motion changes, hip-knee plot in the DEN group displays wider perimeter when compared to the REINN group ($p=0.000$). This increased perimeter results from enlarged hip joint range of motion during walking in DEN group that is approximately twice this joint's range of motion in the other groups. Aside the higher perimeter, the hip-knee plot also reveals interjoint coordination changes in the DEN group. The stance-to-swing transition in sham controls (Sham group) is characterized by reversal of hip motion from extension to flexion with the knee keeping its flexion position during the early part of the swing phase. In contrast, hip flexion in the DEN group initiates with the rat's foot still in ground contact and fulfils approximately half of its flexion range of motion before the foot leaves the ground (swing initiation). Similarly, hip extension in the DEN group starts well in the swing phase, with the foot still off-ground and the knee at its maximal extension angle. Hip-knee plot perimeter is similar in REINN and Sham groups as well as the shape of the angle-angle contour. However, in the REINN group the hip-knee loop is markedly shifted to the left, reflecting the fact that the hip joint is operating at a more flexed position.

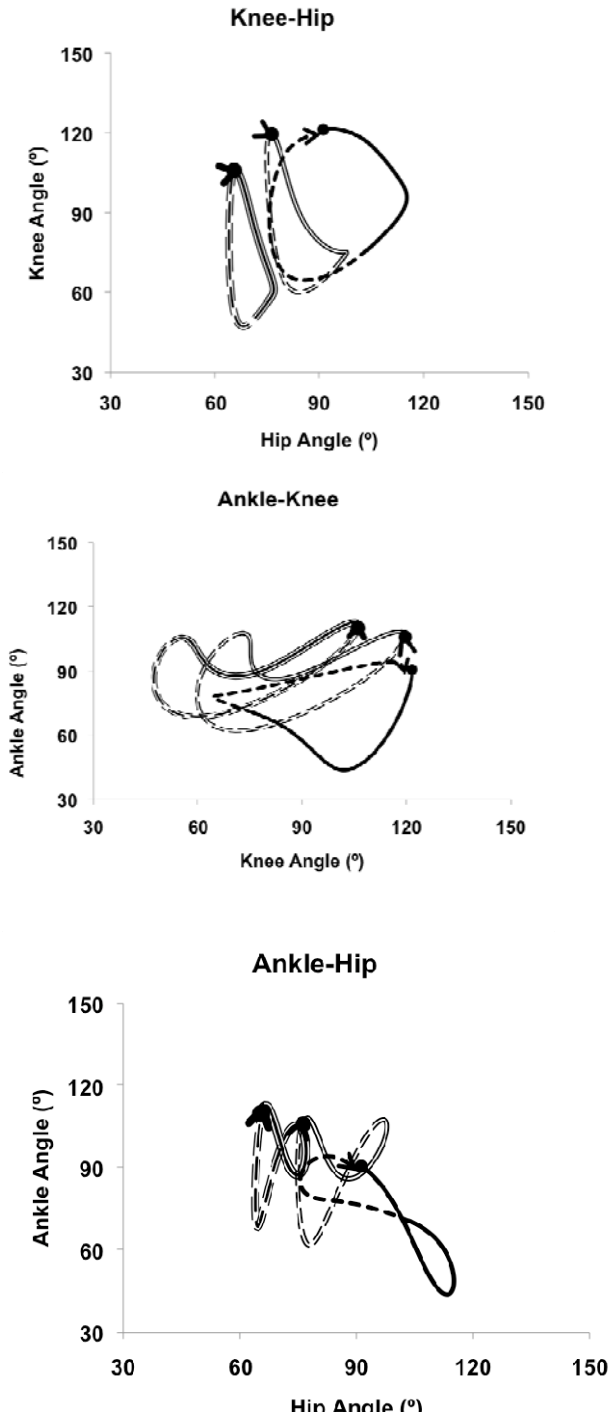

Figure 31 Ankle-knee, knee-hip and ankle-hip loops during the walking cycle for DEN (single line), REINN (triple line) and Sham (double line) groups. Full lines correspond to the stance phase and dashed lines to the swing phase. The start of the walking was taken as the initial paw ground contact and is marked by a full circle. The end of the swing phase is signed with an arrowhead.

The cyclogram for the hip-ankle displays a horizontal eight-shaped pattern, present also in the DEN group. In the REINN and Sham groups, the ankle joint at IC joint reaches maximal plantarflexion and the hip has initiated extension. The DEN group, however, shows altered changes in hip-ankle pattern at this time point, with the ankle

moving already to dorsiflexion and with the hip having completed a significant amount of its extension range of motion. Again, the major distinction between REINN and Sham groups is higher hip flexion in the REINN group that is accompanied by slightly increased ankle plantarflexion. During the stance phase, the range of ankle dorsiflexion in the DEN group is increased when compared to both REINN and Sham groups, as described when presenting individual joint kinematics. The hip-ankle loop pertaining to the DEN group demonstrates that ankle plantarflexion during the stance phase is associated with hip flexion. This suggests that flexion of the hip joint is a strategy that enables foot clearance at the end of stance in sciatic-denervated animals, and compensates the lack of contractile force by plantarflexor muscles.

In the REINN and Sham groups, TO coincide with maximal ankle plantarflexion whereas the knee is maximally flexed at this walking event (see knee-ankle plot, Fig. 2). In these groups, ankle performs a fast dorsiflexion movement during the first half of the swing phase while the knee maintains static its flexion angle. Ankle plantarflexion and knee extension occur during the second half of the swing phase, reaching maximal extension just before IC. In the DEN group, the major change in knee-ankle coordination occurs during the swing phase and is characterized by active knee flexion early during the swing phase, most likely to help raise the paralysed foot off the ground. The perimeters of ankle-knee cyclograms were similar in all groups. Knee-hip cyclogram perimeter shows differences between DEN and REINN groups. Hip-ankle cyclogram perimeter is significantly different in DEN group compared to the REINN and SHAM groups ($p= 0.001$ and $p=0.000$ respectively).

4.4 Discriminant analysis

Four different discriminant models were built: one model based on spatiotemporal data and three other models based on the kinematic data of hip, knee and ankle joints. Peak angle and angular velocity values were not considered for model development. All models correctly classified DEN group animals, excepting the model constructed on the basis of spatiotemporal data that assigned one of animal of the DEN group into the REINN group. Models based on kinematics of the hip, knee and ankle joints showed full sensitivity to identify the animals of the DEN group. Also, none of the animals of REINN and Sham groups was wrongly classified into the DEN group by any of the models. Therefore, the kinematics of the hip, knee or ankle all provide maximal specificity for detecting walking changes in the early phase after sciatic crush injury.

However, the several discriminant models revealed significantly less ability to identify animals of the REINN and Sham groups. In REINN group, the rate of correct assignments, i.e. sensitivity, lowered to 50% when using spatiotemporal data. Surprisingly, the best models to distinguish between animals of the REINN and Sham groups were those based on hip and knee kinematics. Assuming sensitivity as the ability to identify animals of the REINN group, both hip and knee kinematics models reach a sensitivity of 87.5% (7 out of 8 animals correctly classified), remaining unchanged with cross-validation. However, the hip kinematics-based model displayed better specificity, misclassifying just two animals of the Sham group before cross-validation, and three after cross-validation. In contrast, the discriminant model based upon the ankle joint kinematics performed poorly, correctly classifying just five animals (62.5%) of the REINN group. The least sensitive model in finding the sciatic-reinnervated animals was that employing spatiotemparal data. The hip kinematic parameters selected by the stepwise method of linear disciminant model building were hip angle at TO and MSw and hip angular velocity at IC and MSw.

5 Discussion

The assessment of joint kinematics during walking can be useful to evaluate functional recovery after hindlimb peripheral nerve injury in the rat only if its sensitivity and specificity are acceptable. Here, we tested a large set of spatiotemporal and joint kinematics parameters describing rats' walking function, taking for the first time into account data from the hip, knee and ankle joints. We showed that the large majority of spatiotemporal and joint parameters are affected early post sciatic nerve crush injury. Moreover, we demonstrated the ability of joint kinematics to highlight minor walking changes after long term recovery from sciatic crush injury. However, the kinematics changes during walking twelve weeks after sciatic nerve crush were noticed in the hip and knee joints, while ankle joint kinematics had recovered its normal pattern. In line with joint kinematics data, discriminant analysis clearly demonstrated that walking measures, either pertaining spatiotemporal features or hindlimb joint kinematics measures, accurately recognize sciatic-denervated animals and distinguishes them from sciatic-reinnervated animals and sham controls. Only the models employing hip and knee kinematics demonstrated good accuracy when distinguishing animals that had recovered from sciatic crush from sham controls.

5.1 Spatiotemporal and joint kinematics in sciatic-denervated and reinnervated animals

Different factors affect the accuracy and variability of hindlimb joint kinematics during the rat walking, including two- versus three-dimensional analysis (30), the use of anatomical- versus reference-based system (29), skin slippage and the difficulty in tracking bony references (31), over ground versus treadmill walking (32), familiarization, walking velocity and the size and weight of animals (14). However, despite the various sources of variation ankle joint kinematics during walking in the rat displays good day-to-day and inter-observer reliabilities when assessed by 2D video recordings (14). In our study, we adopted a very careful experimental design in order to avoid many of the above mentioned sources of potential bias and to reach accurate measures of hindlimb joint kinematics during walking in rats with different degrees of deficits and in control animals. In this sense, we used a motion capture system with high frame rate and notable tracking precision, thus avoiding data aliasing and spatial

imprecision. Great care was also taken in placing the reflective markers, and this task was always carried out by the same person that followed a strict procedure. In addition, the number of animals in each group was relatively large, the age and weight of sham-operated and REINN animals were similar, and all animals were familiarized with walking in the corridor prior to data collection. Therefore, our data can be viewed as a reference for sagittal hip, knee and ankle kinematics in rats after sciatic nerve crush.

In the first week post sciatic nerve crush, and in the rat, the regenerating axons are elongating in direction of the target organs but the end plates of the target muscles remain denervated (23), which produces paralysis of denervated muscles of the hindleg and foot and severe walking deficits. However, the animals are still capable of locomotion by adopting an abnormal walking pattern that affects either the spatiotemporal features of gait, the joint kinematics, and that is recognizable by simple observation. In the DEN group, we observed slower walking speed and shortened stride length. Also in this group, the stride duration was increased mainly caused by a longer swing phase, while the stance phase duration seemed not to be affected. In contrast, the gait spatiotemporal characteristics in the REINN group were similar to those of the Sham group, indicating total recover of these gait parameters in twelve weeks post sciatic crush, which is in line with previous reports (33). In fact, the recovery of the spatial and temporal features of gait to pre-injury levels takes around four weeks in cases of sciatic nerve crush in the rat (33). The mean walking speed in our study varied from around 16 cm/s, in the DEN group, to 23 cm/s in sham controls, with intermediate velocity of 21 cm/s in the REINN group. Walking velocity in rats varies in a wide range and velocities between 20 to 50 cm/s are considered low (34). This signifies that our reported velocities are at the lower limit of normal rat walking velocity, even in our sham-controls. However, we were very careful selecting the walking cycles for analysis and only those from uninterrupted sequences of three to five walking steps were chosen, discarding steps with arrests or accompanied by evident exploratory behaviours like sniffing.

Ankle joint showed the largest motion changes during walking early post sciatic injury, comparing to the hip and knee joints. This is corroborated by several previous studies using comparable sciatic injuries (5; 14; 25). Most of these studies have focused on the stance phase of walking and they generally report increased ankle dorsiflexion in the weeks immediately after the nerve injury (5; 7; 11; 12; 16; 17). Varejao et al. (19), using computerized high-speed (225 images per second) video system, show increased ankle dorsiflexion (90º angle between leg and foot corresponds to neutral ankle position) during the entire stance phase when animals are assessed one week after

sciatic nerve axonotmesis. Moreover, the degree of ankle dorsiflexion rises from the point of initial contact to near the end of the stance phase. Although we employed a photogrammetric system, our results are in total agreement with this latter study (Figure 30). However, ankle motion changes in the DEN group during the swing phase were also substantial. This is not a unique observation and decreased ankle dorsiflexion angle at midswing, defined as the instant where the swinging leg crosses the contralateral hindlimb, has already been reported after sciatic nerve crush (14; 18). Our data confirms such decreased dorsiflexion at MSw plus decreased plantarflexion angle in the late swing phase, which is compatible with lack of contractile ability by the dorsiflexor and plantarflexor muscles supplied by the peroneal and tibial branches of the sciatic nerve, respectively. Moreover, looking at both ankle angle and angular velocity trajectories (Figure 30) it emerges that it is in the swing phase that ankle motion pattern in the DEN group most deviates from the REINN group and the Sham group. However, since we are not comparing the whole trajectories but simply testing differences in certain kinematic parameters drawn from these trajectories at specific time points, we found similar ankle angular velocity at MSw between all groups. This apparently paradoxical finding is enlightening and shows how is critical the choice of the individual kinematics parameters and exemplifies the chance of finding unaffected parameters in animals presenting severe walking deficits (11).

Our data shows complete recovery of the normal ankle kinematics during walking in twelve weeks after the sciatic crush. This agrees with prior studies with comparable sciatic nerve injury, showing total recovery of ankle motion during walking in 2 to 6 weeks, depending on the particular angle parameter (5; 11; 14; 18). Notwithstanding the fast recovery in ankle joint kinematics, we and other authors have reported subtle and persisting ankle joint motion changes, emerging later in the recovery period (11; 12; 14). However, the exact meaning of these ankle motion changes is unclear. They might indicate abnormal reinnervation of target organs and axon misrouting, causing diskynesis that manifests only in later stages of recovery (18; 35); but the hypothesis that in the sciatic crush model they simply reflect the effect of the various sources of variation affecting the precision of these measures is also a strong possibility, particularly taking into account their inconsistency in repeated measures taken at regular intervals (11; 18).

A major contribution of this study is the reported changes in hip and knee kinematics during walking affecting sciatic-injured rats. This improves our knowledge about the extent of the walking deficits caused by sciatic injury but is particularly relevant since altered patterns of hip and knee motion were encountered not just in the DEN group

but also in the REINN group. In the DEN group, hip and knee motion changes were expected as a mean to overcome the dysfunction at the ankle and foot and for allowing locomotion. Higher level tasks required for walking include foot clearance from the ground and the ability to protract and retract the whole limb during the swing and stance phases, respectively (36). The ankle joint actively contributes to these tasks either by joint rotation, particularly important in the swing phase, or by providing joint stability through contraction of the muscles actuating this joint, which is required for load bearing control during the stance phase. We observed increased hip and knee extension angle in the DEN group during the stance phase. This change in normal hip and knee action are most likely a strategy that compensates the inability of the ankle to perform active plantarflexion. The higher hip range of motion in the DEN group is likely a mean to replace the ankle joint in its functions of both push off and paw forward displacement during the stance and swing phases, respectively. The hindlimb protraction seems to be assisted also by trunk flexion, which is indicated by a visible rounded posture of the rat's torso. However, the contribution of the trunk to locomotion and to the displacement of the affected hindlimb was not objectively measured. In turn, increased knee extension during the stance phase maintains limb length in the absence of ankle plantarflexion (Table 6).

Our data suggests that the hip plays a very important role in keeping limb function during locomotion. In each phase of the walking cycle, the hip undergoes a steady flexion or extension motion. This steady motion is lost in denervated animals. In the DEN group, hip flexion starts before toe off in the stance phase, whereas hip extension begins with the paw still off ground during the swing phase. This changed pattern of hip motion probably emerges as a solution to move the paralytic hindleg using mechanical energy transfer from the hip up to the foot. In the REINN group, the range of motion of the hip joint during walking is similar to sham controls but the joint operates in increased flexion, as demonstrated by the leftward shift of the loop in both the knee-hip and ankle-hip plots of the REINN group (Figure 31). This change in hip motion was unsuspected and could not be detected by simple observation. The reasons explaining such altered hip motion in the REINN group cannot be resolved by our study. However, one simple hypothesis would consider the increased hip flexion as an after effect of the coordination pattern developed at early stages of severe deficit. As we saw, denervated animals rely on trunk and hip flexion to propel the affected limb and this facilitation of flexion may not be resolved even after recovery of the normal ankle joint motion. Other possibility looks at the hip motion changes as an adaptive strategy implemented at whole limb level to adjust for deficits at the ankle that cannot be

disclosed by biomechanical analysis of this individual joint. In the cat, triceps surae and gastrocnemius self-reinnervation are at the origin of motion deficits that surpasses the ankle joint motion and affect the kinematics of the other limb joints (36). Apparently, there are mechanisms that adjust individual joint kinematics in a step-by-step basis to keep a relatively invariant whole limb orientation and length across the walking cycle (36). Though, it is possible that hip motion changes during walking in our reinnervated rats reflect the action of mechanisms that maintain a stable locomotor function in the presence of long-lasting or permanent deficits in force generation ability or proprioceptive feedback of the reinnervated muscles (1; 20). Probably more stringent walking tasks, such as up-hill or downhill walking, are needed to unveil the ankle joint motion deficits in the long term after sciatic nerve crush in the rat (20).

5.2 Discriminant analysis

Several tests based in walking analysis have played an extremely useful role in assessing functional recovery in peripheral nerve research. To assess the efficacy of novel peripheral nerve treatments we require functional test that are very accurate since alternative nerve treatments will most likely be characterized by moderate or small effect size (5; 37). The development of valid and accurate tests for unbiased assessment of functional recovery in the rat is a challenging task considering the difficulty in standardising the testing conditions and the constraint imposed by reduced number of subjects in the experimental groups. Ankle joint kinematics during walking is envisaged as a reliable and accurate test to assess function recovery but we should underline that its testing properties have been evaluated using gross functional deficits and contrasting groups of animals with deficits with large differences in magnitude (15; 16; 24). Here, we directly addressed this limitation by comparing sham controls with animals that had recovered from sciatic crush injury for twelve weeks, a recovery time that is enough to re-establish the normal values in many functional tests (38; 39).

Corroborating the data from several of the measured parameters, our discriminant analysis confirmed the sensitivity of ankle kinematics during walking to highlight functional deficits in sciatic-denervated animals. This level of sensitivity, however, is shared by the discriminant models developed on the basis of hip and knee kinematics as well as on spatiotemporal measures of the rat walking. This means that test sensitivity is not a critical point when testing animals with deficits of great magnitude caused by peripheral nerve injury, and researchers are comfortable choosing from a rather large set of tests to evaluate functional deficits (7; 19; 25; 32; 33; 39; 40). The critical issue is, therefore, how can we measures small differences in functional

recovery that might indicate enhanced nerve regeneration, better re-establishment of end organ reinnervation or changes at the integrative neural circuits at spinal or supraspinal levels using behavioural tests. To date, we were unable to find evidence in the literature that current tests employed to assess functional recovery after sciatic nerve injury demonstrate such potential, particularly considering commonly employed static tests (33). In an attempt to help solving this drawback, we explored the potential of discriminant analysis. This statistical method is a powerful and popular classifier technique and has been previously applied to extract predicting features from complex movement patterns (41). Surprisingly, the discriminant models that employed hip and knee joints parameters showed a very good sensitivity in distinguishing between animals of the REINN and Sham groups. In fact, both hip- and knee-based discriminant models identified correctly seven out of eight animals belonging to the REINN group. This is a good sensitivity level and largely surpassed the sensitivity of the models based on spatiotemporal or ankle joint parameters. Of note, the level of agreement reached by the hip- and knee-based discriminant models was robust and did not diminished with cross-validation.

Many of the variables selected by the discriminant analysis stepwise procedure regard joints' angular velocity. In the case of hip-based discriminant model, the predictor variables selected included hip angular velocities at IC and MSw plus hip angles at TO and MSw. Unlike joint angles, angular velocity is affected by gait speed and this might be a limitation in using angular velocity data when animals walk freely along the corridor. Although we could not find significant differences in group means for spatiotemporal data between the REINN and DEN groups, we found significant correlations between walking velocity and some of the angular velocity parameters when considering only data from these two groups (data not shown). It is possible then that differences between groups in angular velocity data reflect our particular experimental setup and self-paced locomotion. However, our discriminant model using spatiotemporal data consistently showed poorer performance when compared with models using joint kinematics data. Further studies may want to look whether our results are reproduced in more constrained walking conditions, such as using a motorized treadmill.

6 Conclusions

Hip, knee and ankle joint kinematics during walking are all deeply affected following sciatic nerve crush in the rat. After twelve weeks, animals recover the normal pattern of ankle joint motion but kinematics changes affecting the hip and knee joints subsist. The discriminant models using kinematics data of the ankle, knee and hip joints reveal maximal sensitivity and specificity to identify the denervated rats against reinnervated and control counterparts. However, poor classification performance characterized most of the discriminant models when addressing reinnervated and control animals. From all tested spatiotemporal and joint kinematics variables, those describing hip joint motion revealed higher ability to highlight minor walking deficits in the reinnervated animals. We conclude that hip and knee kinematics analysis improves the sensitivity of rat walking test and its potential to single out subtle functional changes in the long term after sciatic injury, which may be essential to prove the advantage of new treatment approaches.

References

1. English AW, Chen Y, Carp JS, Wolpaw JR, Chen XY. Recovery of electromyographic activity after transection and surgical repair of the rat sciatic nerve. [Internet]. Journal of neurophysiology. 2007 Feb;97(2):1127-34.
2. Brushart TM. Preferential reinnervation of motor nerves by regenerating motor axons. [Internet]. The Journal of neuroscience : the official journal of the Society for Neuroscience. 1988 Mar;8(3):1026-31.
3. Geuna S, Papalia I, Tos P. End-to-side (terminolateral) nerve regeneration: a challenge for neuroscientists coming from an intriguing nerve repair concept. [Internet]. Brain research reviews. 2006 Sep;52(2):381-8.
4. Battiston B, Raimondo S, Tos P, Gaidano V, Audisio C, Scevola A, et al. Chapter 11: Tissue engineering of peripheral nerves [Internet]. Elsevier; 2009. 0
5. Amado S, Simões MJ, Armada da Silva PAS, Luís AL, Shirosaki Y, Lopes MA, et al. Use of hybrid chitosan membranes and N1E-115 cells for promoting nerve regeneration in an axonotmesis rat model. [Internet]. Biomaterials. 2008 Nov;29(33):4409-19.
6. Luis AL, Rodrigues JM, Amado S, Veloso AP, Armada-Da-silva PAS, Raimondo S, et al. PLGA 90/10 and caprolactone biodegradable nerve guides for the reconstruction of the rat sciatic nerve [Internet]. Microsurgery. 2007;27(2):125–137.
7. Luís AL, Rodrigues JM, Geuna S, Amado S, Simões MJ, Fregnan F, et al. Neural cell transplantation effects on sciatic nerve regeneration after a standardized crush injury in the rat. [Internet]. Microsurgery. 2008 Jan;28(6):458-70.
8. Brushart TM, Jari R, Verge V, Rohde C, Gordon T. Electrical stimulation restores the specificity of sensory axon regeneration. [Internet]. Experimental neurology. 2005 Jul;194(1):221-9.
9. English AW, Cucoranu D, Mulligan A, Sabatier M. Treadmill training enhances axon regeneration in injured mouse peripheral nerves without increased loss of topographic specificity. [Internet]. The Journal of comparative neurology. 2009 Nov ;517(2):245-55.
10. Angelov DN, Ceynowa M, Guntinas-Lichius O, Streppel M, Grosheva M, Kiryakova SI, et al. Mechanical stimulation of paralyzed vibrissal muscles following facial nerve injury in adult rat promotes full recovery of whisking. [Internet]. Neurobiology of disease. 2007 Apr ;26(1):229-42.

11. Luís AL, Amado S, Geuna S, Rodrigues JM, Simões MJ, Santos JD, et al. Long-term functional and morphological assessment of a standardized rat sciatic nerve crush injury with a non-serrated clamp. [Internet]. Journal of neuroscience methods. 2007 Jun ;163(1):92-104.
12. Varejão ASP, Cabrita AM, Meek MF, Bulas-Cruz J, Gabriel RC, Filipe VM, et al. Motion of the foot and ankle during the stance phase in rats. [Internet]. Muscle & nerve. 2002 Nov;26(5):630-5.
13. Varejão ASP, Cabrita AM, Meek MF, Bulas-Cruz J, Melo-Pinto P, Raimondo S, et al. Functional and morphological assessment of a standardized rat sciatic nerve crush injury with a non-serrated clamp. [Internet]. Journal of neurotrauma. 2004 Nov;21(11):1652-70.
14. Ruiter GC de, Spinner RJ, Alaid AO, Koch AJ, Wang H, Malessy MJ a, et al. Two-dimensional digital video ankle motion analysis for assessment of function in the rat sciatic nerve model. [Internet]. Journal of the peripheral nervous system : JPNS. 2007 Sep;12(3):216-22.
15. Santos PM, Williams SL, Thomas SS. Neuromuscular evaluation using rat gait analysis. [Internet]. Journal of neuroscience methods. 1995 ;61(1-2):79-84.
16. Lin FM, Pan YC, Hom C, Sabbahi M, Shenaq S. Ankle stance angle: a functional index for the evaluation of sciatic nerve recovery after complete transection. [Internet]. Journal of reconstructive microsurgery. 1996 Apr ;12(3):173-7.
17. Amado S, Rodrigues JM, Luís AL, Armada-da-Silva P a S, Vieira M, Gartner A, et al. Effects of collagen membranes enriched with in vitro-differentiated N1E-115 cells on rat sciatic nerve regeneration after end-to-end repair. [Internet]. Journal of neuroengineering and rehabilitation. 2010 Jan;77.
18. Ruiter GCW de, Malessy MJ a, Alaid AO, Spinner RJ, Engelstad JK, Sorenson EJ, et al. Misdirection of regenerating motor axons after nerve injury and repair in the rat sciatic nerve model. [Internet]. Experimental neurology. 2008 Jun;211(2):339-50.
19. Varejão ASP, Cabrita AM, Meek MF, Bulas-Cruz J, Filipe VM, Gabriel RC, et al. Ankle kinematics to evaluate functional recovery in crushed rat sciatic nerve [Internet]. Muscle & nerve. 2003;27(6):706–714.
20. Maas H, Prilutsky BI, Nichols TR, Gregor RJ. The effects of self-reinnervation of cat medial and lateral gastrocnemius muscles on hindlimb kinematics in slope walking. [Internet]. Experimental brain research. 2007 Aug;181(2):377-93.

21. Sefton JM, Hicks-Little CA, Hubbard TJ, Clemens MG, Yengo CM, Koceja DM, et al. Sensorimotor function as a predictor of chronic ankle instability. [Internet]. Clinical biomechanics (Bristol, Avon). 2009 Jun;24(5):451-8.
22. Press SJ, Wilson S. Choosing Between Logistic Regression and Discriminant Analysis [Internet]. 2007 Nov ;
23. Jaweed MM, Herbison GJ, Ditunno JF. Denervation and reinnervation of fast and slow muscles. A histochemical study in rats. [Internet]. The journal of histochemistry and cytochemistry : official journal of the Histochemistry Society. 1975 Nov ;23(11):808-27.
24. Medinaceli L de, Freed WJ, Wyatt RJ. An index of the functional condition of rat sciatic nerve based on measurements made from walking tracks. [Internet]. Experimental neurology. 1982 Sep ;77(3):634-43.
25. Varejão ASP, Cabrita AM, Patricio JA, Bulas-Cruz J, Gabriel RC, Melo-Pinto P, et al. Functional assessment of peripheral nerve recovery in the rat: gait kinematics [Internet]. Microsurgery. 2001 ;21(8):383–388.
26. Beer GM, Steurer J, Meyer VE. Standardizing nerve crushes with a non-serrated clamp. [Internet]. Journal of reconstructive microsurgery. 2001 Oct ;17(7):531-4.
27. Sporel-Ozakat RE, Edwards PM, Hepgul KT, Savas A, Gispen WH. A simple method for reducing autotomy in rats after peripheral nerve lesions. [Internet]. Journal of neuroscience methods. 1991 Feb ;36(2-3):263-5.
28. Kerns JM, Braverman B, Mathew A, Lucchinetti C, Ivankovich AD. A comparison of cryoprobe and crush lesions in the rat sciatic nerve. [Internet]. Pain. 1991 Oct ;47(1):31-9.
29. João F, Amado S, Veloso A, Armada-da-silva P, Maurício AC. Anatomical Reference Frame versus Planar Analysis : Implications for the Kinematics of the Rat Hindlimb during Locomotion. Reviews in the Neurosciences. 2010 ;485469-485.
30. Couto P a, Filipe VM, Magalhães LG, Pereira JE, Costa LM, Melo-Pinto P, et al. A comparison of two-dimensional and three-dimensional techniques for the determination of hindlimb kinematics during treadmill locomotion in rats following spinal cord injury. [Internet]. Journal of neuroscience methods. 2008 Aug ;173(2):193-200.
31. Filipe VM, Pereira JE, Costa LM, Maurício AC, Couto P a, Melo-Pinto P, et al. Effect of skin movement on the analysis of hindlimb kinematics during treadmill locomotion in rats. [Internet]. Journal of neuroscience methods. 2006 May ;153(1):55-61.

32. Pereira JE, Cabrita AM, Filipe VM, Bulas-Cruz J, Couto P a, Melo-Pinto P, et al. A comparison analysis of hindlimb kinematics during overground and treadmill locomotion in rats. [Internet]. Behavioural brain research. 2006 Sep ;172(2):212-8.
33. Bozkurt A, Deumens R, Scheffel J, O'Dey DM, Weis J, Joosten EA, et al. CatWalk gait analysis in assessment of functional recovery after sciatic nerve injury. [Internet]. Journal of neuroscience methods. 2008 Aug ;173(1):91-8.
34. Koopmans GC, Deumens R, Brook G, Gerver J, Honig WMM, Hamers FPT, et al. Strain and locomotor speed affect over-ground locomotion in intact rats. [Internet]. Physiology & behavior. 2007 Dec ;92(5):993-1001.
35. Ijkema-Paassen J, Meek MF, Gramsbergen A. Reinnervation of muscles after transection of the sciatic nerve in adult rats. [Internet]. Muscle & nerve. 2002 Jun ;25(6):891-7.
36. Chang Y-H, Auyang AG, Scholz JP, Nichols TR. Whole limb kinematics are preferentially conserved over individual joint kinematics after peripheral nerve injury. [Internet]. The Journal of experimental biology. 2009 Nov ;212(Pt 21):3511-21.
37. Yao L, Ruiter GCW de, Wang H, Knight AM, Spinner RJ, Yaszemski MJ, et al. Controlling dispersion of axonal regeneration using a multichannel collagen nerve conduit. [Internet]. Biomaterials. 2010 Aug ;31(22):5789-97.
38. Bodine-Fowler SC, Meyer RS, Moskovitz A, Abrams R, Botte MJ. Inaccurate projection of rat soleus motoneurons: a comparison of nerve repair techniques. [Internet]. Muscle & nerve. 1997 Jan ;20(1):29-37.
39. Hare GM, Evans PJ, Mackinnon SE, Best TJ, Bain JR, Szalai JP, et al. Walking track analysis: a long-term assessment of peripheral nerve recovery. [Internet]. Plastic and reconstructive surgery. 1992 Feb ;89(2):251-8.
40. Varejão a S, Meek MF, Ferreira a J, Patrício J a, Cabrita a M. Functional evaluation of peripheral nerve regeneration in the rat: walking track analysis. [Internet]. Journal of neuroscience methods. 2001 Jul ;108(1):1-9.
41. Cavalheiro GL, Almeida MFS, Pereira AA, Andrade AO. Study of age-related changes in postural control during quiet standing through linear discriminant analysis. [Internet]. Biomedical engineering online. 2009 Jan ;835.

Chapter 6 - The effect of active and passive exercise in nerve regeneration and functional recovery after sciatic nerve crush in the rat

S Amado, AL Luis, S Raimondo, M Fornaro, MG Giacobini-Robecchi, S Geuna, F João, AP Veloso, AC Maurício , PAS Armada-da-Silva (2012). *Neuroscience* (submitted)

1. Abstract

For the first time the effects of exercise after peripheral nerve injury was assessed with quantitative method of kinematic analysis. There is growing evidence that both active and passive exercise improve peripheral nerve regeneration and functional recovery. With the aim of contributing to this mounting evidence, we investigated the effect of treadmill walking exercise and the effect of passive mobilization of the entire hindlimb in the sciatic morphology and functional recovery after a sciatic crush injury in the rat. The injured animals were separated in a treadmill exercise group (EXa), passive mobilization group (EXp) and a group without any further treatment intervention (Crush). A sham-operated control group was also included (Sham). Active exercise consisted on 30 minutes daily of treadmill walking at a speed of 10 m/min, while passive mobilization consisted on 3 minutes repetitive triple flexion and triple extension (i.e. simultaneous flexion or extension of the hip, knee and ankle joints) with slight stretching at the two movement extremes. The two types of exercise slightly improved nerve morphology at 12-weeks survival time, reducing the total number of regenerated myelinated fibers to values similar to intact nerves. This effect of exercise on nerve regeneration seems to operate through different mechanisms dependent on whether the exercise is active or passive, since nerve fibers density was significantly increased in the Exp group, in contrast to the sciatic-injured groups. Functional recovery was assessed using gait variable and hindlimb joint kinematics during level self-paced walking. At the end of the 12-weeks survival time spatiotemporal gait variables were similar in all groups. Similarly, ankle kinematics recovered the normal motion pattern in all groups. In contrast, hip and knee kinematics in the Crush group were still abnormal at the end of the survival time, while these joints in both exercise groups displayed a pattern of motion during walking that was indistinct from that of the sham control animals. It is concluded that either active or passive exercise positively affect sciatic nerve regeneration after a crush injury. We suggest that the positive role of passive exercise results from a general stimulus induced by the movement and possibly mediated by a direct mechanical effect onto the regenerating nerve.

2 Introduction

Peripheral nerve injuries cause motor, sensory and autonomic dysfunction in the denervated territory. After injury and repair, the injured axons grow from the proximal nerve stump in direction to the target organs. However, and irrespective of the good ability of peripheral nerves to regenerate, the degree of reinnervation and of functional recovery after peripheral nerve injury is typically disappointing (1). Dysfunction after peripheral nerve injury and repair is manifold. In the rat sciatic nerve crush model, several studies show increased number of nerve fibers as well as decreased nerve fibers' diameter and decreased myelin thickness in regenerated nerves (2-4). The increase in the number of nerve fibers distally to the injured site results from multiple branching of the severed axons (5-7). The many collaterals branching from single proximal axon often disperse and lead to inappropriate reinnervation, including reinnervation of multiple muscle groups possibly with antagonistic function (8). A second wave of axonal sprouting occurs when regenerating axons reach the target muscle. In this case, axon terminal splits in several small sprouts that course through bridges formed by extensive Schwann cells processes. In this way, multiple fine axonal branches spread to re-innervate multiple end-plates. The poly-neuronal innervation caused by increased density of sibling collaterals reaching the denervated muscle groups and by terminal axon sprouting, disturbs force generation control and contributes to poor functional recovery (8). Sciatic nerve injury also affects sensitive function. Deafferentiation causes adaptive changes at the dorsal root ganglion and the dorsal horn of the spinal cord, disrupting the normal processing of afferent inflow and spinal reflexes integration (9). At a higher level, remapping of central controlling neural circuitry may occur in order to cope with muscle paralysis and to maintain motor function. All these changes contribute to dyskinesia, dysreflexia and hyperalgesia that typically develop after peripheral nerve transaction and that severely compromise functional recovery.

The poor functional outcome after peripheral nerve repair and its clinical relevance have raised the interest in the development of rehabilitation strategies to enhance nerve regeneration and improve functional recovery. Physical exercise is one of such rehabilitation strategies and has been the focus of intense research recently. Many different types of exercise have been tested, including active (3; 10-14) and passive exercise (15; 16). Treadmill walking is a common procedure to stimulate the denervated territories and the regenerating axons in rodents. This type of exercise

uses a natural pattern of locomotion and its intensity can be easily adjusted, turning treadmill walking a very useful exercise model. Studies in mice show that active treadmill walking at both mild and high intensity increases the rate of axonal elongation after nerve transection (12) as well as it leads to a higher intensity in axonal collateral branching but without accompanying increase in incorrect reinnervation (17). The latter effect contrasts to that of electrical nerve stimulation delivered at the time of nerve repair that has been shown to increase collateral axonal branching at the lesion site but also causing excessive axonal misrouting (18). Positive effect of treadmill walking is also reported for adult rats (16). In these animals, daily treadmill walking produced an increase in the number of myelinated nerve fibers in transected and end-to-end repaired sciatic nerves and enhanced muscle reinnervation, demonstrated by increased M-wave amplitude in the gastrocnemius, soleus and plantaris muscles of the affected hindlimb (16). In this study, active walking exercise also resulted in improved spinal reflex activity and in a decrease in H-reflex facilitation that is manifested after peripheral nerve injury and non-exercised animals (9; 16).

The positive effect of exercise stimulus on nerve regeneration and in the extent and precision of target organs reinnervation seems to apply also to passive exercise. Increased mechanical stimulation of the vibrissal muscles and whisker muscle pad of rats restored the normal vibrissae function after transection and direct coaptation of the facial nerve (15). Here, manual stimulation had no effect on the degree of axonal collateral branching, which occurs in a large extent after facial nerve injury in rats, but instead reduced the amount of motor end-plate polyinnervation (15). This positive effect of manual mobilization of the denervated facial nerve territory seems to rely on intact sensory function conveyed by uninjured trigeminal nerve sensory endings (19). In the rat sciatic nerve model, passive exercise has also been shown to positively affect nerve regeneration and muscle reinnervation, demonstrating that the beneficial effect of passive mobilization after peripheral nerve injury also applies to lesions of mixed nerve trunks and is not strictly dependent on normal sensory input (16).

By causing muscle paralysis, denervation is associated with reduced movement of the affected limbs and mechanical unloading of muscles and other soft tissues. The lack of normal movement pattern of the joints and surrounding tissues leads to the development of tissue contractures and joint ankylosis in severe cases. These conditions may be prevented by passive exercise, joint mobilization and gentle muscle stretching. By helping maintain the normal muscle structure and joint mobility, this type of exercise may contribute to functional recovery.

In this study we tested for the effect of brief manual mobilization of the hindlimb joints and muscles on nerve regeneration and functional recovery after sciatic nerve crush in

the rat, and compared to the effect of active treadmill walking and to non-treated conditions. Our manual mobilization technique involved moving the hip, knee and ankle joints through their full range of motion thus applying a slight stretching to the muscles crossing these joints as well as to the other soft tissues.

3 Methods

A total of 32 adult Sprague-Dawley male rats were randomly separated in the following groups: (1) sciatic crush plus treadmill-walking (EXa), (2) sciatic crush plus passive exercise (EXp), (3) sciatic crush (Crush) and (4) sham-operated control (Sham). Our procedure to cause sciatic nerve crush has been detailed elsewhere. Briefly, we utilized a non-serrated clamp (Institute of Industrial Electronic and Material Sciences, University of Technology, Vienna, Austria), that exerts a constant force of 54 N onto the nerve. The pressure was applied for duration of 30 seconds, generating a 3mm-long crush of the sciatic nerve and complete axonotmesis. The right sciatic nerve was crushed 1 cm above the bifurcation into tibial and common fibular nerves. This procedure was demonstrated to cause complete axonotmesis of the sciatic nerve (4; 20-22).

Animals in the EXa group exercised for 30 min on a 10-lane motorized treadmill at a constant speed of 10 m/min with zero incline. The exercise was performed 5 days a week starting at week 2 post-injury and maintained until week 12 post sciatic nerve crush (Figure 32). At least two weeks before sciatic crush injury, animals in the EXa were acclimated to treadmill walking during five to ten minutes daily for one week. Twelve days after the surgery, rats were again tested to ascertain their ability to walk on the treadmill. All animals initiated the walking training protocol at day fourteen after sciatic nerve crush.

Figure 32 - image of rats on the treadmill after sciatic nerve injury.

Passive exercise consisted on manual mobilization of the entire right hindlimb. The passive mobilization of the hindlimb included movement of the hip, knee and ankle joints in concert, and alternating flexion and extension of the joints. During extension, a slight stretching was applied at the end of the movement amplitude. The passive

exercise sessions took approximately three minutes and were undertaken with animals fully awake with the head and upper torso covered with a scarf to help keep the animals relaxed. The animals tolerated the passive exercise sessions without signs of pain or discomfort. The exercise was performed 5 days a week and along the same recovery period as the EXa group.

Animals of the Crush and Sham groups remained in their cages during the 12-weeks recovery period with no other intervention. All animals were socially housed within a single room. Dry food and water were provided *ad libitum*. All procedures were performed with the approval of the Veterinary Authorities of Portugal in accordance with the European Communities Council Directive of November 1986 (86/609/EEC).

3.1 Kinematic analysis

Gait analysis was performed before training protocol (one week post-injury) and at weeks 4, 8 and 12 post-injury. This analysis used an optoelectronic system of six infrared cameras (Oqus-300, Qualisys, Sweden) operating at a frame rate of 200Hz to record the motion of the right hindlimb during the rat level gait. After skin shaving, seven reflective markers with 2 mm diameter were attached to the right hindlimb at bony prominences: (1) tip of fourth finger, (2) head of fifth metatarsal, (3) lateral malleolus, (4) lateral knee joint, (5) trochanter major, (6) anterior superior iliac spine, and (7) ischial tuberosity. The retroreflective markers were in all instances placed by the same operator using the marked skin as a guide. Animals walked on a Perspex track with length, width and height of respectively 120, 12 and 15 cm. Two darkened cages were placed at the extremities of the corridor as a mean to facilitate the animals to cross the walking corridor. All rats previously performed two or three conditioning trials to be familiarized with the corridor. Cameras were positioned to minimize light reflection artifacts and to allow recording 4-5 consecutive walking cycles, defined as the time between two consecutive initial ground contacts (IC) of the right fourth finger. The motion capture space was calibrated regularly using a fixed set of markers and a wand of known length (20 cm) moved across the recorded field. Calibration was accepted when the standard deviation of wand's length measure was below 0.4 mm. Planar motion in the sagittal plane of the hip, knee and ankle joint was calculated with Visual 3D software (C-Motion, Inc, Germantown, USA) by a computational procedure implementing the dot product between the skeletal segments articulated by these joints. Joint velocity was also calculated using the first derivative of joint angle motion. The trajectory of the reflective markers was smoothed using a Butterworth low-pass filter with a 6 Hz cut-off. Data for each animal at each recording session consisted on

an average of six walking cycles. Each walking cycle was time normalized by interpolation using spline fitting. Our angles convention was: 1) decreasing hip angle value – hip flexion; 2) decreasing knee angle value – knee flexion; 3) positive ankle angle value – dorsiflexion. Positive angular velocity indicates increasing angle values (i.e. hip and knee extension). This also applies to the ankle joint where a positive angular velocity means increase dorsiflexion angle. Joint angle and angular velocity values were measured at the instants of initial ground contact (IC), defined as the time point where horizontal velocity of the toe reflective marker becomes zero, midstance (MSt), the point of fifty per cent duration of the stance phase, toe-off (TO), defined as the instant the horizontal velocity of the toe's reflective marker increases from zero, and midswing (MSw), defined as the point of fifty per cent duration of the swing phase. Additional kinematics parameters recorded included peak angles and angular velocities during both phases of the walking cycle.

Spatiotemporal parameters, including walking velocity, walking cycle duration, stride length, stance duration, and swing duration, were directly obtain from kinematic model developed under Visual 3D software based on horizontal displacement of the reflective markers.

3.2 Design-based quantitative nerve morphology

At the end of the 12-weeks follow-up time, rats were anaesthetised and a 10-mm-long segment of the sciatic nerve that included the injured portion was collected, fixed, and prepared for morphological analysis and histomorphometry of myelinated nerve fibers. A 10-mm segment of uninjured sciatic nerve was also withdrawn from the 8 control animals. Immediately after collecting the nerve, rats were euthanized through an intracardiac injection of 5% sodium pentobarbital (Eutasil®). Sciatic nerve samples were immersed immediately in a fixation solution, containing 2.5% purified glutaraldehyde and 0.5% saccarose in 0.1M Sorensen phosphate buffer for 6-8 hours. Specimens were then washed in 0.1M Sorensen phosphate buffer (1.5% saccarose), post-fixed in 1% osmium tetroxide, dehydrated and embedded in Glauerts' embedding mixture of resins (23). Series of semi-thin transverse sections (2-µm thick) were then cut starting from the distal nerve stump and stained by Toluidine blue for high resolution light microscopy examination and design-based stereology (24). Systematic random sampling and 2-D disector were adopted (25-27). The following predictors of nerve regeneration were assessed: mean fiber density (D), total fibers number (N); circle-fitting diameter of fiber (D) and axon (d), and the g-ratio (d/D). The sampling scheme was designed in order to keep the coefficient of error (CE) below 0.10, a level which assures enough accuracy for neuromorphological studies (28).

4 Statistical analysis

Differences between groups for each of the variables were tested by univariate ANOVA and the post hoc Tukey's HSD test. Significance was accepted at $p<0.05$. Data are presented as mean and standard deviation (SD). Statistical analysis was performed using SPSS software package (version 17, SPSS Inc).

5 Results

During surgery, the sciatic nerve crushed resulted in visible crush of nerve but without interrupting its continuity. Muscle paralysis of the operated foot was observed following crush injury. All rats survived, with no wound infection or automutilation.

1.1 Gait spatiotemporal data

All animals could walk with steady pace in the corridor during the testing sessions carried out in the recovery period. As a consequence of sciatic nerve injury and sham surgery, most gait spatiotemporal features changed along the recovery time. During the 12-weeks recovery, stride length increased [$F_{(3,84)}$ = 17.239, p = 0.000] either in sciatic-injured groups and Sham group [non-significant main effect of group; $F_{(2,28)}$ = 2.688, p = 0.066], while gait cycle time diminished [$F_{(3,84)}$ =19.794,p=0.000] again in all groups. The shortened gait cycle duration was associated with decreased swing phase duration [$F_{(3,84)}$ = 27.133 , p = 0.000], while that of the stance phase showed no changes in any of the groups at any joint in time. A trend for the rise of gait speed rise with time of recovery was noticed (p=0.054). At week 1 post-injury, gait speed ranged from 0.161±0.038 $m.s^{-1}$ in EXp group to 0.116±0.028 $m.s^{-1}$ in Crush group. By week twelve, mean gait speed varied from 0.239±0.052 $m.s^{-1}$ in EXa group to 0.210±0.047 $m.s^{-1}$ in Crush group (Table 8).

Table 8 - Walking velocity and cycle time data if the right hindlimb in sciatic-crushed animals and sham-operated controls; n=8 in each group

	Gait velocity (m/s)		stride lenght (m)		cycle duration (s)		stance duration (s)		swing duration (s)	
Group	**W01**	**W12**	**W01**	**W12**	**W01**	**W12**	**W01**	**W12**	**W01**	**W12**
EXa	0.15 ±0.04	0.24 ±0.05	0.14 ±0.01	0.17 ±0.01	0.92 ±0.16	0.73 ±0.17	0.23 ±0.05	0.20 ±0.03	0.20 ±0.05	0.13 ±0.01
EXp	0.16 ±0.03	0.23 ±0.09	0.13 ±0.01	0.16 ±0.02	0.85 ±0.16	0.76 ±0.20	0.24 ±0.09	0.25 ±0.06	0.17 ±0.03	0.13 ±0.01
Crush	0.12 ±0.03	0.21 ±0.05	0.13 ±0.01	0.15 ±0.02	1.11 ±0.27	0.73 ±0.10	0.28 ±0.04	0.26 ±0.03	0.19 ±0.03	0.12 ±0.01
Sham	0.15 ±0.03	0.23 ±0.04	0.14 ±0.01	0.16 ±0.01	0.96 ±0.13	0.70 ±0.09	0.28 ±0.08	0.25 ±0.04	0.17 ±0.01	0.13 ±0.01

1.2 Hindlimb joint kimematics

Ankle kinematics

Sciatic nerve crush causes paralysis of the hindleg and foot muscles. Therefore, we start by presenting ankle joint kinematics data followed by that of the hip and knee joints.

Ankle kinematics was most affected at week 1 post sciatic nerve injury (Figure 33). Exaggerated dorsiflexion during the whole stance phase characterizes movement about this joint in sciatic-injured animals, with differences to sham-operated controls being most evident at midstance and toe-off time points. Clear changes in ankle angular velocity were also induced by sciatic injury. Ankle angular velocity at week 1 post injury shifted from negative to positive values in sciatic-injured animals either at initial paw contact and midstance, contrasting to the negative values of sham controls. Conversely, at toe-off time point (Table 10), ankle angular velocity was negative in sciatic nerve-injured animals and positive in Sham group. Ankle kinematics at midswing (Table 12) was less affected by sciatic nerve crush. At week 1, sciatic crushed animals demonstrated a decreased ability to perform ankle dorsiflexion at midswing, compared to animals in the Sham group, but ankle angular velocity was similar in all groups. A good recovery of the normal pattern of ankle kinematics during walking occurred during the 12 weeks of follow up, and no consistent differences in the extent of this recovery were observed due to treatment modality (Figure 34).

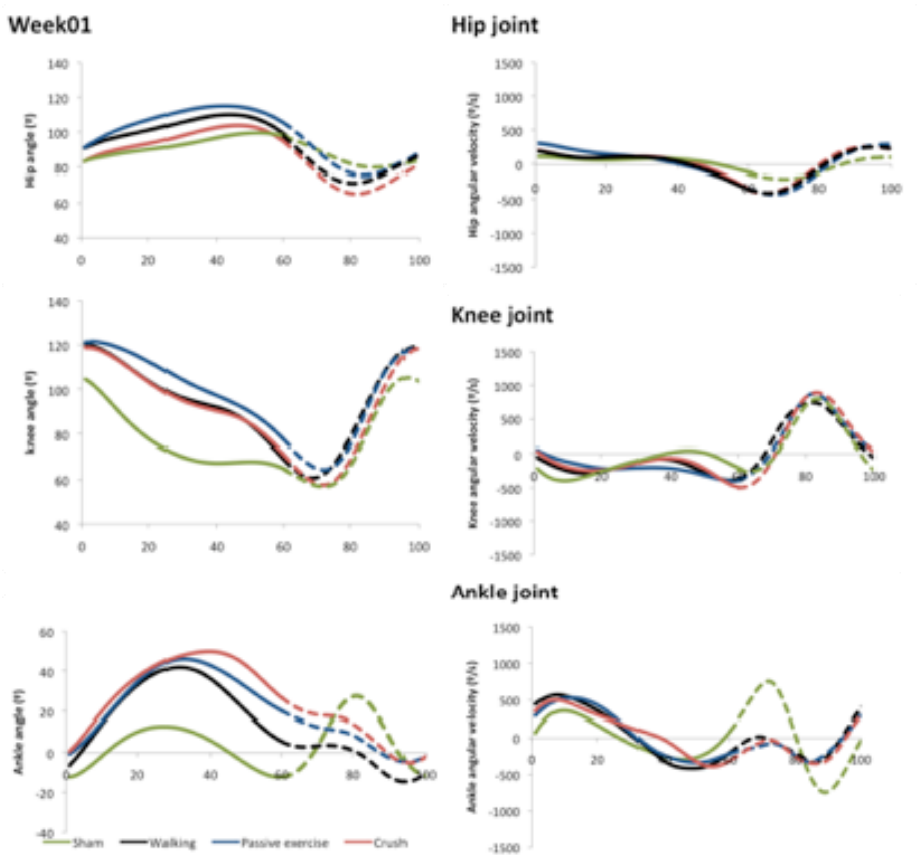

Figure 33 - Mean trajectories for hip (upper graphs), knee (middle graphs) and ankle (lower graphs) joint angle (left hand graphs) and angular velocity (right hand graphs) during the rat's walking cycle. Full lines correspond to the stance phase and dashed lines correspond to the swing phase of the walking cycle: crush group (red line); EXa (black line); EXp (blue line); Sham Group (green line). All groups n=8

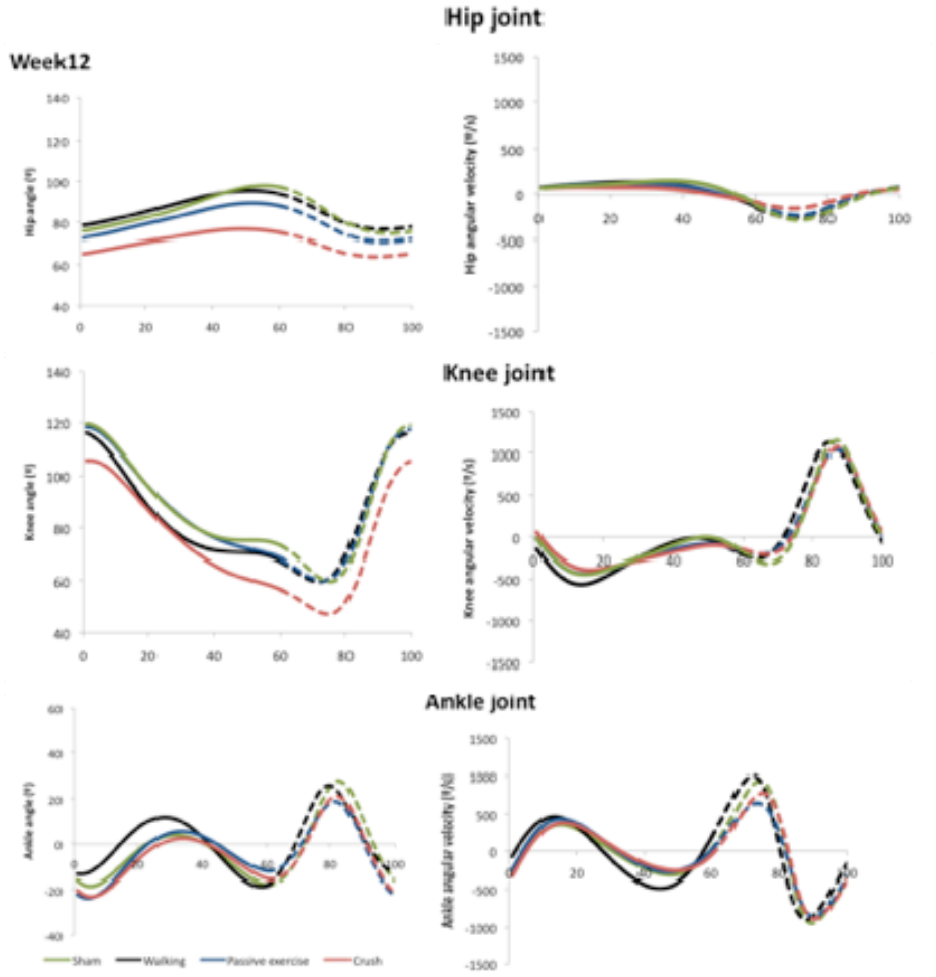

Figure 34 - Mean trajectories for hip (upper graphs), knee (middle graphs) and ankle (lower graphs) joint angle (left hand graphs) and angular velocity (right hand graphs) during the rat's walking cycle. Full lines correspond to the stance phase and dashed lines correspond to the swing phase of the walking cycle: crush group (red line); EXa (black line); EXp (blue line); Sham Group (green line). All groups n=8.

Hip kinematics

Hip kinematics during walking was also affected as a consequence of sciatic nerve crush. Significant differences between groups in hip kinematics were acutely observed after sciatic denervation being these differences were still noticeable at the end of the 12-weeks recovery. In the week immediately after surgery, changes in normal hip joint motion during walking were noticed only in angular velocity values. At this point in time, sciatic injured animals walk with increased hip angular velocity either at initial toe contact (i.e. swing-to-stance transition) and toe off (i.e. stance-to-swing transition), compared to Sham group animals. Despite such changes in hip angular velocity, no significant alterations in hip position at the relevant phases of gait were recorded in sciatic denervated animals. Sciatic nerve reinnervation led to the recovery of the normal hip motion pattern during walking in exercised animals (i.e. EXa and EXp groups) but differences between Crush and Sham groups emerged. In fact, all kinematic parameters obtained from the stance phase were significantly different in Crush group, compared to Sham control at the 12-weeks time point. The changes were characterized by more acute hip angles at the entire stance phase and significantly lower hip angular velocity in Crush group.

Knee kinematics

Sciatic denervation was also accompanied by compensatory changes in knee joint kinematics as a mean to enable successful walking. Early after sciatic nerve crush, changes in knee kinematics occurred mainly during the stance phase. At the instant of paw touch down, knee angle shows similar values in all groups but its angular velocity was distinctly higher in sciatic-injured animals. At midstance (Table 11), and at week 1 post injury, sciatic denervated animals display a more extended knee, when compared to the sham operated animals. This can be reasonably interpreted as a compensatory response to the more plantigrade pattern of walking resulting from paralysis of the muscle crossing the ankle joint thus avoiding excessive shortening of the overall limb length. At this particular instant of the step cycle, knee joint velocity was not affected by the sciatic nerve injury. Conversely, at the stance-to-swing transition knee angular velocity in the sciatic-injured animals is greatly augmented compared to Sham group, meaning fast knee flexion motion in the former animals. A recovery of the normal knee pattern of motion during walking occurred in the weeks after sciatic nerve crush. This recovery was, however, enhanced by both walking exercise and manual mobilization. At week 12 post injury, and when compared to Sham group, animals in Crush group walked with exaggerated knee flexion at the instants of initial toe ground contact and toe off.

Table 9 - Values of hindlimb joints joint angle and angular velocity at initial contact (IC)

Joint	Group	Angle (º)		Velocity (º/s)	
		week01	week12	week01	week12
Ankle	EXa	-6.6±4.4	-13.3±2.9	446.2±123.4	-67.2±114.6
	EXp	-0.6±4.6	-22.7±3.5	321.8±145.8	-243.0±165.0
	Crush	1.0±4.2	-20.1±4.4	365.4±122.8	-313.4±100.7
	Sham	-11.7±4.8	-16.4±3.4	57.2±100.8	-280.9±127.4
Knee	EXa	117.1± 18.42	116.1±7.3	-59.8±99.5	-153.4±91.5
	EXp	121.1±14.5	118.2±9.6	26.5±69.3	-46.9±134.3
	Crush	115.0±15.6	105.5±14.3	23.7±67.2	9.0±82.3
	Sham	104.9±15.8	119.7±11.8	-214.3±106.4	-58.4±54.7
Hip	EXa	89.1±11.3	78.3±11.4	201.9±38.4	75.6±36.5
	EXp	90.5±14.8	72.6±7.0	294.7±85.8	70.3±30.4
	Crush	83.2±14.6	65.4±10.2	218.3±94.7	62.5±32.6
	Sham	83.6±9.4	76.4±10.1	109.5±52.5	71.4±29.9

Table 10 - Values of hindlimb joints angle and angular velocity at toe-off (TO)

Joint	Group	Angle (º)		Velocity (º/s)	
		week01	week12	week01	week12
Ankle	EXa	12.09±14.32	-19.25±9.92	-367.97±254.35	320.36±109.10
	EXp	17.09±9.43	-15.00±9.44	-361.44±237.79	363.65±146.06
	Crush	23.63±11.57	-14.59±13.62	-447.27±212.76	431.40±113.60
	Sham	-17.89±9.48#	-17.03±11.00	74.36±187.84	486.84±104.15
Knee	EXa	72.30±12.80	66.29±10.31	-563.86±183.40	-281.72±83.49
	EXp	79.40±13.55	63.82±12.44	-621.61±137.42	-325.02±69.60
	Crush	65.50±15.47	50.70±13.34	-557.37±108.77	-265.91±65.89
	Sham	67.04±16.21	68.25±12.65	-205.83±102.05	-363.16±87.63
Hip	EXa	103.32±8.86	93.02±19.35	-336.71±167.08	-173.18±89.81
	EXp	109.42±13.51	85.07±9.72	-347.56±116.73	-208.12±67.99
	Crush	93.82±19.59	71.06±14.41	-367.31±138.26	-155.40±49.02
	Sham	97.42±16.27	93.40±14.80	-155.10±76.60	-236.47±55.28

Table 11 - Values of hindlimb joints angle and angular velocity at midstance (MSt)

Joint	Group	MSt angle (º)		MSt velocity (º/s)	
		week01	week12	week01	week12
Ankle	EXa	42.10±10.54	11.65±12.28	175.98±119.89+	-134.35±84.06
	EXp	46.22±8.43	6.99±12.28	200.32±91.63-	23.16±85.33
	Crush	48.04±12.96	4.24±14.12	163.38±118.21-	1.43±56.25
	Sham	13.61±13.19	4.73±15.17	-58.63±61.23	-52.19±81.85
Knee	EXa	94.05±15.01	75.15±6.85	-137.36±76.77	-224.36±60.35
	EXp	105.33±16.04	80.42±14.86	-161.26±84.53	-247.41±35.48
	Crush	91.09±10.28	69.66±13.70	-142.49±81.28	-255.12±28.54
	Sham	68.31±15.44	80.06±7.41	-121.79±43.65	-213.98±69.05
Hip	EXa	106.21±10.76	89.80±16.38	109.07±73.71	137.18±94.40
	EXp	112.50±8.70	84.30±7.20	125.43±83.40	124.89±44.64
	Crush	99.01±17.72	74.76±13.11	115.21±67.04	73.92±48.24
	Sham	93.38±11.15	89.01±11.16	95.19±70.18	157.03±44.71

Table 12 - Values of hindlimb joints angle and angular velocity at midswing (MSw)

Joint	Groups	MSw Angle (º)		MSw velocity (º/s)	
		week01	week12	week01	week12
Ankle	EXa	4.54±10.39	27.38±12.18	-274.44±310.80	-276.94±129.49
	EXp	11.40±11.32	22.06±6.99	-227.98±256.05	-422.19±133.67
	Crush	16.09±11.00	23.09±15.11	-313.59±292.90	-402.28±91.21
	Sham	35.41±11.38	29.06±13.91	-282.91±263.38	-383.13±220.56
Knee	EXa	71.18±19.46	73.74±5.71	860.40±333.73	1035.40±145.63
	EXp	72.13±17.87	74.79±12.39	872.07±230.25	1099.15±94.48
	Crush	61.88±14.04	64.75±12.20	976.08±249.34	1073.30±101.82
	Sham	65.96±14.70	76.72±10.27	844.78±165.17	1100.27±173.29
Hip	EXa	71.25±9.53	78.38±12.15	109.07±100.53	137.18±96.65
	EXp	75.38±15.71	71.89±7.19	125.43±86.07	124.89±75.40
	Crush	63.69±13.66	63.94±11.47	115.21±140.41	73.92±78.72
	Sham	80.63±11.15	77.26±10.80	95.19±83.82	157.03±107.46

1.3 Nerve stereology

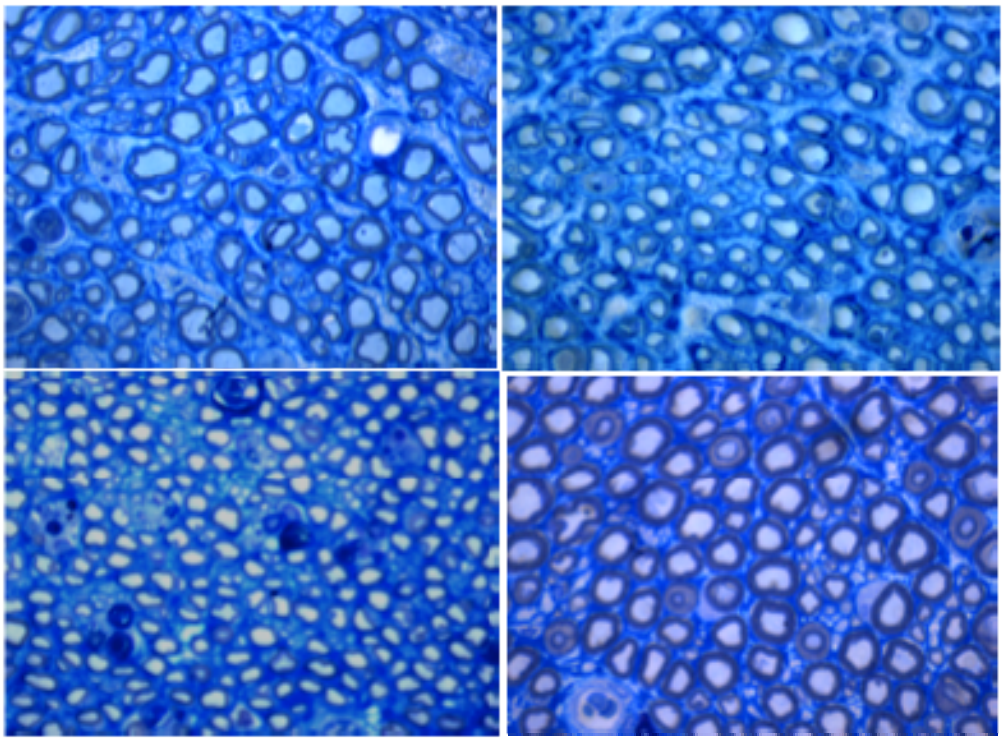

Figure 35 - Representative micrographs toluidine blue stained semithin sections from EXa (A), Exp (B), Ctrl (C) and Sham (D) groups. The presence smaller myelinated nerve fibers can be appreciated in all axonotmesis groups (A-C) in comparison to controls (D). Morphometrical changes have been quantified by stereology and results are reported in table 6. Original magnification = 1,000x.

Figure 35 shows representative images of myelinated nerve fibers from nerves belonging to the four experimental groups included in this study. The results of the stereological analysis of myelinated nerve fibers are reported in Table 13. Overall, regenerated sciatic nerves present increased number and density of myelinated nerve fibers in comparison to intact nerves. The regenerated nerve fibers are also characterized by smaller diameter and lower myelin sheet thickness. Slight effects of exercise were observed in the morphology of the regenerated sciatic nerves. When compared to the Sham group, the increase in total number of myelinated fibers was only significant for the Crush group ($p<0.05$), suggesting that both types of exercise prevented an excessive increase in regenerating axonal collaterals. Despite this apparently positive effect of active and passive exercise, nerve density was increased in EXp group only, when compared to Sham control group ($p<0.05$). Other morphological features characterizing the myelinated nerve fibers, i.e. diameter of

nerve fiber (D) and axon (d) and the g-ratio (D/d), were all significantly different in regenerated sciatic nerves, compared to the intact nerves.

Table 13 - stereological analysis of myelinated nerve fibers

Group	Density of myelinated nerve fibers (N/mm^2)	Total number of myelinated nerve fibers (N)	d - axonal diameter (µm)	D - nerve fiber diameter (µm)	d/D (g-ratio)
EXa	14786 ± 4186	9255 ± 1618	3.90 ± 0.32	5.37 ± 0.41	0.72 ± 0.02
EXp	18146 ± 4691	8974 ± 1918	3.85 ± 0.37	5.35 ± 0.44	0.71 ± 0.03
Crush	16701 ± 4251	10473 ± 1487	3.72 ± 0.31	5.22 ± 0.42	0.71 ± 0.04
Sham	11680 ± 1282	6883 ± 1222	5.35 ± 0.35	8.22 ± 0.38	0.65 ± 0.04

6 Discussion

In this study we evaluated the role of two different methods of exercise on sciatic nerve regeneration and functional recovery after a sciatic nerve crush lesion. The two exercise modes consisted on treadmill exercise walking and passive mobilization of the affected hindlimb. The effect of both exercise programs was evaluated in contrast to a non-exercise group of sciatic nerve crushed animals and sham operated controls. The results showed marginal effects of both active and passive exercise on functional recovery, assessed by hindlimb joint kinematics during level walking. Although the impact of exercise on functional recovery was relatively modest it was nonetheless accompanied by improved nerve morphology, particularly by preventing excessive increase in total number of myelinated fibers in regenerated sciatic nerves.

Physical exercise has received much interest recently due to its potential effect in enhancing nerve regeneration and reinnervation in different models of peripheral nerve pathology (11; 13; 15-17; 29; 30). The results of the majority of these studies point to a small to moderate positive effect of the active exercise stimulus in nerve regeneration after sciatic injury and repair in rodents either when used alone (16; 17; 31) or in combination with nerve electrical stimulation (13), as well as in the degree of reinnervation and extent of functional recovery (12; 13; 16; 31).

To date, the exact mechanisms explaining the beneficial effect of active exercise on nerve regenerations are still not completely elucidated; although several mechanisms have been alluded. After sciatic nerve transection and repair, walking exercise has been shown to increase the number of myelinated nerve fibers distal to injury site (13; 16), as well as to enhance the rate of axonal elongation in the common fibular nerve of mice (12). After being cut, elongating axons are well known to divide profusely in a variable number of collaterals that, afterwards, may either travel in parallel along the same nerve or take a divergent route through alternative nerve pathway leading to inappropriate reinnervation. Increased axonal branching, although important in the sense that it contributes with more regenerating nerve fibers to reinnervation, has a downside consequence if accompanied by aberrant reinnervation of target organs. Studies in mice demonstrate that nerve regeneration is considerably enhanced by electrical stimulation applied to the proximal nerve stump for a brief period of time just prior to nerve repair, as well as by distal nerve stump treatment with chondroitinase ABC, an enzyme that removes the axonal growth-inhibiting glycosaminoglycans from chondroitin sulfate proteoglycans (18). This conclusion is driven by the use of different retrograde fluorescent tracers applied to the tibial and common fibular branches of the

sciatic nerve and consequent enumeration of labeled motoneurons at the anterior horn of the spinal cord (18). However, the increased number of labeled motoneurons was most pronounced two weeks after sciatic transection, lowering to almost control levels at four weeks survival time. Importantly, the enhanced nerve regeneration, noticed two weeks after the sciatic nerve injury, was manifested with clear loss of the normal spinal topographical organization of tibial and common fibular motoneurons, consequent to elongating axon collaterals entering erroneous ending nerves, which in turn might compromise function (18). Comparable increase in the number of labeled motoneurons of the sciatic motor nucleus also occurred at 2-week and 4-week after sciatic nerve transection and repair when animals performed either mild-intensity continuous or high-intensity intermittent treadmill exercise during the two recovery periods of time, with more robust effect with the more intense treadmill exercise protocol (17). Treadmill exercise, however, not just enhanced nerve regeneration but importantly had such effect without simultaneously raising inappropriate target reinnervation. In addition, treadmill exercise seems to exert a sustained nerve regeneration enhancing effect, with the number of tibial nerve labeled motoneurons in exercised animals increasing from week-2 to week-4 after sciatic nerve transection and repair whereas this number remained unchanged between these two recovery times in animals that had nerve regeneration accelerated by treatment with electrical stimulation and chondroitinase ABC (17; 18).

Active treadmill exercise was also shown to improve nerve regeneration in the rat after sciatic transection and direct repair (13; 16). Morphological evaluation at the level of the tibial nerve reveals increased number of regenerated myelinated fibers in the active exercise group, compared to the non-exercise, control group (16). Detailed morphometry of regenerated sciatic crushed nerve in the rat again supports a positive role of treadmill endurance exercise in nerve regeneration (31). In this latter study, treadmill exercise started two weeks after the sciatic nerve injury and was maintained throughout the next five weeks, with animals of the endurance exercise group walking at 50% of their maximal exercise capacity determined pre-operatively, corresponding to a mean walking velocity of around 9 m/min, thus comparable to that we used in the present study. When compared to untrained control animals, the endurance-trained group depicted better nerve regeneration, demonstrated by greater myelin thickness, higher area fraction of myelinated nerve fibers and less of that of endoneurial connective tissue in regenerated sciatic nerves (31).

A major aim of the present study was to test for the effect of brief passive manual mobilization of the affected hindlimb on sciatic nerve regeneration and functional recovery. Our data of the sciatic nerve morphology collected distally to injury site again

showed signs of better regeneration as a result of passive hindlimb mobilization and gentle stretching. As for the EXa group, and when excluding outliers from statistical testing, mean total number of myelinated fibers in the EXp group was indistinct from that of the Sham group. To some extent , this agrees with other studies investigating the effect of passive exercise on sciatic nerve regeneration after transection injury and direct cooptation (16). Udina et al. (16) tested the effect of passive bicycling in the rat on sciatic regeneration and noticed improved sciatic regeneration to a similar degree to that registered for active treadmill exercise. It is difficult to interpret, and thus it deserves further research, the discrepancy between the results of this authors who revealed an increase in the number of myelinated axons and our results, which evidenced the opposite.

In the case of the facial nerve, manual mobilization of the whisker pad reduced muscle fibers poly-innervation two months after nerve transection and repair. In this case, however, the passive exercise showed no effect on the degree of regenerating nerve fibers misdirection (15). Thus, our results of a seemingly positive role of manual mobilization on sciatic nerve regeneration add to those of the latter studies, and reinforce the notion that passive exercise is an effective strategy to stimulate nerve regeneration.

Despite the importance of nerve regeneration, a successful nerve treatment is much dictated by the degree of reinnervation and of functional recovery. Here, we conducted gait analysis to track functional recovery and assessed motion changes at the hip, knee and ankle joints during voluntary level walking. Several motion changes occurred that can be attributed to the sciatic nerve injury and that affected all recorded joints. In the weeks following the sciatic nerve crush and before initiating either active or passive exercise, relevant changes in hip and knee kinematics were noticed, particularly during the stance phase. Higher hip joint velocity and overall increase in knee extension characterized walking of sciatic-injured animals acutely post injury. This profound reorganization of the role played by each individual joint reveals most likely a strategy to overcome dysfunction at the level of ankle joint and to permit walking. Similar to other studies (2; 32; 33), twelve weeks after sciatic injury ankle kinematics was recover in all sciatic-injured groups, taking into account either the ankle angle and the ankle angular velocity during both the stance and swing phases. Complete recovery of the normal ankle kinematics during level walking in a walkway is a common observation after a sciatic nerve crush, however some studies report few kinematic changes appearing late during recovery suggesting that walking is altered after this type of injury (32; 33). Also, it should be kept in mind that the morphology of regenerated crushed

sciatic nerves are clearly distinct from intact nerves, which suggest that complete functional recovery is unlikely to occur on these animals. However, and in contrast to ankle joint kinematics, hip and knee joint kinematics in the Crush group clearly deviated to that of the Sham group. Such changes in the normal hip and knee kinematics during walking were not noticed in both the EXa and EXp groups. We interpret these results as a demonstration that the hindlimb motion pattern during level walking is not fully reestablished after sciatic crush injury and those compensatory changes at the hip and knee joint kinematics emerges that masks disability at the ankle joint. The mechanisms guiding these changes cannot be discerned by our data, but studies have shown altered pattern of electromyographical activity of the muscles crossing the ankle joint after sciatic nerve transection that are best explained by changes at spinal neural output (34). A possibility is that hip and knee motion pattern changes result from altered proprioceptive feedback originating from muscles crossing the ankle joint and other hindleg afferents (35; 36). A simpler explanation, and probably one that better adjusts to our results, is that hip and knee kinematic changes reflect past compensatory changes that are not corrected even if their purpose is not justified anymore. In fact, the stimulus of active and passive exercise corrected hip and knee motion changes during level walking in our exercised animals.

This study was not designed to investigate the mechanisms by which active or passive exercise improves nerve regeneration and functional recovery. The mechanisms are potentially many and might operate at several levels and at distinct organs, including the spinal cord (19; 37), the regenerating nerve (Sabatier, Redmon et al. 2008) and the reinnervated muscles (15; 38). The enhancing effect of active exercise on nerve regeneration and reinnervation probably expresses the maintenance of an adequate degree of stimulation onto the affected motor groups at the spinal cord level. This stimulus might come either from the descending pathways that are active when animals attempt to walk, even if due to denervation the movement itself does not happen, or from afferent pathways originating from non-denervated hindlimb territories but projecting onto the sciatic motoneuron pools (15; 39). It is known from cultured retinal ganglion cells that neuronal outgrowth does not occur spontaneously and is dependent on soluble neurotrophic factors and neuronal electrical activity (40). It is likely that both active and passive exercise originate bursts of electrical activity at the neuronal soma in the spinal cord that then travel along the severed axons and stimulate axonal outgrowth.

The positive effect of passive exercise on nerve regeneration and functional recovery is probably less anticipated, compared to active exercise. Previous studies used a passive exercise stimulus that was designed to closely resemble natural active

movements and behaviors. For instance, passive bicycling used by Udina et al. (16) emulated the range of motion of hindlimb joints observed during walking in the rat. Similarly, the manual strokes of the whisker pad implemented by Angelov et al. (15) took into consideration the normal sweep exploratory motions of the vibrissae in these animals. Our manual passive mobilization of the hindlimb was not planned to mimic any specific task but otherwise to move the hip, knee and ankle joints through most of their movement amplitude and to cause a mild stretch of the muscles crossing the ankle joint. This protocol is in line with rehabilitation techniques aiming to maintain the joint amplitude and prevent muscle shortening and contracture. However, the stimulus caused by this rather unspecific passive motion proves also to have a positive effect on the regenerating nerve morphology and in overall hindlimb motion pattern during walking. Such apparent positive direct effect on nerve regeneration might result from increased afferent input due to the movement stimulus (19; 37). Another possibility is that our passive movement induced rhythmic mechanical load onto the regenerating nerve inducing local cellular and molecular responses that enhance nerve regeneration (41).

Lastly, some limitations of our study must be addressed. Our active walking exercise might be envisaged as a mild-intensity endurance exercise, consisting of daily sessions of 30 minutes continuous level walking at a 10 m/min speed. This exercising protocol was initiated two weeks after sciatic nerve crush, when injured axons start reinnervating the target muscles. However, there is evidence that the nerve regeneration enhancing effect of exercise might be dose-dependent, being endurance high-intensity, intermittent physical exercise capable of inducing higher effect than mild-intensity (17). Also, some protocols use treadmill exercise of one-to two-hours duration (13; 16; 31). It is then possible that our slight positive effect of active exercise on nerve regeneration and functional recovery is the reflection of a relatively low exercise stimulus. Also, our walking conditions used to test functional recovery might not challenge the walking animals to a degree sufficient to uncover the disability associated to faulty reinnervation or changes at spinal neural output (42).

In summary, active continuous walking exercise and passive mobilization of whole hindlimb had a positive effect on the morphology of regenerating crushed sciatic nerves and improved overall hindlimb kinematics during the rat gait. These results are in line with growing evidence that not just active exercise but passive exercise as well are suitable strategies to help nerve regeneration after injury and, most important, to aid in function restoration. Moreover, the positive effect of passive exercise after sciatic nerve injury does not require a strict task-specific movement and might alternatively result

from a general action of movement stimulation, including a direct mechanical effect on the nerve and muscles. Clearly, further studies are needed for in vivo investigation of the mechanism responsible for the effect of passive exercise.

References

1. Raimondo S, Fornaro M, Tos P, Battiston B, Giacobini-Robecchi MG, Geuna S. Perspectives in regeneration and tissue engineering of peripheral nerves. [Internet]. Annals of anatomy = Anatomischer Anzeiger : official organ of the Anatomische Gesellschaft. 2011 Mar 12;
2. Amado S, Simões MJ, Armada da Silva PAS, Luís AL, Shirosaki Y, Lopes MA, et al. Use of hybrid chitosan membranes and N1E-115 cells for promoting nerve regeneration in an axonotmesis rat model. [Internet]. Biomaterials. 2008 Nov ;29(33):4409-19.
3. Malysz T, Ilha J, Nascimento PSD, Angelis KD, Schaan BD, Achaval M. Beneficial effects of treadmill training in experimental diabetic nerve regeneration [Internet]. Clinics. 2010 ;65(12):1329-1337.
4. Varejão AS, Melo-Pinto P, Meek MF, Filipe VM, Bulas-Cruz J. Methods for the experimental functional assessment of rat sciatic nerve regeneration. [Internet]. Neurological research. 2004 Mar ;26(2):186-94.
5. Bodine-Fowler SC, Meyer RS, Moskovitz A, Abrams R, Botte MJ. Inaccurate projection of rat soleus motoneurons: a comparison of nerve repair techniques. [Internet]. Muscle & nerve. 1997 Jan ;20(1):29-37.[
6. Brushart TM. Preferential reinnervation of motor nerves by regenerating motor axons. [Internet]. The Journal of neuroscience : the official journal of the Society for Neuroscience. 1988 Mar ;8(3):1026-31.
7. Ruiter GCW de, Malessy MJ a, Alaid AO, Spinner RJ, Engelstad JK, Sorenson EJ, et al. Misdirection of regenerating motor axons after nerve injury and repair in the rat sciatic nerve model. [Internet]. Experimental neurology. 2008 Jun ;211(2):339-50.
8. Bernstein JJ, Guth L. Nonselectivity in establishment of neuromuscular connections following nerve regeneration in the rat. [Internet]. Experimental neurology. 1961 Sep ;4262-75.
9. Valero-Cabré A, Navarro X. H reflex restitution and facilitation after different types of peripheral nerve injury and repair. [Internet]. Brain research. 2001 Nov 23;919(2):302-12.
10. Meeteren NL van, Brakkee JH, Helders PJ, Gispen WH. The effect of exercise training on functional recovery after sciatic nerve crush in the rat. [Internet]. Journal of the peripheral nervous system : JPNS. 1998 Jan ;3(4):277-82.

11. Marqueste T, Alliez J-R, Alluin O, Jammes Y, Decherchi P. Neuromuscular rehabilitation by treadmill running or electrical stimulation after peripheral nerve injury and repair. [Internet]. Journal of applied physiology (Bethesda, Md. : 1985). 2004 May ;96(5):1988-95.
12. Sabatier MJ, Redmon N, Schwartz G, English AW. Treadmill training promotes axon regeneration in injured peripheral nerves [Internet]. Experimental neurology. 2008 ;211(2):489–493.
13. Asensio-Pinilla E, Udina E, Jaramillo J, Navarro X. Electrical stimulation combined with exercise increase axonal regeneration after peripheral nerve injury. [Internet]. Experimental neurology. 2009 Sep ;219(1):258-65.
14. English AW, Cucoranu D, Mulligan A, Sabatier M. Treadmill training enhances axon regeneration in injured mouse peripheral nerves without increased loss of topographic specificity. [Internet]. The Journal of comparative neurology. 2009 Nov ;517(2):245-55.
15. Angelov DN, Ceynowa M, Guntinas-Lichius O, Streppel M, Grosheva M, Kiryakova SI, et al. Mechanical stimulation of paralyzed vibrissal muscles following facial nerve injury in adult rat promotes full recovery of whisking. [Internet]. Neurobiology of disease. 2007 Apr ;26(1):229-42.
16. Udina E, Puigdemasa A, Navarro X. Passive and active exercise improve regeneration and muscle reinnervation after peripheral nerve injury in the rat. [Internet]. Muscle & nerve. 2011 Feb ;1-10.
17. English AW, Cucoranu D, Mulligan A, Sabatier M. Treadmill training enhances axon regeneration in injured mouse peripheral nerves without increased loss of topographic specificity. [Internet]. The Journal of comparative neurology. 2009 Nov ;517(2):245-55.
18. English AW. Enhancing axon regeneration in peripheral nerves also increases functionally inappropriate reinnervation of targets. [Internet]. The Journal of comparative neurology. 2005 Oct ;490(4):427-41.
19. Pavlov SP, Grosheva M, Streppel M, Guntinas-Lichius O, Irintchev A, Skouras E, et al. Manually-stimulated recovery of motor function after facial nerve injury requires intact sensory input. [Internet]. Experimental neurology. 2008 May ;211(1):292-300.
20. Beer GM, Steurer J, Meyer VE. Standardizing nerve crushes with a non-serrated clamp. [Internet]. Journal of reconstructive microsurgery. 2001 Oct ;17(7):531-4.
21. Varejão ASP, Cabrita AM, Meek MF, Bulas-Cruz J, Melo-Pinto P, Raimondo S, et al. Functional and morphological assessment of a standardized rat sciatic

nerve crush injury with a non-serrated clamp. [Internet]. Journal of neurotrauma. 2004 Nov ;21(11):1652-70.

22. Luís AL, Amado S, Geuna S, Rodrigues JM, Simões MJ, Santos JD, et al. Long-term functional and morphological assessment of a standardized rat sciatic nerve crush injury with a non-serrated clamp. [Internet]. Journal of neuroscience methods. 2007 Jun ;163(1):92-104.
23. Di Scipio F, Raimondo S, Tos P, Geuna S. A simple protocol for paraffin-embedded myelin sheath staining with osmium tetroxide for light microscope observation. [Internet]. Microscopy research and technique. 2008 Jul ;71(7):497-502.
24. Raimondo S, Fornaro M, Di Scipio F, Ronchi G, Giacobini-Robecchi MG, Geuna S. Chapter 5: Methods and protocols in peripheral nerve regeneration experimental research: part II-morphological techniques. [Internet]. International review of neurobiology. 2009 Jan ;8781-103.[
25. Geuna S, Gigo-Benato D, Rodrigues A de C. On sampling and sampling errors in histomorphometry of peripheral nerve fibers. [Internet]. Microsurgery. 2004 Jan ;24(1):72-6.
26. Geuna S, Tos P, Battiston B, Guglielmone R. Verification of the two-dimensional disector, a method for the unbiased estimation of density and number of myelinated nerve fibers in peripheral nerves. [Internet]. Annals of anatomy = Anatomischer Anzeiger : official organ of the Anatomische Gesellschaft. 2000 Jan ;182(1):23-34.
27. Geuna S. The revolution of counting “tops”: two decades of the disector principle in morphological research. [Internet]. Microscopy research and technique. 2005 Apr ;66(5):270-4.
28. Pakkenberg B, Gundersen HJ. Neocortical neuron number in humans: effect of sex and age. [Internet]. The Journal of comparative neurology. 1997 Jul 28;384(2):312-20.
29. Nascimento PS do, Malysz T, Ilha J, Araujo RT, Hermel EES, Kalil-Gaspar PI, et al. Treadmill training increases the size of A cells from the L5 dorsal root ganglia in diabetic rats. [Internet]. Histology and histopathology. 2010 Jun ;25(6):719-32.
30. Malysz T, Ilha J, Nascimento PS do, Angelis KD, Schaan BD, Achaval M. Beneficial effects of treadmill training in experimental diabetic nerve regeneration. [Internet]. Clinics (São Paulo, Brazil). 2010 Jan ;65(12):1329-37.
31. Ilha J, Araujo RT, Malysz T, Hermel EES, Rigon P, Xavier LL, et al. Endurance and resistance exercise training programs elicit specific effects on sciatic nerve

regeneration after experimental traumatic lesion in rats. [Internet]. Neurorehabilitation and neural repair. 2008 ;22(4):355-66.

32. Luis AL, Rodrigues JM, Lobato JV, Lopes MA, Amado S, Veloso AP, et al. Evaluation of two biodegradable nerve guides for the reconstruction of the rat sciatic nerve. [Internet]. Bio-medical materials and engineering. 2007 Jan ;17(1):39-52.
33. Varejão ASP, Cabrita AM, Meek MF, Bulas-Cruz J, Filipe VM, Gabriel RC, et al. Ankle kinematics to evaluate functional recovery in crushed rat sciatic nerve [Internet]. Muscle & nerve. 2003 ;27(6):706–714.
34. Sabatier MJ, To BN, Nicolini J, English AW. Effect of slope and sciatic nerve injury on ankle muscle recruitment and hindlimb kinematics during walking in the rat. [Internet]. The Journal of experimental biology. 2011 Mar 15;214(Pt 6):1007-16.
35. Maas H, Prilutsky BI, Nichols TR, Gregor RJ. The effects of self-reinnervation of cat medial and lateral gastrocnemius muscles on hindlimb kinematics in slope walking. [Internet]. Experimental brain research. Experimentelle Hirnforschung. Expérimentation cérébrale. 2007 Aug ;181(2):377-93.
36. Chang C-J. The effect of pulse-released nerve growth factor from genipin-crosslinked gelatin in schwann cell-seeded polycaprolactone conduits on large-gap peripheral nerve regeneration. [Internet]. Tissue engineering. Part A. 2009 Mar ;15(3):547-57.
37. Chen Y, Wang Y, Chen L, Sun C, English AW, Wolpaw JR, et al. H-reflex up-conditioning encourages recovery of EMG activity and H-reflexes after sciatic nerve transection and repair in rats. [Internet]. The Journal of neuroscience : the official journal of the Society for Neuroscience. 2010 Dec 1;30(48):16128-36.
38. Cebasek V, Kubínová L, Janácek J, Ribaric S, Erzen I. Adaptation of muscle fibre types and capillary network to acute denervation and shortlasting reinnervation. [Internet]. Cell and tissue research. 2007 Nov ;330(2):279-89.
39. Udina E, Voda J, Gold BG, Navarro X. Comparative dose-dependence study of FK506 on transected mouse sciatic nerve repaired by allograft or xenograft. [Internet]. Journal of the peripheral nervous system : JPNS. 2003 Sep ;8(3):145-54.
40. Goldberg JL, Espinosa JS, Xu Y, Davidson N, Kovacs GTA, Barres BA. Retinal ganglion cells do not extend axons by default: promotion by neurotrophic signaling and electrical activity. [Internet]. Neuron. 2002 Feb 28;33(5):689-702.
41. Heidemann SR, Buxbaum RE. Mechanical tension as a regulator of axonal development. [Internet]. Neurotoxicology. 1994 Jan ;15(1):95-107.

42. Sabatier MJ, To BN, Nicolini J, English AW. Effect of axon misdirection on recovery of electromyographic activity and kinematics after peripheral nerve injury. [Internet]. Cells, tissues, organs. 2011 Jan ;193(5):298-309.

Chapter 7 - General discussion and conclusions

1 General discussion

The main objective of this thesis was to investigate functional recovery of rats' hindlimb after therapeutic strategies for peripheral nerve repair in axonotmesis and neurotmesis injuries. The results obtained in the experimental studies included in this thesis allowed to verify functional and morphological differences between different therapeutic strategies, when using tissue engineering and cellular therapies based on new biomaterials. Chitosan (Chapter 3) and collagen (Chapter 4) associated to a cellular system capable of neurotrophic factors production are the different therapeutic strategies. Exercise-based neurorehabilitation was also studied in chapter 6.
The relevance of rat model in this thesis is related with the possibility to isolate several levels of complexity to understand biological systems and develop cellular systems to promote nervous tissue regeneration. It was possible to evaluate functional recovery *in vivo* after therapeutic intervention for peripheral nerve repair during a follow-up period with morphological evaluation of the nerve at the end of the experiment. Our experimental model was the sciatic nerve, and we have verified that the possibility of peripheral nerve repair is a promising reality. Peripheral nerve regeneration can be studied in a number of different experimental models based on the use of nerves from both forelimb and hindlimb (1-3). The experimental animal model of choice for many researchers remains the rat sciatic nerve. It provides an inexpensive source of mammalian nervous tissue of identical genetic stock that it is easy to work with and well studied (4) and shows a similar capacity for regeneration in rats and sub-humans primates (5). The rat sciatic nerve is a widely used model for the evaluation of motor as well as sensory nerve function at the same time (3).

Our studies of sciatic nerve regeneration include a post-surgery follow-up period of 20 weeks after neurotmesis and 12 weeks after axonotmesis based on the assumption that, by the end of this time, functional and morphological recovery are complete (6-9). Although both morphological and functional data have been used to assess neural regeneration after induced neurotmesis and axonotmesis injuries, the correlation between these two types of assessment is usually poor (10-12). Classical and newly developed methods of assessing nerve recovery, including histomorphometry, retrograde transport of horseradish peroxidase and retrograde fluorescent labelling (13; 14) do not necessarily predict the reestablishment of motor and sensory functions (10; 15-17). Although such techniques are useful in studying the nerve regeneration process, they generally fail in assessing functional recovery (10). In this sense,

research on peripheral nerve injury needs to combine both functional and morphological assessment. The use of biomechanical techniques and rat's gait kinematic evaluation is a progress in documenting functional recovery (17). Indeed, the use of biomechanical parameters has given valuable insight into the effects of the sciatic denervation/reinnervation, and thus represents an integration of the neural control acting on the ankle and foot muscles (17-20).

After peripheral nerve injury, acute changes were particularly evident during push off phase during stance, reflected in increased dorsiflexion at Toe Off (TO). With time, there was a somewhat limited recovery towards normality during stance phase with less pronounced dorsiflexion at TO, suggesting that extensor muscles regained the ability to partially perform the push off action.
In sciatic-crushed (i.e. axonotmesis) animals, functional recovery is fast and by week 6 to 8 most of the kinematic parameters show values similar to those post-surgery. However, some of the parameters remain altered even after a 12-weeks recovery period which contrasts to other functional test that recover within 8 weeks following sciatic crush injury (8).

After axonotmesis injury, hybrid chitosan membranes were used for peripheral nerve regeneration. Chitosan has recently attracted particular attention because of its biocompatibility, biodegradability, low toxicity, low cost, enhancement of wound-healing and antibacterial effects. Its potential usefulness in nerve regeneration have been demonstrated both *in vitro* and *in vivo* (7; 22). Chitosan is a partially deacetylated polymer of acetyl glucosamine obtained after the alkaline deacetylation of chitin (23). Chitosan matrices have been shown to have low mechanical strength under physiological conditions and to be unable to maintain a predefined shape for transplantation, which has limited their use as nerve guidance conduits in clinical applications. The improvement of their mechanical properties can be achieved by modifying chitosan with a silane agent. γ-glycidoxypropyltrimethoxysilane (GPTMS) is one of the silane-coupling agents, which has epoxy and methoxysilane groups. The epoxy group reacts with the amino groups of chitosan molecules, while the methoxysilane groups are hydrolyzed and form silanol groups, and the silanol groups are subjected to the construction of a siloxane network due to the condensation. Thus, the mechanical strength of chitosan can be improved by the crosslinking between chitosan and GPTMS and siloxane network. Chitosan and chitosan-based materials

have been proven to promote adhesion, survival, and neuritis outgrowth of neural cells (7).

The normal pattern of ankle motion during stance characterized by initial dorsiflexion followed by plantarflexion (push off action) was lost and dorsiflexion continues up to the end of the stance phase caused by inability of the leg muscles to generate plantarflexion moment (21). The ankle joint angle at Initial Contact changed significantly after the sciatic crush. Such changes were transient and by week4 ankle joint angle at Initial Contact was indistinguishable from baseline. Ankle joint angle at Opposite Toe-off was significantly affected after the crush injury but by week 4 of recovery joint position at this point of stance had recovered to normal values. At Heel Rise ankle joint angle was significantly altered after the sciatic nerve injury until week 12. Ankle joint angle at Toe-Off was significantly altered after the sciatic nerve injury. At week 12 ankle's joint angle mean value at Toe-Off was similar to the one registered before the sciatic nerve injury.

Group differences were observed, being the values at Initial Contact in the *ChitosanII* group different from all the other four groups. Ankle joint angular position at Opposite Toe in the *ChitosanII* group, throughout the study, were significantly different from *Crush* and *ChitosanIII* groups. At Heel Rise, it was possible to verify differences between *ChitosanII* and the *Crush* and *ChitosanIIICell* groups. Ankle's joint angle at Toe-Off was different between *ChitosanII* and *ChitosanIIICell* groups.

Ankle angular velocity at Opposite Toe was significantly affected after the crush injury and returned to preoperative values at week 4. Instantaneous ankle's joint velocity at Heel Rise was significantly affected after axonotmesis with differences from normal values until week 4 of recovery. Ankle's joint velocity at Toe-Off was significantly affected after the crush injury and did not recover completely within the 12-weeks follow up time.

There were significant differences between the groups for ankle joint velocity at Opposite Toe with significant differences between *ChitosanII* and *ChitosanIICell* groups. Differences between *ChitosanII* and *ChistosanIICell* groups were registered at Heel Rise. At Toe-Off, differences between *ChitosanIICell*, from one hand and *Crush*, *ChitosanIII* and *ChistosanIIICell* groups, on the other were found. At week12, results of the gait kinematic analysis of the experimental groups revealed that the group using

ChitosanIII group differs from *Crush* group in a smaller number of variables. This indicates that at the end of the recovery period animals in *ChitosanIII* group presented a degree of functional recovery similar to that registered in the *Crush* group.

Sciatic functional index (SFI) and Static Sciatic Index (SSI) results showed that SFI values changed significantly after the crush injury. SFI values were different from baseline until week 7 of recovery.
The effect of group was observed for SFI values indicating that values from *ChitosanIICell* group were different from those of the *ChitosanII* and *ChitosanIII* groups. Analysis on SSI data was similar to the reported SFI results. However, SSI results from the *ChitosanIIICell* group were different from those of the *Crush*, *ChitosanII* and *ChitosanIICell* groups.

The Extensor Postural Trust (EPT) values obtained during the healing period of 12 weeks were significantly affected by the crush injury and at week 12, EPT had still not recovered to baseline values.
There were significant differences in EPT values between the experimental groups analysis shows that the EPT values from the *Crush* group were significantly different from those of the *ChitosanIICell* and *ChitosanIIICell*, suggesting a negative effect of the N1E 115-differentiated cells on motor recovery after sciatic crush injury.

Withdrawal Reflex Latency (WRL) assessed nociceptive function and it was affected up to week 8. Beyond this time point, WRL values, the experimental groups pooled together, were similar to those preoperatively.
The effect of group was found for WRL data and analysis showed that differences were significant between *ChitosanII* group from one side and *ChitosanIICell*, *ChitosanIII* and *ChitosanIIICell* groups on the other side. These results are suggestive of a slower rate of recovery in WRL with the use of type II chitosan.

Functional assessment partially supported the histomorphometric results since results of the WRL, EPT, SFI and SSI tests suggest that chitosan type II and the N1E-115 cells have a reduced degree of functional recovery which is in line with results of histomorphometric analysis. Histological appearance of control normal sciatic nerve cross sections in comparison to cross sections of the regenerated nerve fibers in all five experimental groups were organized in microfascicles and were smaller than control nerve fibers. In the two experimental groups in which cell delivery was carried

out, the presence of unusual cell profiles, interpretable as the transplanted cells, was detectable at the periphery of the nerves. This was seldom observed in inner parts of the nerve suggesting that only few transplanted cells colonized the inner nerve interstice. Electron microscopy confirms that a good regeneration pattern of both unmyelinated and myelinated nerve fibers occurred in all experimental groups, irrespectively of the enrichment with neural stem cells. The border zone of the nerve still shows the presence of some chitosan debris integrated with the collagen fibers of the epineurium. Moreover, in the two experimental groups in which cell delivery was carried out, it was possible to find some of transplanted cells localized in the border zone of the regenerated nerve. Results of the design-based morphoquantitative analysis of regenerated myelinated nerve fibers permitted to quantitatively compare the different experimental groups. As expected, fiber density was significantly higher in all experimental groups in comparison to control sciatic nerves, while mean axon and fiber diameter and myelin thickness were significantly lower. On what regards the number of regenerated myelinated nerve fibers, was found to be significantly higher in comparison to controls in four out of the five experimental groups only; in fact, *ChitosanIII* group showed a number of fibers not significantly different in comparison to normal control nerves. The peculiarity of the experimental group, characterized by type III chitosan membrane enwrapment, was also confirmed by statistical analysis of inter-group variability among experimental groups which demonstrated that *ChitosanIII* group presented a significantly higher mean fiber and axon diameter and myelin thickness in comparison with all other experimental crush groups.

We also studied the effects on nerve regeneration when using collagen membranes after neurotmesis without gap (end-to-end microsurgical technique) associated with *in vitro* differentiated cellular system (chapter 3). After 20 weeks animals were sacrificed and the repaired sciatic nerves were processed for histological and stereological analysis. SFI was not possible to perform because of automutilation of the fingers after sciatic nerve injury.

In the weeks following sciatic nerve transection, ankle joint motion became severely abnormal, particularly throughout the second half of stance corresponding to the push-off sub-phase. In clear contrast to the normal pattern of ankle movement, at week-2 post-injury animals were unable to extend this joint and dorsiflexion continued increasing during the entire stance. This result could be associated to the paralysis of plantarflexor muscles. The pattern of the ankle joint motion seemed to have improved only slightly during recovery. For OT velocity and HR angle no differences were found

before and after sciatic nerve transection, whereas for OT angle differences from pre-injury values were significant only at weeks 2 and 16 of recovery. The angle at IC showed a unique pattern of changes, being unaffected at week-2 post-injury and altered from normal in the following weeks of recovery. Probably the most consistent results are those of HR velocity, TO angle and TO velocity. These parameters were affected immediately after the nerve injury and remained abnormal along the entire 20-weeks recovery period.

Generally, no differences in the kinematic parameters were found between the groups. Exceptions were IC velocity in the *End-to-EndMembCell* group, which was different from the other two groups, and OT angle in the *End-to-EndMemb* group that was also different from the other two groups.

Reflex activity also revealed relevant information concerning functional recovery. The EPT response steadily improved during recovery but at week-20 the EPT values of the injured side were still significantly lower compared to values at week-0.
A significant main effect for treatment was found, with better recovery of the EPT response in the *End-to-EndMembCell* group when compared to the other two experimental groups: at week-20, motor deficit decreased to 27% in the *End-to-EndMembCell* and to 34% and 42% in the *End-to-End* and *End-to-EndMemb* groups, respectively.

During the following weeks after injury there was recovery in paw nociception**,** which was more clearly seen between weeks 6 and 8 post-surgery. At week-6, half of the animals still had no withdrawal response to the noxious thermal stimulus in the operated side, which is in contrast with week-8, when all animals presented a consistent, although delayed, response. Despite such improvement in WRL response, persistence of sensory deficit in all groups by the end of the 20-weeks recovery time was reported. No difference between the groups was observed in the level of WRL impairment after the sciatic nerve neurotmesis.

After neurotmesis, regeneration of axons was organized in many smaller fascicles in comparison to controls. No significant difference regarding any of the morphological parameters investigated in the regenerated axons from the three experimental groups. On the other hand, comparison between regenerated and control nerves showed, as expected, the presence of a significantly higher density and total number of myelinated

axons in experimental groups accompanied by a significantly lower fiber diameter. Results showed that enwrapment of the rapair site with a collagen membrane, with or without neural cell enrichment, did not lead to any significant improvement in most of functional and stereological predictors of nerve regeneration. The exception was EPT which recovered significantly better after neural cell enriched membrane employment. Results of this study revealed that this particular type of nerve tissue engineering approach has very limited effects on nerve regeneration after sciatic end-to-end nerve reconstruction in the rat.

We have concluded that the sciatic nerve regeneration after neurotmesis and end-to-end suture can be improved by *in vitro* differentiated N1E-115 neural cells seeded on a type III equine collagen membrane, enwrapped around the injury site. The N1E-115 cell line has been established from a mouse neuroblastoma (24) and have already been used, with conflicting results due to its neoplasic origin, as a cellular system to locally produce and deliver neurotrophic factors (25). *In vitro*, the N1E-115 cells undergo neuronal differentiation in response to dimethylsulfoxide (DMSO), adenosine 3', 5'- cyclic monophosphate (cAMP), or serum withdrawal (24). Upon induction of differentiation, proliferation of N1E-115 cells ceases, extensive neurite outgrowth is observed and the membranes become highly excitable (8; 9; 26-30). The interval period of 48 hours of differentiation was previously determined by measurement of the intracellular calcium concentration ($[Ca^{2+}]i$). Notice that at this time, the N1E-115 cells present, already, the morphological characteristics of neuronal cells, nevertheless cell death due to increased $[Ca^{2+}]i$ is not yet occurring as described elsewhere (8; 9; 26; 29-36).

Neurotrophic factors play an important role in nerve regeneration after injury or disease and it is conceivable that if neurotrophic factors are applied in the close vicinity of the injured nerve their healing potency is optimized. In spite of these assumptions and contrary to our initial hypothesis, the N1E-115 cells did not facilitate either nerve regeneration or functional recovery and, as far as morphometrical parameters are concerned, results showed that the presence of this cellular system reduced the number and size of the regenerated fibers. These results suggest that this type of nerve guides can partially impair nerve regeneration, at least from a morphological point of view (8; 9; 26; 29-36). The impaired axonal regeneration seems to be the result of N1E-115 cells surrounding and invading the regenerating nerve, since numerous of these cells where seen colonizing the nerve and might have deprived regenerated nerve fibers blood supply (8; 9; 26-30). The use of N1E-115 cells did not promote nerve

healing and their use might even derange the nerve regenerating process. Whereas the effects on nerve regeneration were negative, an interesting result of this study was the demonstration that the cell delivery system that we have used was effecting in enabling long-term colonization of the regenerated nerve by transplanted neural cells. Whether the negative effects of using N1E-115 cells as a cellular aid to peripheral neural tissue regeneration extends to other types of cells is not known at present and further studies are warranted to assess the role of other cellular systems, e.g. mesenchymal stem cells, as a foreseeable therapeutic strategy in peripheral nerve regeneration. Our experimental results with this cellular system are also important in the perspective of stem cell transplantation employment for improving posttraumatic nerve regeneration with patients (8; 9; 26; 29-36). Undoubtedly, great enthusiasm has raised among researchers and in the general public about cell-based therapies in regenerative medicine (8; 9; 26; 29-36). There is a widespread opinion that this type of therapy is also very safe in comparison to other pharmacological or surgical therapeutic approaches. By contrast, recent studies showed that cell-based therapy might be ineffective for improving nerve regeneration (8; 9; 26; 29-36) or even have negative effects by hindering the nerve regeneration process after tubulisation repair. Whereas the choice of the cell type to be used for transplantation is certainly very important for the therapeutic success, our present results suggest that the paradigm that donor tissues guide transplanted stem cells to differentiate in the direction that is useful for the regeneration process it is not always true and the possibility that transplanted stem cells choose another differentiation line potentially in contrast with the regenerative process should be always taken in consideration.

From a functional point of view, it was verified that independently from the type of sciatic nerve injury, ankle motion is severely affected in the weeks immediately after the injury. After neurotmesis (chapter 4), automutilation, chronic foot deformities, inversion or eversion deformations were the main methodological source of limitation for the functional assessment with the use of others widely used behavioural tests, i.e. Sciatic Functional Index (SFI) and Static Sciatic Index (SSI) (12; 37). Despite this limitation SFI is a widely used parameter because of its reliability (38), but recent studies revealed that SFI method is only reliable from the 3rd week on after a severe lesion (39). Although SFI is a quantitative method, it only considers stance phase and several aspects have been reported as methodological limitations since some of the measurements (i.e. Print Length factor) are dependent on the walking velocity and pressure exerted by the foot on the floor influenced for instance by the weight of the

animal. Performing kinematic analysis for assessment of gait as dynamic function, as it describes the trajectory of a joint during the movement, was a good alternative. Although kinematics are only the description of movement and only takes into consideration joint angles, it represent a good approach to understand joint coordination and changes in kinematics during walking could be indicative of the role of muscles in regulating locomotor activity. Using 2D video analysis and dedicated software for motion analysis, our group reported measures of both angle and angular velocity of the ankle joint during the stance phase (8; 26). Angular velocity data were calculated in an attempt to raise the precision of joint motion analysis and to increase its power in detecting subtle differences in functional recovery when testing alternative treatments after sciatic crush (26). We reasoned that functional deficits during walking in rat nerve models might be masked by the high redundancy and adaptability of the motor apparatus in response to sensorimotor alterations (12; 37).

Almost all the kinematics parameters analysed regarding ankle motion during the whole phase of the rat walk reveals a persistent abnormal pattern. Muscles innervated by sciatic nerve *rami* includes both dorsiflexors and plantarflexors and although in previous studies we focused our kinematic analysis only in the stance phase, including analysis of all joints also during the swing phase provided additional information. However, a key question regarding joint motion analysis is which parameters present enough sensitivity to evaluate function after different types of sciatic injury. We have evaluated the sensitivity and the specificity of ankle motion analysis to detect functional deficits in the rat sciatic model (Chapter 5). By using a set of kinematic variables describing angle and velocity during walking, a statistical model was generated that robustly separates animals shortly after sciatic crush from sham-operated controls and animals after 12 weeks of recovery. Moreover, the model displayed a moderate ability to separate between the two latter groups of animals. Therefore, 2D kinematic analysis of joint motion is sensitive to detect motor deficit caused by sciatic nerve injury even when functional deficits are minimized by long-term recovery.

All kinematic measures were significantly altered in the time shortly after the sciatic crush, when compared to sham-operated and recovered animals, with the exception of angular velocity at mid-swing, which apparently is not affected by the sciatic nerve crush and therefore seems not to be of great utility to assess functional status in the rat sciatic model. Moreover, the introduction of interjoint coordination was also important in order to have insights about the behaviour of all hindlimb joints, considering the denervated chain of muscles after injury. Sciatic nerve gives off branches to the hip

extensors and leg flexors and continues its courses beneath the gluteus medius muscle into the thigh, in the mid-thigh the nerve trifurcates into the peroneal, tibial and sural branches; the peroneal nerve subsequently innervates the tibialis anterior and extensor *digitorum longus*, while the tibial nerve supplies the plantar flexor, toe flexors, and the tibialis posterior. Thus, it is expected that after sciatic nerve injury hip, knee and ankle motion reflect functional deficits. Although kinematics is only the description of movement and only takes into consideration joint angles, it represents a good approach to understand joint coordination. Recent studies revealed that different joint positions were combined to achieve functional movement during cat walking after peripheral nerve injury (12; 37). The whole limb position and orientation were considered a preferable parameter than joint position (38). Therefore, inter segmental transfer of energy might also be a mechanisms of economical movement production after muscle denervation.

Our data suggest that joint kinematics has the ability to highlight minor walking changes after long-term recovery from sciatic crush injury. However, the kinematics changes during walking twelve weeks after sciatic nerve crush were noticed in the hip and knee joints, while ankle joint kinematics had recovered its normal pattern. In line with joint kinematics data, discriminant analysis clearly demonstrated that walking measures, either spatiotemporal features or hindlimb joint kinematics, accurately recognize sciatic-denervated animals and distinguishes them from sciatic-reinnervated animals and sham controls. Spatiotemporal parameters like gait velocity, stride length, stance phase duration and swing phase duration are relevant for the study of pathological pattern of gait after peripheral nerve injury in experimental rat model (39). Stance phase duration measured the time hind foot was in contact with the floor. After sciatic nerve injury, the injured limb has a smaller stance phase duration. Step length, is accurately measured using the location of the middle metatarsal head to metatarsal head in successive steps (8; 26) and walking speed is considered a parameter that influences stance phase and step length after sciatic crush injury (26).

The relevance of spatiotemporal parameters is related with mechanical aspects of locomotion and its functional relevance for performance. Considering that the basic functions of locomotion are propulsion, stance stability, shock absorption and energy conservation (40; 41), gravitational forces are important in walking and gait disturbances reduces the ability to use gravity and inertia in ambulation and therefore must resort to actual muscle work, which means that they have to spend more energy to cover certain distance.

Finally, it was possible to detect subtle differences between two types of therapeutic exercise widely used in neurorehabilitation clinical practice. The two exercise modes consisted on treadmill exercise walking and passive mobilization of the affected hindlimb and their effect was evaluated in contrast to a non-exercise group of sciatic nerve crushed animals and sham operated controls. Passive exercise consisted on manual mobilization of the entire right hindlimb. The manual mobilization included movement of the hip, knee and ankle joints in concert, and alternating flexion and extension of the joints. The results demonstrate marginal effects of both active and passive exercise on functional recovery, assessed by hindlimb joint kinematics during level walking. Although the impact of exercise on functional recovery was relatively modest it was nonetheless accompanied by improved nerve morphology, particularly by preventing excessive increase in total number of myelinated fibers in regenerated sciatic nerves.

Kinematic analysis distinguished recovery of movement pattern between groups. Twelve weeks after injury, ankle joint was similar between groups. In contrast to ankle joint kinematics, hip and knee joint kinematics in the Crush group clearly deviated to that of the Sham group. Such changes in the normal hip and knee kinematics during walking were not noticed in both the active and passive exercise groups. We interpret these results as a demonstration that the hindlimb motion pattern during level walking is not fully reestablished after sciatic crush injury and that compensatory change at the hip and knee joint kinematics masking disability at the ankle joint. The mechanisms underlying these changes cannot be discerned by our data. The stimulus caused by this rather unspecific passive motion proves also to have a positive effect on the regenerating nerve morphology and in overall hindlimb motion pattern during walking. Such apparent positive direct effect on nerve regeneration might result from increased afferent input due to the movement stimulus (38). Another possibility is that our passive movement induced rhythmic mechanical load onto the regenerating nerve inducing local cellular and molecular responses that enhance nerve regeneration (39)

Comparison between regenerated and non-injured nerves showed morphological differences. Signs of better regeneration as a result of passive hindlimb mobilization were observed. As for the active exercise group, mean total number of myelinated fibers in the passive exercise group was indistinct from that of the Sham group. Interpretation of these results is difficult, and thus it deserves further research, the

discrepancy between different authors who revealed an increase in the number of myelinated axons and our results, which evidenced the opposite. Thus, results from exercise-based neurorehabilitation are promising. In conclusion, passive and active joint movement causes joint kinematics and nerve morphological changes. Results of this study suggest that mechanical load plays a role on functional recovery after peripheral nerve repair. However, further studies are needed to understand the functional meaning of results.

2 Future perspectives

2.1 Nerve regeneration

Enwrapment of the site of a nerve crush lesion with a chitosan type III membrane significantly improves nerve regeneration in the rat, whereas enrichment of chitosan membranes with N1E-115 neural cells does have positive effects. Whereas transposition of animal studies to patients should always be dealt with caution, the results obtained in this experimental study opened interesting perspectives for the clinical use of hybrid chitosan membranes in peripheral nerve reconstruction.

More complex devices will be needed, such as multilayered tube guides where growth factors are entrapped in polymer layers with varying physicochemical properties or tissue engineered tube guides containing viable stem cells (8; 26). The combination of two or more growth factors will likely exert a synergistic effect on nerve regeneration, especially when the growth factors belong to different families and act via different mechanisms. Combinations of growth factors can be expected to enhance further nerve regeneration, particularly when each of them is delivered at individually tailored kinetics (26). The determination and control of suitable delivery kinetics for each of several growth factors will constitute a major hurdle both technically and biologically with the biological hurdle lying in the compliance with the naturally occurring cross talk between growth factors and cells. A solution to this problem may be the use of mesenchymal autologous or heterologous stem cells because they can synthesize several growth factors and differentiate into Schwann cells which are critical for very long gaps (40; 41).

Tissue engineering advances promotes the development of other biomaterials to enhance peripheral nerve regeneration. The choice of the cellular system to be applyed is crucial for the therapeutic success. Using another cell line other than N1E-115 could have led to better results, concerning for instance, the emerging knowledge about autologous or heterologous mesenchymal stem cells from extra-fetal sources (38). Moreover, the construction of more appropriate tube-guides with integrated growth factor delivery systems and/or cellular components could improve the effectiveness of nerve tissue engineering. In fact, single-molded tube guides may not give sufficient control over both the mechanical properties and the delivery of bioactive agents.

2.2 Methodological improvement of functional assay

Kinematic analysis has improved the sensitivity of functional recovery assessment after peripheral nerve injury in experimental animals and its importance seems will increase in the future as a result of advanced technology and improved biomechanical models. From a biomechanical perspective, joint rotational velocity has a more direct relationship with the forces actuating onto the hindlimb segments and therefore velocity measures may be better indicators of dysfunction caused by nerve injury. Moreover, ankle position data is sometimes difficult to interpret, for example in those cases where ankle joint angle remains unaffected in the weeks immediately after sciatic nerve crush (8; 26). This shows that measures of ankle joint angle taken at snapshots during walking may lack sensitivity to assess functional impairment. In the near future, other statistical methods should be considered. Individual joint kinematics either in control or nerve-injured animals is characterized by high variability, with notable differences between different animals and even from step to step (42). Such high level of variability, which seems to be an intrinsic property of normal quadruped walking, seriously affects the precision of joint kinematic measures of functional recovery after nerve injury. Reducing this variability is a challenge for efficient use of walking analysis to assess functional recovery. Attempts to overcome this limitation include constraining walking velocity by using treadmill walking instead of self-paced locomotion (28; 43-48). This, of course, is likely to reduce step-by-step variability in joint kinematics but has the disadvantage of requiring expensive equipment and limits the possibility of combining kinematic analysis with other data, such as ground reaction forces. Other possibilities look at a global, limb-level movement analyses as an alternative to individual joints kinematics (28; 43-48). Also, systematic changes in the biomechanical and movement control constraints of the locomotor task, such as using up- and down-slope walking might also increase the accuracy of walking analysis within the context of peripheral nerve research (28; 43-48).

Study the influence of gait velocity on functional parameters. Yu et al (2001) (37) showed that gait analysis method is highly sensitive and studied seven spatial and kinematic parameters. It was also pointed out that when the spontaneous walking speed exceeded 55 cm/s was approached the limit of walking. When the walking speed was less than 25cm/s the rats looked nervous and overcautious. Moreover, the stance phase and step length, accurately measured by middle metatarsal head to metatarsal head distance, was affected by walking speed.

Bilateral hindlimb model should be constructed. Yu et al. (2001) defined the right:left stance/swing ratio (SS); right:left step length ratio (SLR); angle of the ankle joint at terminal stance (ATS); angle of the ankle joint at midswing (AMS); tail height; tail deviation, and midline deviation (MID). Concerning to tail and midline deviation, they verified that the tail of normal rats deviated towards the side where the hindlimb was at terminal stance, and during walking the body leans towards the contralateral side when the hindlimb is at midswing. During a gait cycle after sciatic nerve injury produces ankle dorsiflexion deformity presumably due to the dominance of tibial nerve innervation in the lower extremities. Based on discriminant analysis these authors concluded that right:left stance/swing ratio, right:left step length ratio and ankle joint at terminal stance contributed significantly to the equation developed to obtain sciatic injury score.

Methodological errors related with skin movement artefacts should be studied in kinematic analysis with optimization methods. In fact, the main sources of error affecting in vivo estimation of the pose of a skeletal bone with a non invasive skin markers technique are related with skin slippage, namely soft tissue artefacts (37), anatomical landmarks misallocation and instrumental noise (40; 41), and efforts have been made to overcome this limitation. While the estimation of instrumental errors is not problematic, the in vivo quantification of soft tissue artefacts and their effect on the determination of the bone position and orientation is still an open issue. Rats have excessive skin mobility that can generate large soft tissue artefacts therefore increasing the kinematic and kinetics data error during motion analysis. Thus, it was verified that using tattooing the anatomical landmarks misallocation and consequent inter-test variability was controlled (50). Soft tissue artefacts were verified to be problematic at the knee joint (51). The position of the knee joint is loosed by skin coverage; (8; 26) proposed that it could be calculated by using hip and ankle joint position and external individual measurements of femur and tibia length. (26), used high speed X-ray video and reported that the largest error between skin and bone derived angles occurred immediately before the paw contact, and at toe-off the error was the smallest. It was also reported that skin-derived kinematics overestimated angular values and the knee position was the joint most affected. The choice of skin marker placement is a critical aspect for discussion about motion analysis, and comparisons between studies should consider this aspect when interpreting for instance joint angle values. Sagittal values derived from skin markers are only approximation of the actual movements of the bones that comprises a joint of interest.

Another problem in kinematic studies related with protocol is the accurate determination of cycle landmarks such as Initial contact and toe-off. Ground reaction forces will improve the accuracy of determination of stance phase events. The introduction of optoelectronic motion capture system (Chapter 4) improved accuracy of the kinematic model, allowing instantaneous position estimation and reducing the error introduced by digitalization process, improving data processing. Position estimation is performed automatically and when a marker is missing it is estimated with mathematical algorithm considering the coordinates of the following frames. Data using this system has surprisingly showed that unlike our previous stance phase based results showing significant improvement in ankle joint motion after sciatic injury, analysis of swing phase shows that the abnormal ankle motion pattern remains without significant improvement over the entire recovery period. Using optoelectronic technology it will be possible to introduce anthropometric characteristics. In what concerns biomechanical model, the relative position of anatomical segments is important to perform biomechanical modelling. Reconstruction and analysis of *in vivo* skeletal system kinematics using optoelectronic stereophotogrammetric data will allows the joint kinematic description providing segment morphology (40; 41). Anatomical 3D analyses (42) will be possible to quantify observable functional deficits in others planes of movement further than sagittal, like rotation of the injured paw, curvation and inversion of the feet (37; 49).

2.3 Functional meaning

From animal models we know that neural control of locomotion operates automatically at a basic level, without conscious perception. There is a spinal network, which generates a detailed muscle-specific spatio-temporal pattern similar to what is observed during walking. However, this automatic level does not operates in isolation, the final muscle activation pattern is also influenced by sensory feedback from joint, muscle, and skin receptors (37). During ongoing movement fundamental mechanical variables of force, length, and velocity are monitored within muscles by Golgi tendon organs and by muscle spindle receptors, respectively. Thus, kinematics description of motor behaviour provides a foundation for integrating morphology and physiology with mechanics and function (28; 43-48). Moreover, force generated by a muscle depends on activation by nerve impulses as well as the length and velocity of the muscle. The functional meaning of recovery after peripheral nerve injuries implies the study of motor control since peripheral nerves enclose both sensory and motor information, which are important to produce controlled movement. From our results, we demonstrated that

joint angular displacement and joint velocity during locomotion movement might quantify functional recovery after peripheral nerve injury. Moreover, nociception was the first variable achieving signs of recovery. How could these quantities be related with neuromuscular function and have functional meaning and clinical implications?
When we analyze joint kinematics data, it should be taken into consideration that these results are also related with neural and muscle function thus being relevant to perform a comprehensive description of movement of individual muscle action within the joint or the joints it crosses. Dynamics of muscle function is usually examined by indirect assessment of muscle length change based on kinematics (51) and muscle moment arms, or estimates of fascicle length change that must take into account in-series elastic stretch of a tendon and a simplification of the effects of muscle architecture. Knowledge of the more complex, but a realistic pattern of 3D movement is important for understanding its neuromuscular control, as well as the principles of musculoskeletal design (52) that are crucial to the production of movement. During dynamic conditions, combining kinematic data with kinetics and electromyography would be desirable to make a comprehensive understanding of movement patterns and its changes as well as the study of inefficient movement after injury. The study of the relationship between joint angular velocity and muscle moments would contribute to understand muscle contraction and work production. Results from the last study awake us for the relevance of mechanical load, fatigue and the influence of joint rotational velocity, which should be explored to understand performance and make available results translation for motor rehabilitation.

Understanding functional results after peripheral nerve injury is complex, especially when both sensory and motor pathways are impaired. Moreover, some limitation of WRL and EPT should be considered and the interpretation of functional results should be made carefully. Motor reflex deficit was assessed by extensor postural test (EPT) that is characterized by the exertion of force on the ground, in a hand-controlled loading condition, quantified with a scale. The reduction in this force, representing reduced extensor muscle tone, was considered a deficit of motor function. Moreover, the muscles that has been considered for interpretation of the results was the ankle extensors i.e. gastrocnemius and soleus muscles. Also for sensory function, some authors considered that the influence of mecanoreceptors should be controlled for the interpretation of the results controlling the pressure exerted on the thermal platform. Although WRL reflex was originally named flexion-withdrawal reflex (42), it has since been shown to involve other muscles besides flexors (52). The WRL can vary because

it depends on which afferents are stimulated and signals transmitted over polysynaptic pathways. This means that the input signal can be modified along its path. The recovery of sensory function is undertaken by several afferent fibers and may not be explained by the outgrowth of regenerating axons from the sectioned proximal sciatic nerve stumps but also by collateral sprouts from intact fibers in the skin surrounding the denervated zone. In fact, the recovery of sensory nerve function might be started with the expansion of the territory of intact neighbouring fibers (28; 43-48). Regenerated sciatic nerve began to regain function between 3 (28; 43-48) to 7 (52) weeks after injury. The borderline between a sensory-motor response involving both sensory ascending and descending motor pathways and a pain-based withdrawal reflex-response is not always possible. It cannot always be sure that all responses are based on proper temperature sensing. Reflex activity should be integrated in a dynamic model, assessed during movement, since it might comprise an important aspect on motor control with functional meaning for the position of the limb and movement. Mathematical modelling is a possible solution to simplify and understand the potential environmental effect with similar neural control and exclude neural feedback. Efforts will be made to improve the biomechanical modelling with musculoskeletal model and methodologies to understand the reflex mechanisms involved in the sensory and motor recovery of function.

In summary, gait analysis is a promising method to assess functional recovery after hindlimb nerve injury. However, in order to provide accurate measures of functional recovery, gait analysis after hindlimb peripheral nerve injury should evolve from a simple ankle kinematics analysis to a full 3D biomechanical description of complete hindlimb motion, meaning analysis of hip, knee and ankle joints. Further refinements of gait analysis in the field of peripheral nerve research using the rat model should include the combined use of joint kinematics, ground reaction forces and electromyography data.

Innervation regulates muscle mass and muscle phenotype (53) and peripheral nerve injury in the rat is a widely used model to investigate nerve regeneration and can also be employed as a model of muscle inactivity and muscle atrophy (54). Previous work of our research team has been devoted to enhance nerve regeneration after injury, including the use of biomaterials and cellular systems (26). By combining motor and sensory function tests, biomechanical analysis of the rat gait and nerve morphology assessment by unbiased stereological methods, we could demonstrate that animals

almost fully recover from sciatic nerve crush in 12 weeks (8). However, nerve morphology remains significantly different in control and injured animals as well as ankle joint motion during walk (8). Muscle function was not assessed in our previous work. Aside incomplete nerve regeneration, changes in the muscles may contribute to functional deficit after nerve injury (54-56).

Denervation induces muscle atrophy and, 25 months post denervation, muscle fibres crossectional area of the EDL muscle diminish to only 2.5% of control animals although their fascicular organization is maintained (57). The effect of denervation on muscle atrophy is both activity-dependent and activity-independent since the degree of hindlimb muscle atrophy after spinal isolation (activity-independent nerve influence) is less when compared to the atrophy caused by removal of all nerve influences by transecting the sciatic nerve (53). Two basic mechanisms are responsible for denervation-induced muscle atrophy. First, there is augmented activity of the ubiquitin-proteasome pathway and proteolysis (58). Second, there is cell death and myonuclei apoptosis conjugated with decreased capacity of satellite cell-dependent reparative myogenesis (54; 57). Together with atrophy, denervated/reinnervated muscles undergo phenotypical changes and conversion between muscle fibre types (55).

The relative increase in type I or type II muscle fibres following denervation seems to depend on the type of muscle fibres predominant in the muscle, with type II muscle fibres (fast fibres) increasing in proportion in soleus (slow muscle) and type I muscle fibre number increasing in gastrocnemius and tibialis anterior muscles (54). Likewise, the degree of muscle fibre atrophy in short-term denervation (4 weeks) has been noticed to be greater in the muscle fibre type that is more abundant in the affected muscles (59). However, it must be stressed that for many purposes there is a lack of detailed morphological description of denervated/reinnervated muscles since in most cases the morphoquantitative methods employed lack accuracy and completeness.

Muscle architectural changes, and also likely remodeling of the enveloping connective tissue (60) might contribute to altered function in denervated/reinnervated muscles. Ideally, muscle contractile properties are evaluated in minimally dissected muscle-nerve preparations in which muscle contractions are elicited by electrical stimulation of the nerve (61). Using such approach, fundamental properties of hindlimb muscles of the rat, like isometric peak force, range of active force, slack length, and passive length-force curve can be obtained. All these parameters are potentially affected by changes in muscle morphology secondary to denervation/reinnervation (60). Unlike the classical view, skeletal muscles are not isolated units and their mechanical properties are dependent on the context, meaning the mechanical load in surrounding muscles

and connective tissue (62). The transmission of force out from the muscle fibres to the skeleton follows both myotendinous and myofascial links (63). The latter involves load being transmitted to synergistic and antagonistic muscles (60) and occurs through the muscular and non-muscular connective tissues (e.g. neurovascular tracts, i.e. the collagen fiber reinforced tissues surrounding nerves and blood vessels). Surgical reconstruction of the peripheral nerves affects the mechanical properties of the neurovascular tract supplying leg muscles in unknown ways as well as the architecture of denervated muscles. In addition, altered properties of supportive connective tissue may affect myofascial force transmission and overall function (60). In situ testing of muscle function, keeping the connective tissue that envelops the muscle or muscle groups undamaged, is a unique method to evaluate possible changes in myofascial force transmission (62), and by measuring the force produced at the proximal and distal ends of the EDL an indication of myofascial force transmission is obtained (64).
In recent years, great emphasis has been placed on kinematic analysis of the rat locomotion [(19). Although gait analysis is an elegant and meaningful way to assess functionality, it is limited in evaluating physiological and mechanical properties of the affected muscles. The potential for biomechanical gait analysis to assess hindlimb muscle function requires precise motion capture system combined with ground reaction force data (65) and a geometrical model of the rat hindlimb musculoskeletal system (66).

The development of biological and material therapeutic strategies to enhance functional recovery is the major interest of several research areas such as Biology, Engineering, and Medicine. The assessment of functional recovery is a complex question that has many different facts to be addressed in detail. A common feature of these problems is that they address relationships between morphological, physiological and behavioural aspects of information processing in nervous system (“structure-function” relationships). Movement Sciences should be considered for the interdisciplinary approaches across established neuroscience disciplines. Moreover, functional recovery after peripheral nerve injury assessed with dynamical model of locomotion might represent an integrative approach to have deep knowledge about neural activity, mechanical and structural relationship.

REFERENCES

1. Yang C-C, Shih Y-H, Ko M-H, Hsu S-Y, Cheng H, Fu Y-S. Transplantation of human umbilical mesenchymal stem cells from Wharton's jelly after complete transection of the rat spinal cord. [Internet]. PloS one. 2008 Jan ;3(10):e3336.
2. Höke A. Mechanisms of Disease: what factors limit the success of peripheral nerve regeneration in humans? [Internet]. Nature clinical practice. Neurology. 2006 Aug ;2(8):448-54.
3. Jensen JN, Tung THH, Mackinnon SE, Brenner MJ, Hunter DA. Use of anti-CD40 ligand monoclonal antibody as antirejection therapy in a murine peripheral nerve allograft model. [Internet]. Microsurgery. 2004 Jan ;24(4):309-15.
4. Geuna S, Raimondo S, Ronchi G, Di Scipio F, Tos P, Czaja K, et al. International Review of Neurobiology Volume 87 [Internet]. Elsevier; 2009.
5. Hu D, Hu R, Berde CB. Neurologic evaluation of infant and adult rats before and after sciatic nerve blockade. [Internet]. Anesthesiology. 1997 Apr ;86(4):957-65.[
6. Amado S, Rodrigues JM, Luís AL, Armada-da-Silva P a S, Vieira M, Gartner A, et al. Effects of collagen membranes enriched with in vitro-differentiated N1E-115 cells on rat sciatic nerve regeneration after end-to-end repair. [Internet]. Journal of neuroengineering and rehabilitation. 2010 Jan ;77.
7. Simões MJ, Amado S, Gärtner A, Armada-Da-Silva P a S, Raimondo S, Vieira M, et al. Use of chitosan scaffolds for repairing rat sciatic nerve defects. [Internet]. Italian journal of anatomy and embryology = Archivio italiano di anatomia ed embriologia. 2010 Jan ;115(3):190-210.
8. Luís AL, Amado S, Geuna S, Rodrigues JM, Simões MJ, Santos JD, et al. Long-term functional and morphological assessment of a standardized rat sciatic nerve crush injury with a non-serrated clamp. [Internet]. Journal of neuroscience methods. 2007 Jun ;163(1):92-104.
9. Luís AL, Rodrigues JM, Geuna S, Amado S, Simões MJ, Fregnan F, et al. Neural cell transplantation effects on sciatic nerve regeneration after a standardized crush injury in the rat. [Internet]. Microsurgery. 2008 Jan ;28(6):458-70.
10. Shen N, Zhu J. Application of sciatic functional index in nerve functional assessment. [Internet]. Microsurgery. 1995 Jan ;16(8):552-5.
11. Kanaya F, Firrell JC, Breidenbach WC. Sciatic function index, nerve conduction tests, muscle contraction, and axon morphometry as indicators of regeneration.

[Internet]. Plastic and reconstructive surgery. 1996 Dec ;98(7):1264-71, discussion 1272-4.

12. Dellon AL, Mackinnon SE. Sciatic nerve regeneration in the rat. Validity of walking track assessment in the presence of chronic contractures. [Internet]. Microsurgery. 1989 Jan ;10(3):220-5.
13. Mackinnon SE, Dellon AL, O'Brien JP. Changes in nerve fiber numbers distal to a nerve repair in the rat sciatic nerve model. [Internet]. Muscle & nerve. 1991 Nov ;14(11):1116-22.
14. Mackinnon SE, Hudson AR, Hunter DA. Histologic assessment of nerve regeneration in the rat. [Internet]. Plastic and reconstructive surgery. 1985 Mar ;75(3):384-8.
15. Almquist E, Eeg-Olofsson O. Sensory-nerve-conduction velocity and two-point discrimmination in sutured nerves. [Internet]. The Journal of bone and joint surgery. American volume. 1970 Jun ;52(4):791-6.
16. Medinaceli L de, Freed WJ, Wyatt RJ. An index of the functional condition of rat sciatic nerve based on measurements made from walking tracks. [Internet]. Experimental neurology. 1982 Sep ;77(3):634-43.
17. Varejão ASP, Cabrita AM, Meek MF, Bulas-Cruz J, Filipe VM, Gabriel RC, et al. Ankle kinematics to evaluate functional recovery in crushed rat sciatic nerve [Internet]. Muscle & nerve. 2003 ;27(6):706–714.
18. Varejão ASP, Cabrita AM, Patricio JA, Bulas-Cruz J, Gabriel RC, Melo-Pinto P, et al. Functional assessment of peripheral nerve recovery in the rat: gait kinematics [Internet]. Microsurgery. 2001 ;21(8):383–388.
19. Varejão ASP, Cabrita AM, Meek MF, Bulas-Cruz J, Gabriel RC, Filipe VM, et al. Motion of the foot and ankle during the stance phase in rats. [Internet]. Muscle & nerve. 2002 Nov ;26(5):630-5.
20. Varejão ASP, Cabrita AM, Meek MF, Bulas-Cruz J, Melo-Pinto P, Raimondo S, et al. Functional and morphological assessment of a standardized rat sciatic nerve crush injury with a non-serrated clamp. [Internet]. Journal of neurotrauma. 2004 Nov ;21(11):1652-70.
21. Luis A, Amado S, Geuna S, Rodrigues J, Simoes M, Santos JD, et al. Long-term functional and morphological assessment of a standardized rat sciatic nerve crush injury with a non-serrated clamp [Internet]. Journal of neuroscience methods. 2007 ;16392–104.
22. Chandy T, Sharma CP. Chitosan--as a biomaterial. [Internet]. Biomaterials, artificial cells, and artificial organs. 1990 Jan ;18(1):1-24.

23. Senel S, McClure SJ. Potential applications of chitosan in veterinary medicine. [Internet]. Advanced drug delivery reviews. 2004 Jun ;56(10):1467-80.
24. Amano T, Richelson E, Nirenberg M. Neurotransmitter synthesis by neuroblastoma clones (neuroblast differentiation-cell culture-choline acetyltransferase-acetylcholinesterase-tyrosine hydroxylase-axons-dendrites). [Internet]. Proceedings of the National Academy of Sciences of the United States of America. 1972 Jan ;69(1):258-63.
25. Shirosaki Y, Tsuru K, Hayakawa S, Osaka A, Lopes MA, Santos JD, et al. In vitro cytocompatibility of MG63 cells on chitosan-organosiloxane hybrid membranes. [Internet]. Biomaterials. 2005 Feb ;26(5):485-93.
26. Amado S, Simões MJ, Armada da Silva PAS, Luís AL, Shirosaki Y, Lopes MA, et al. Use of hybrid chitosan membranes and N1E-115 cells for promoting nerve regeneration in an axonotmesis rat model. [Internet]. Biomaterials. 2008 Nov ;29(33):4409-19.
27. Luis AL, Rodrigues JM, Amado S, Veloso AP, Armada-Da-silva PAS, Raimondo S, et al. PLGA 90/10 and caprolactone biodegradable nerve guides for the reconstruction of the rat sciatic nerve [Internet]. Microsurgery. 2007 ;27(2):125–137.
28. Luís AL, Rodrigues JM, Geuna S, Amado S, Shirosaki Y, Lee JM, et al. Use of PLGA 90:10 scaffolds enriched with in vitro-differentiated neural cells for repairing rat sciatic nerve defects. [Internet]. Tissue engineering. Part A. 2008 Jun ;14(6):979-93.
29. Rodrigues JM, Luís AL, Lobato JV, Pinto MV, Faustino A, Hussain NS, et al. Intracellular Ca2+ concentration in the N1E-115 neuronal cell line and its use for peripheric nerve regeneration. [Internet]. Acta médica portuguesa. 2005 ;18(5):323-8.
30. Rodrigues JM, Luís AL, Lobato JV, Pinto MV, Lopes MA, Freitas M, et al. Determination of the intracellular Ca2+ concentration in the N1E-115 neuronal cell line in perspective of its use for peripheric nerve regeneration. [Internet]. Bio-medical materials and engineering. 2005 Jan ;15(6):455-65.
31. Kimhi Y, Palfrey C, Spector I, Barak Y, Littauer UZ. Maturation of neuroblastoma cells in the presence of dimethylsulfoxide. [Internet]. Proceedings of the National Academy of Sciences of the United States of America. 1976 Feb ;73(2):462-6.
32. Laat SW de, Saag PT van der. The plasma membrane as a regulatory site in growth and differentiation of neuroblastoma cells. [Internet]. International review of cytology. 1982 Jan ;741-54.

33. Reagan LP, Ye XH, Mir R, DePalo LR, Fluharty SJ. Up-regulation of angiotensin II receptors by in vitro differentiation of murine N1E-115 neuroblastoma cells. [Internet]. Molecular pharmacology. 1990 Dec ;38(6):878-86.
34. Larcher JC, Basseville M, Vayssiere JL, Cordeau-Lossouarn L, Croizat B, Gros F. Growth inhibition of N1E-115 mouse neuroblastoma cells by c-myc or N-myc antisense oligodeoxynucleotides causes limited differentiation but is not coupled to neurite formation. [Internet]. Biochemical and biophysical research communications. 1992 Jun ;185(3):915-24.
35. Prasad KN. Differentiation of neuroblastoma cells: a useful model for neurobiology and cancer. [Internet]. Biological reviews of the Cambridge Philosophical Society. 1991 Nov ;66(4):431-51.
36. Prasad KN, Kentroti S, Edwards-Prasad J, Vernadakis A, Imam M, Carvalho E, et al. Modification of the expression of adenosine 3',5'-cyclic monophosphate-induced differentiated functions in neuroblastoma cells by beta-carotene and D-alpha-tocopheryl succinate. [Internet]. Journal of the American College of Nutrition. 1994 Jun ;13(3):298-303
37. Yu P, Matloub HS, Sanger JR, Narini P. Gait analysis in rats with peripheral nerve injury. [Internet]. Muscle & nerve. 2001 Feb ;24(2):231-9.
38. Meek MF, Den Dunnen WF, Schakenraad JM, Robinson PH. Long-term evaluation of functional nerve recovery after reconstruction with a thin-walled biodegradable poly (DL-lactide-epsilon-caprolactone) nerve guide, using walking track analysis and electrostimulation tests. [Internet]. Microsurgery. 1999 Jan ;19(5):247-53.
39. Monte-Raso VV, Barbieri CH, Mazzer N. Índice funcional do ciático nas lesões por esmagamento do nervo ciático de ratos. Avaliação da reprodutibilidade do método entre examinadores [Internet]. Acta Ortopédica Brasileira. 2006 ;14(3):133-136.
40. Canu M-H, Garnier C, Lepoutre F-X, Falempin M. A 3D analysis of hindlimb motion during treadmill locomotion in rats after a 14-day episode of simulated microgravity. [Internet]. Behavioural brain research. 2005 Feb ;157(2):309-21.
41. Canu M-H, Garnier C. A 3D analysis of fore- and hindlimb motion during overground and ladder walking: comparison of control and unloaded rats. [Internet]. Experimental neurology. 2009 Jul ;218(1):98-108.
42. Chang Y-H, Auyang AG, Scholz JP, Nichols TR. Whole limb kinematics are preferentially conserved over individual joint kinematics after peripheral nerve

injury. [Internet]. The Journal of experimental biology. 2009 Nov ;212(Pt 21):3511-21.

43. Lundborg G. Alternatives to autologous nerve grafts. [Internet]. Handchirurgie, Mikrochirurgie, plastische Chirurgie : Organ der Deutschsprachigen Arbeitsgemeinschaft für Handchirurgie : Organ der Deutschsprachigen Arbeitsgemeinschaft für Mikrochirurgie der Peripheren Nerven und Gefässe : Organ der Vereinigung der Deut. 2004 Feb ;36(1):1-7.
44. Schmidt CE, Leach JB. Neural tissue engineering: strategies for repair and regeneration. [Internet]. Annual review of biomedical engineering. 2003 Jan ;5293-347.
45. Battiston B, Raimondo S, Tos P, Gaidano V, Audisio C, Scevola A, et al. Chapter 11: Tissue engineering of peripheral nerves [Internet]. Elsevier; 2009.
46. Zacchigna S, Giacca M. Chapter 20: Gene therapy perspectives for nerve repair. [Internet]. International review of neurobiology. 2009 Jan ;87381-92.
47. Terenghi G, Wiberg M, Kingham PJ. Chapter 21: Use of stem cells for improving nerve regeneration. [Internet]. International review of neurobiology. 2009 Jan ;87393-403.
48. Dahlin L, Johansson F, Lindwall C, Kanje M. Chapter 28: Future perspective in peripheral nerve reconstruction. [Internet]. Elsevier; 2009.
49. Santos PM, Williams SL, Thomas SS. Neuromuscular evaluation using rat gait analysis. [Internet]. Journal of neuroscience methods. 1995 ;61(1-2):79-84.
50. Perry J. Gait analysis: Normal and Pathological Function. SLACK Incorporated; 1992.
51. Cavanagh P. Biomechanics of distance running [Internet]. Champaign, Illinois: Human Kinetics Books; 1990.
52. Meek MF, Werff JFA van der, Klok F, Robinson PH, Nicolai JPA, Gramsbergen A. Functional nerve recovery after bridging a 15 mm gap in rat sciatic nerve with a biodegradable nerve guide. [Internet]. Scandinavian journal of plastic and reconstructive surgery and hand surgery / Nordisk plastikkirurgisk forening [and] Nordisk klubb for handkirurgi. 2003 Jan ;37(5):258-65.
53. Hyatt J-PK, Roy RR, Baldwin KM, Edgerton VR. Nerve activity-independent regulation of skeletal muscle atrophy: role of MyoD and myogenin in satellite cells and myonuclei. [Internet]. American journal of physiology. Cell physiology. 2003 Nov ;285(5):C1161-73.

54. Ijkema-Paassen J, Meek MF, Gramsbergen A. Reinnervation of muscles after transection of the sciatic nerve in adult rats. [Internet]. Muscle & nerve. 2002 Jun ;25(6):891-7.
55. Edgerton VR, Roy RR. How selective is the reinnervation of skeletal muscle fibers? [Internet]. Muscle & nerve. 2002 Jun ;25(6):765-7.
56. Borisov AB, Dedkov EI, Carlson BM. Abortive myogenesis in denervated skeletal muscle: differentiative properties of satellite cells, their migration, and block of terminal differentiation [Internet]. Anatomy and Embryology. 2005 Mar 11;209(4):269-279.
57. Dedkov EI, Kostrominova TY, Borisov AB, Carlson BM. Reparative myogenesis in long-term denervated skeletal muscles of adult rats results in a reduction of the satellite cell population. [Internet]. The Anatomical record. 2001 Jun 1;263(2):139-54.
58. Bruusgaard JC, Gundersen K. In vivo time-lapse microscopy reveals no loss of murine myonuclei during weeks of muscle atrophy. [Internet]. The Journal of clinical investigation. 2008 Apr ;118(4):1450-7.
59. Cebasek V, Radochová B, Ribaric S, Kubínová L, Erzen I. Nerve injury affects the capillary supply in rat slow and fast muscles differently. [Internet]. Cell and tissue research. 2006 Mar ;323(2):305-12.[
60. Huijing P a, Jaspers RT. Adaptation of muscle size and myofascial force transmission: a review and some new experimental results. [Internet]. Scandinavian journal of medicine & science in sports. 2005 Dec ;15(6):349-80.
61. Meijer HJM, Rijkelijkhuizen JM, Huijing PA. Effects of firing frequency on length-dependent myofascial force transmission between antagonistic and synergistic muscle groups. [Internet]. European journal of applied physiology. 2008 Oct ;104(3):501-13.
62. Rijkelijkhuizen JM, Baan GC, Haan a de, Ruiter CJ de, Huijing P a. Extramuscular myofascial force transmission for in situ rat medial gastrocnemius and plantaris muscles in progressive stages of dissection. [Internet]. The Journal of experimental biology. 2005 Jan ;208(Pt 1):129-40.
63. Huijing P a. Muscle as a collagen fiber reinforced composite: a review of force transmission in muscle and whole limb. [Internet]. Journal of biomechanics. 1999 Apr ;32(4):329-45.
64. Maas H, Meijer HJM, Huijing PA. Intermuscular interaction between synergists in rat originates from both intermuscular and extramuscular myofascial force transmission. [Internet]. Cells, tissues, organs. 2005 Jan ;181(1):38-50.

65. Howard CS, Blakeney DC, Medige J, Moy OJ, Peimer C a. Functional assessment in the rat by ground reaction forces. [Internet]. Journal of biomechanics. 2000 Jun ;33(6):751-7.

66. Johnson WL, Jindrich DL, Roy RR, Reggie Edgerton V. A three-dimensional model of the rat hindlimb: musculoskeletal geometry and muscle moment arms. [Internet]. Journal of biomechanics. 2008 Jan ;41(3):610-9.